2013

Non-destructive Analysis Of Trace Textile Fiber Evidence Via Room-temperature Fluorescence Spectrocopy

Krishnaveni Appalaneni
University of Central Florida

NON-DETSRUCTIVE ANALYSIS OF TRACE TEXTILE FIBER EVIDENCE VIA ROOM-TEMPERATURE FLUORESCENCE SPECTROSCOPY

by

KRISHNAVENI APPALANENI
M.S. University of Central Florida 2012

A dissertation submitted in partial fulfillment of the requirement
for the degree of Doctor of Philosophy
in the Department of Chemistry
in the College of Sciences
at the University of Central Florida
Orlando, Florida

Summer Term
2013

Major Professor: Andres D. Campiglia

ABSTRACT

Forensic fiber evidence plays an important role in many criminal investigations. Non-destructive techniques that preserve the physical integrity of the fibers for further court examination are highly valuable in forensic science. Non-destructive techniques that can either discriminate between similar fibers or match a known to a questioned fiber - and still preserve the physical integrity of the fibers for further court examination - are highly valuable in forensic science. When fibers cannot be discriminated by non-destructive tests, the next reasonable step is to extract the questioned and known fibers for dye analysis with a more selective technique such as high-performance liquid chromatography (HPLC) and/or gas chromatography-mass spectrometry (GC-MS). The common denominator among chromatographic techniques is to primarily focus on the dyes used to color the fibers and do not investigate other potential discriminating components present on the fiber. Differentiating among commercial dyes with very similar chromatographic behaviors and almost identical absorption spectra and/or fragmentation patterns is a challenging task.

This dissertation explores a different aspect of fiber analysis as it focuses on the total fluorescence emission of fibers. In addition to the contribution of the textile dye (or dyes) to the fluorescence spectrum of the fiber, we investigate the contribution of intrinsic fluorescence impurities – i.e. impurities imbedded into the fibers during fabrication of garments - as a reproducible source of fiber comparison. Differentiation of visually indistinguishable fibers is achieved by comparing excitation-emission matrices (EEMs) recorded from single textile fibers with the aid of a commercial spectrofluorimeter coupled to an epi-fluorescence microscope. Statistical data comparison was carried out via principal component analysis. An application of

this statistical approach is demonstrated using challenging dyes with similarities both in two-dimensional absorbance spectra and in three dimensional EEM data. High accuracy of fiber identification was observed in all the cases and no false positive identifications were observed at 99% confidence levels.

This thesis is dedicated to

My parents

Lakshmi and Sambasiva Rao

My husband

Rishi

My sisters

Lalitha and Sushma

For their endless love, support and encouragement.

ACKNOWLEDGMENTS

I would like to acknowledge my advisor, Dr. Andres D. Campiglia, for his encouragement and guidance to carry out this research and my dissertation committee for their valuable suggestions. I would like to thank Dr. Emily Heider for inspiring me towards chemometrics.

I would like to take this opportunity to thank my parents – I am who I am today because of their hard work and support. My special "thank you" goes out to my husband for his patience and his sacrifices to support my graduate life. I would also like to acknowledge my sisters, who stood by me during all days of hardships.

I would like to thank my family – Siva, Manoj, I.B.Rao, I.V. Lakshmi, Bindu and Prasad; my friends Lakshmi, Razi, Sharath, Sneha, Sushrutha, Swapna, Vamshi, Vinay and a special mention goes out to Srishanth, Rahul and Pranavi.

TABLE OF CONTENTS

LIST OF FIGURES

LIST OF TABLES

CHAPTER 1: GENERAL INTRODUCTION

1.1. Introduction

Forensic fiber evidence plays an important role in many criminal cases[1-2]. Non-destructive techniques that can either discriminate between similar fibers or match a known to a questioned fiber – and still preserve the physical integrity of the fibers for further court examination - are highly valuable in forensic science. Current microscopy based techniques for fiber comparison include polarized light microscopy[3], infrared microscopy[4-6], microspectrophotometry (MSP)[7-13] and scanning electron microscopy coupled to energy dispersive spectrometry[14]. Differences in cross-sectional shape, type of fiber material (natural or synthetic), weave and color often make possible to rule out a common source for the two samples. The main advantage of these techniques is their non-destructive nature, which preserves the physical integrity of the fibers for further court examination. Beyond microscopy but still under the category of minimally destructive techniques is pyrolysis coupled to gas chromatography. This tool is capable to compare the polymeric nature of synthetic and natural fibers at expenses of partial sample consumption[15].

When fibers cannot be discriminated by non-destructive tests, the next step usually consists of extracting the textile dye – or dyes – from both the known and questioned fiber. Solvent extraction [16], enzymatic [17-18] and alkaline [18-19] hydrolysis have been used to release dyes from the various types of fibers. Thin-layer chromatography (TLC) [17-19], high-performance liquid-chromatography (HPLC) [20] and capillary electrophoresis (CE) [21-23] have been used to separate and identify colored dyes in fiber extracts. TLC is a long-standing tool for the separation of common classes of fiber dyes, with silica gel being the most used stationary phase.

Unfortunately, no single solvent system exists that can separate all classes of dyes and some amount of prescreening is usually necessary. Specific methods have been reported for the analysis of dyes in cotton[17, 24], wool[19, 25-27], and various synthetic fabrics[24, 28-30]. This is a major disadvantage for forensic comparisons, mainly if one considers that each loose fiber in a forensic investigation represents and must be handled as a unique item of evidence.

HPLC presents several advantages over TLC, including better chromatographic resolution and quantitative capability. Reversed-phase HPLC has been used to separate and determine anionic, cationic, nonionic, and ionic dyes. When coupled to absorption single channel detectors, the identification of dyes is solely based on their chromatographic retention times. Additional selectivity is possible with the use of multichannel wavelength detection systems that record real-time absorption spectra for comparison of eluted components to spectral databases[20]. Initial attempts to develop CE methods for fiber dyes rendered irreproducible migration times, poor sensitivity, and the inability to separate non-ionizable dyes[21]. The introduction of micelles in the electrophoretic buffer (micellar electrokinetic chromatography or MEKC) has now made possible the separation of water insoluble dyes extracted from wool fiber samples[22]. A considerable improvement in sensitivity was obtained by coupling sample induced isotachophoresis to MEKC. With this approach, it was possible to analyze the dye content of single natural and synthetic fibers[23].

The detection scheme that holds the best selectivity for fiber discrimination is mass spectrometry (MS). The discrimination power of this approach has been demonstrated with thermospray HPLC-MS (TSP-HPLC-MS)[31] and electrospray ionization HPLC-MS (ESI-HPLC-MS)[16, 32-34]. CE-MS was successfully applied to the discrimination of four types of textile fibers,

namely acrylic, nylon, cotton and polyester[35]. The sensitivity of the mass spectrometer allows fibers as small as 2 mm to be successfully analyzed. Recent advances in MS of textile fibers have focused on matrix-assisted laser desorption ionization (MALDI) time-of-flight (TOF) MS. With this technique, it was possible to discriminate between single fibers pre-dyed with acidic and basic dyes by gathering both positive and negative ion mass spectra[36]. Direct analysis of textile fibers was demonstrated using Infrared matrix-assisted laser desorption electrospray ionization (IR-MALDESI) as a source for MS[37]. A minimally destructive, high-sensitivity analysis of acid dyes on nylon fibers was demonstrated using time of flight secondary ionization mass spectrometry (TOF-SIMS) method[38]. Unfortunately, MS techniques destroy the fiber just like all the other methods that provide chemical information based on previous dye extraction.

New approaches to the non-destructive analysis of fibers include diffuse reflectance infrared Fourier transform spectroscopy (DRIFTS) and Raman spectroscopy. Both techniques base comparisons on spectral characteristics of textile dyes imbedded in the fibers. When coupled to chemometric methods for spectral interpretation such as principal component analysis (PCA) and soft independent modeling of class analogies (SIMCA), DRIFTS was able to discriminate both dye color and reactive dye state on cotton fabrics[39-41]. Attempts on the discrimination of single fibers were not reported. Raman microprobe spectroscopy was able to characterize dyes in both natural and synthetic fibers via a combination of Fourier transform-Raman spectra and PCA analysis[42-44]. Due to the inherently weak nature of the infrared absorption signal and the Raman signal, the identification of minor fiber dyes via Fourier Transform infrared spectroscopy and Raman spectroscopy has not been possible. The inability to detect small concentrations of dyes that could add valuable information to the signature of fibers

certainly reduces the discrimination power of these techniques. The weak nature of their signals also poses serious limitations in the analysis of lightly dyed fibers[7-9, 30, 45-49].

To the extent of our literature search, no efforts have been made to investigate the full potential of fluorescence microscopy for forensic fiber examination. Most fluorescence microscopy articles report measurements made with excitation and emission band-pass filters[50-53], i.e. an approach that takes no advantage of the information content that exists in the spectral signatures of textile fibers. This dissertation introduces a highly discriminating approach based on fluorescence microscopy. It focuses on the total fluorescence emission of fibers. In addition to the contribution of the textile dye (or dyes) to the fluorescence spectrum of the fiber, we examined the contribution of intrinsic fluorescence impurities – i.e. impurities imbedded into the fibers during fabrication of garments - as a reproducible source of fiber comparison. Fiber comparison is made via data formats known as room-temperature fluorescence excitation-emission matrices (RTF-EEM). Collection of two-dimensional (2D) spectra and EEM directly from the fiber is carried out with the aid of an epi-fluorescence microscope connected to a commercial spectrofluorimeter via fiber optic probes. Statistical figures of merit for correct identification of fiber dyes via principal component cluster analysis are described so that matching single evidential fibers to other single fibers, threads, or bulk materials may be accomplished with 99 % confidence.

1.2. Principles of fluorescence:

Absorption of a photon by a molecule in the ground electronic state, S_0, allows promotion of the molecule into one of the excited electronic states, S_n. Absorption of photons is rapid,

requiring 10^{-14} to 10^{-15} S. Following excitation, excited molecules in the condensed phase rapidly relax to a Boltzmann distribution of the vibrational levels in the first excited singlet state, S_1,. This relaxation occurs on the pico second time scale and is due to internal conversion and vibrational relaxation. As Kasha's rule states, fluorescence from the states higher than the first excited singlet state, S_1, is uncommon[54].

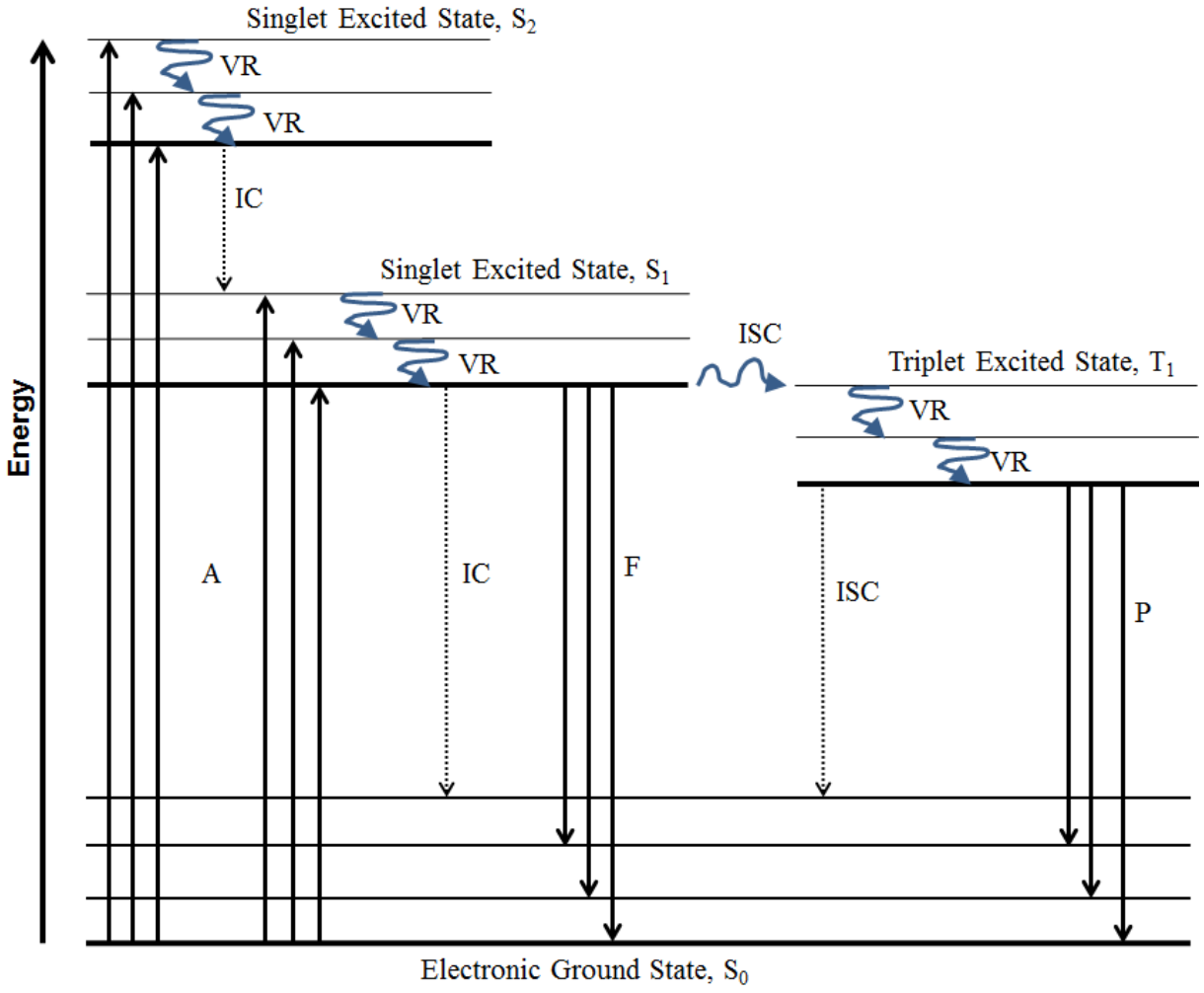

Figure 1.1. Partial energy level diagram indicating the electronic processes of photoluminescence. where A = absorption, VR = vibrational relaxation, IC = internal conversion, ISC = intersystem crossing, F = fluorescence emission and P = phosphorescence emission

A variety of mechanisms contribute to the deactivation of the molecule from S_1. These processes are depicted in the Jablonski diagram as shown in Figure 1.1. Non-radiative processes such as internal conversion (IC), external conversion (EC) and intersystem crossing (ISC) contribute to deactivation from S_1. IC is an intermolecular process by which the excited molecule drops to a lower-energy electronic state without the emission of radiation[55]. IC is especially efficient when two electronic levels are close enough that their vibrational energy levels can overlap. External conversion involves energy transfer from the excited molecule to the solvent or other solute molecules, and can also include quenching processes. Intersystem crossing is the process in which the multiplicity of the molecule changes from the first excited singlet state to the lowest excited triplet state. In this case, the change in multiplicity occurs due to spin-orbit coupling in which the character of both singlet and triplet states is mixed as the spin and orbital angular momenta interact.

The intensity of fluorescence emission is directly proportional to quantum yield (ϕ_F). The fluorescence emission yield is given by the following equation

$$\phi_F = \frac{k_F}{k_F + k_{ISC} + k_{IC} + k_{EC}} \qquad \text{Equation 1.1}$$

Where k_f is the fluorescence rate constant; k_{ISC} is the rate constant of intersystem crossing and k_{IC} and k_{EC} are the internal conversion and external conversion rate constants, respectively. The ideal quantum yield approaches unity. Equation 1.1 illustrates that enhanced fluorescence is attained when non-radiative transitions are kept at a minimum. The structure of the analyte molecule is the main factor contributing to the magnitude of k_F. Molecules with rigid, fused ring structures exhibit increased fluorescence.

1.3. Excitation-Emission matrices (EEMs):

The most popular data format in fluorescence spectroscopy is a two-dimensional (2D) plot correlating fluorescence intensities to emission wavelengths. The usual procedure for recording 2D fluorescence spectra consists of measuring the emission spectrum at a fixed excitation wavelength. Similarly, 2D excitation spectra are recorded by monitoring the excitation wavelength at a fixed fluorescence wavelength. In most cases, the fluorescence spectral profile of a pure compound is independent of the excitation wavelength. The same is true for its excitation spectral profile, which remains the same independent of the monitored emission wavelength. Maximum fluorescence intensity is always obtained at the maximum excitation wavelength of the fluorophor.

Recording a 2D fluorescence spectrum from a mixture with numerous fluorescence components only provides partial information on the total fluorescence of the mixture. The emission profile of a mixture with numerous fluorescence components varies with the relative positions of the excitation wavelength and the excitation maxima of the fluorophors in the mixture. Individual fluorophor contributions to the total fluorescence spectrum of the sample also depend on the fluorescence quantum yields of the fluorophors and possible quenching due to synergistic effects. For a sample of unknown composition, therefore, variations in the fluorescence profile with variations in the excitation wavelength suggest that more than fluorescence compound is present in the sample. A similar statement could be made from variations in its excitation profile with the monitored emission wavelengths.

The total fluorescence of the sample, which includes possible quenching and synergistic effects, can be gathered in a single data format known as excitation-emission matrix (EEM)[56-57].

The experimental procedure for collecting EEMs is rather simple. It consists of recording fluorescence spectra at various excitation wavelengths. The resulting I by J data matrix (EEM) is compiled from an array of 2D fluorescence spectra while the excitation wavelength is increased incrementally between each scan[58-59]. Each I row in the EEM corresponds to the emission spectrum at the *ith* excitation wavelength. Each J column in the EEM corresponds to the excitation spectrum at the *jth* emission wavelength. For a single emitting species in a sample, the elements of the EEM are given by:

$$\mathbf{M}_{ij} = 2.303\Phi_F \boldsymbol{I}_0(\lambda_i)\boldsymbol{\varepsilon}(\lambda_i)bc\boldsymbol{\gamma}(\lambda_j)\boldsymbol{\kappa}(\lambda_j) \qquad \text{Equation 1.2}$$

where $\boldsymbol{I}_0(\lambda_i)$ is the intensity of the incident light exciting the sample in units of quanta/s; $2.303\boldsymbol{\varepsilon}(\lambda_i)bc$ represents the optical density of the sample, which results from the product of the analyte's molar absorptivity $\boldsymbol{\varepsilon}(\lambda_i)$, the optical path-length b, and the concentration of the emitting species c; Φ_F is the quantum yield of fluorescence; $\boldsymbol{\gamma}(\lambda_j)$ is the fraction of fluorescence photons emitted at wavelength λ_j and $\boldsymbol{\kappa}(\lambda_j)$ is an instrumental factor that represents the wavelength dependence of the spectrofluorimeter's sensitivity[58]. The condensed version of equation 1.2 may be expressed as:

$$\mathbf{M}_{ij} = \boldsymbol{\alpha} x_i y_j \qquad \text{Equation 1.3}$$

where $\boldsymbol{\alpha} = 2.303\Phi_F bc$ is a wavelength independent factor containing all of the concentration dependence, $x_i = \boldsymbol{I}_0(\lambda_i)\boldsymbol{\varepsilon}(\lambda_i)$ and $yi = \boldsymbol{\gamma}(\lambda_j)\boldsymbol{\kappa}(\lambda_j)$. The observed relative fluorescence excitation spectrum may be represented by x_i, the wavelength sequenced set, and thought of as a column vector, x in λ_i space. The wavelength sequenced set, y_i, may be thought of as a row vector y in λ_i space, representing the observed fluorescence emission spectrum. Therefore, for a single component, **M** is simply represented as:

$$\mathbf{M} = \boldsymbol{\alpha}xy \qquad \text{Equation 1.4}$$

Where **M** is the product of the vectors x and y multiplied by the compound specific parameter **α**. When data is taken from a sample containing multiple, r, different species, M is given by the following expression:

$$M = \sum_{k=1}^{r} \alpha_k x^k y^k \qquad \text{Equation 1.5}$$

where k is used to detail the species. For a recorded M, the spectral characterization of single components then relies on finding r, $\boldsymbol{\alpha}_k$, x^k, and y^k.

Figure 1.2 and Figure 1.3 provides a schematic representation of an EEM of a compound obeying Kasha's rule[60]. The 2D excitation and fluorescence spectra are depicted along the sides of the EEM plot. Within the defined contour levels, this pure compound adheres to the two properties of excitation and emission previously discussed, i.e. its fluorescence profile does not change with the excitation wavelength and vice-versa. As always observed from an EEM of a pure compound, the center of the contour plot corresponds to the maximum excitation and emission wavelengths of the fluorophor.

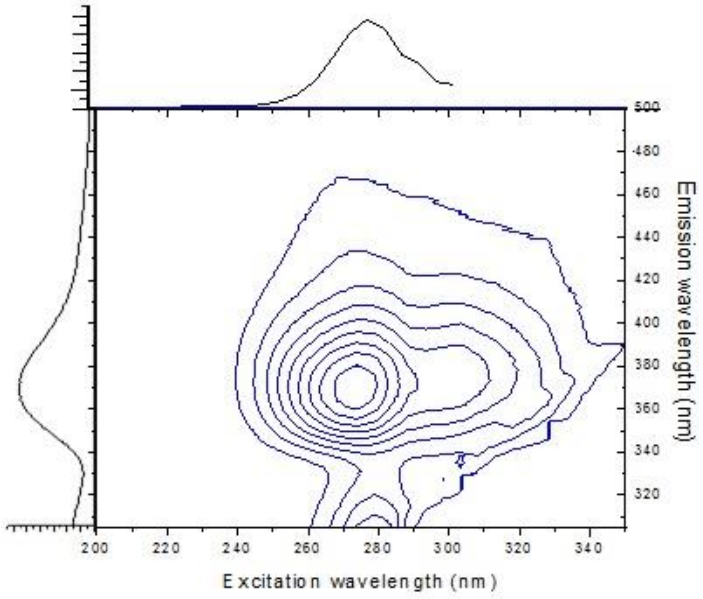

Figure 1.2 Contour map of EEM of basic green 4 reagent dye solutions in 50% v/v acetonitrile/water.

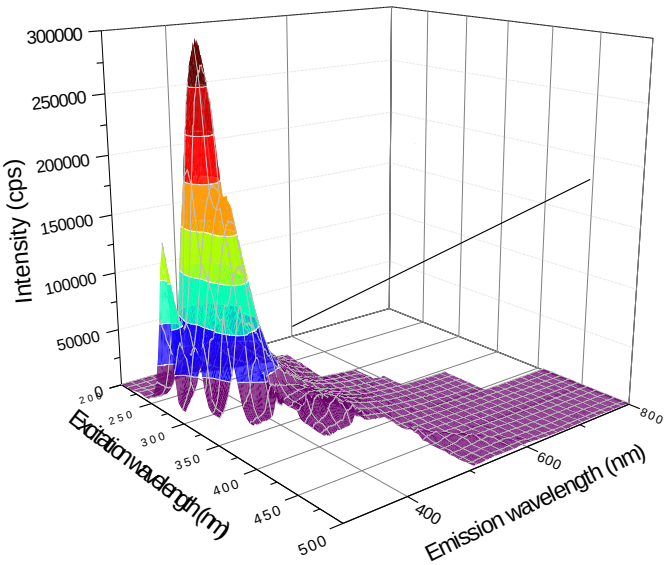

Figure 1.3. Color map surface of EEM of basic green 4 reagent dye solution in 50% v/v acetonitrile/water.

Figure 1.4 provides an example of a more complex EEM recorded from a multicomponent fluorescence mixture[61]. Evidence of the multicomponent nature of the EEM becomes clear with the multiple changes of the emission profile due to variations in the excitation wavelength. The same is true for the variations in excitation spectra with emission wavelengths. The number of changes noted in the emission or excitation profiles provides visual indication of the number of fluorescence components in the mixture.

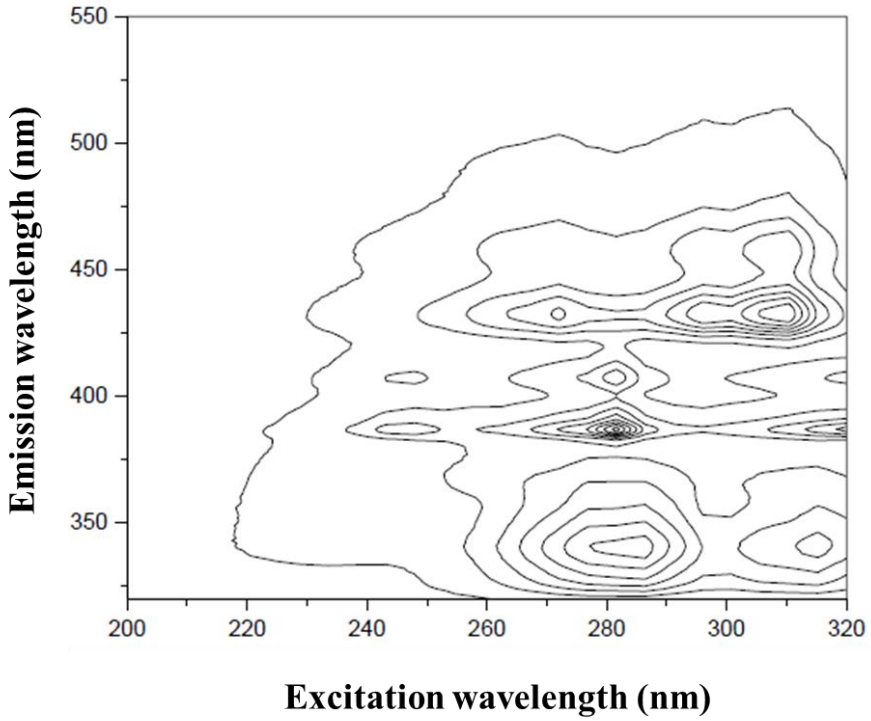

Figure 1.4. Contour plot of an EEM of a six-component mixture of polycyclic aromatic hydrocarbon compounds namely 1-hydroxynaphthalene (75ng/mL), 2-hydroxynaphthalene (300 ng/mL), 1-hydroxypyrene (100 ng/mL), 3-hydroxybenzo[a]pyrene (120 ng/mL), 2-hydroxyfluorene (350 ng/mL) and 9-hydroxyphenanthrene (90 ng/mL) in methanol

CHAPTER 2:POTENTIAL OF FLUORESCENCE SPECTROSCOPY FOR THE FORENSIC EXAMINATION OF FIBER EXTRACTS

2.1. Introduction

When non-destructive preliminary textile fiber examination cannot provide discrimination, known and questioned fibers are subjected to extraction and analyzed using various analytical methods like ultraviolet, visible and infrared absorption spectrometry[62-63], thin-layer chromatography[62-63], HPLC[16, 62-64] and LC-MS [65]. All these techniques focus on the analysis of the dye itself which can present several problems such as: (i) Commercial dyes are rarely ever pure and may contain multiple dyes or impurities that can vary from batch to batch. These other dyes and impurities can make it difficult to correctly identify the dye of interest by causing peak overlap, broadening or other interferences; (ii) Dyes may be present in concentrations too low to measure, especially if the fiber sample is very small; (iii) Many of these dyes are visually and structurally similar. Most methods, with the exception of LC-MS, do not provide information about molecular structure of the dye and cannot differentiate between structurally similar dyes.

Little has been done in the area of fluorescence for forensic study of fibers and dyes. Fluorescence microscopy has been reported for forensic fiber analysis[65], but this typically makes use of filters as wavelength selectors and doesn't provide the detailed spectra and peak information that room temperature fluorescence does. Typically fluorescence emission of fibers only investigates the optical brighteners used to treat textiles. These brighteners are not always present on fibers and when they are, show broad peaks emitting in the same wavelength region. Examining fluorescence of the dyes themselves is not very useful as many of them do not fluoresce.

In this chapter a different aspect of forensic fiber analysis is presented. Fluorescent impurities present on forensic textile fiber are used for their discriminating analysis and the reproducibility of these fluorescent impurities is analyzed. Several types of dye standards (disperse, direct, basic and acid) and extracts from dyed fibers are analyzed via room temperature fluorescence. Fluorescence spectra of fiber extracts show the presence of impurities not present in the dye standards. HPLC absorption and fluorescence chromatograms are used to compare dye standards with extracts and confirm the presence of these impurities.

2.2. Materials and methods

Table 2.1 summarizes the fourteen types of fibers investigated in this study, which were purchased in the form of fabric and dyed cloths of different shapes and sizes from Testfabrics Inc.; West Pittston, Pennsylvania, USA. All samples were received in sealed packages and kept as received in the dark to avoid environmental exposure.

Table 2.2 lists the dye standards used in this study. All standards were purchased from Sigma-Aldrich at reagent grade purity. No additional information was provided by Sigma-Aldrich on the complete chemical composition of the dye reagents.

Fiber threads were pulled from cloths using tweezers. Each thread was cut into a strand of appropriate length (4cm, 2cm or 5mm) using scissors or razor blades. Tweezers, scissors and razor blades were previously cleaned with methanol and visually examined under ultraviolet light (254nm) to prevent the presence of fluorescence contamination. Each 4cm or 2cm strand was cut into pieces of approximately 5 mm in length. 5 mm strands were used as such. The

number of fibers per thread depended on the cloth material and varied from 30 – 50 fibers. Depending on the cloth material, the total extracted mass varied from 0.38 to 1.58 mg. The mass of extracted fibers was measured with a Mettler-Toledo balance, Model AB135-S/FACT. Fibers were solvent extracted following the procedure recommended by the Federal Bureau of Investigations (FBI) [66]. All pieces from one fiber thread were placed in a 6 x 50 mm glass culture tube. 200 µL of extracting solvent were added to each tube. The tubes were sealed by melting with a propane torch. Sealed tubes were placed in an oven at 100° C for one hour. Tubes were removed from the oven, scored and broken open. The solvent was removed with a micro-pipette and placed in a plastic vial for storage. All solvents were HPLC grade and were purchased from Fisher Scientific. Nanopure water was used throughout and obtained from a Barnstead Nanopure Infinity water purifier. Glass culture tubes were acquired from Fischer Scientific.

Table 2.1. Type of fibers and respective dyes

Type of Fiber	*Respective Textile Dye*	*Cloth Size*
Acetate 154	Disperse Red 1	1meter x 1meter
Polyester 777	Disperse Red 4	1meter x 1meter
Polyester 777	Disperse Red 13	30cm x 30cm
Polyester 777	Disperse Blue 56	10cm x 10cm
Poly-acrylic 864	Basic Green 4	1meter x 1meter
Polyester 777	Basic Red 9	30cm x 30cm
Polyester 777	Basic Violet 14	30cm x 30cm
Cotton 400	Direct Blue 1	11cm x 15cm (100 pieces)
Cotton 460	Direct Blue 71	10cm x 10cm
Cotton 400	Direct Blue 90	11cm x 15 cm (100 pieces)
Nylon 361	Acid Red 151	11cm x 15cm (100 pieces)
Nylon 361	Acid Yellow 17	30cm x 30cm
Nylon 361	Acid Yellow 23	30cm x 30cm
Nylon 361	Acid Green 27	30cm x 30cm

Table 2.2. List of dye standards

Dye	*Dye Content (%)*[a]
Disperse Red 1	95
Disperse Red 4	NA [b]
Disperse Red 13	95
Disperse Blue 56	NA [b]
Basic Green 4	80
Basic Red 9	85
Basic Violet 14	NA [b]
Direct Blue 1	NA [b]
Direct Blue 71	50
Direct Blue 90	NA [b]
Acid Red 151	40
Acid Yellow 17	60
Acid Yellow 23	90
Acid Green 27	65

Two dimensional (2D) spectra and excitation and emission matrices (EEMs) were recorded using a commercial spectrofluorimeter (FluoroMax-P from Horiba Jobin-Yvon) equipped with a continuous 100 W pulsed xenon lamp with broadband illumination from 200 to 1100 nm. The

excitation and emission monochromators had the same reciprocal linear dispersion (4.2 nm·mm^{-1}) and accuracy (±0.5 nm with 0.3 nm resolution). Both diffraction gratings had the same number of grooves per unit length (1200 grooves·mm^{-1}) and were blazed at 330 nm (excitation) and 500 nm (emission). A photomultiplier tube (Hamamatsu, model R928) with spectral response from 185 to 650 nm was used for fluorescence detection operating at room temperature in the photon-counting mode. Commercial software (DataMax) was used to computer-control the instrument. Measurements were made by pouring un-degassed liquid solutions into micro-quartz cuvettes (1 cm path length x 2 mm width) that held a maximum volume of 400 μL. Fluorescence was collected at 90° from excitation using appropriate cutoff filters to reject straight-light and second order emission.

2D spectra were recorded via the classic method of setting one monochromator to a constant wavelength while scanning the other. EEMs were collected at 5nm excitation steps from longer to shorter wavelengths to reduce the risk of potential photo-degradation due to extensive sample excitation. The same procedures were used for blank samples to account for fluorescence background subtraction.

HPLC analysis of fiber extracts were carried out using an HPLC system from Hitachi (San Jose, CA, USA) equipped with the following basic components: a gradient pump (L-7100), a UV (L-7400 UV) and a fluorescence (L-7485) detector, an online degasser (L-761) and a control interface (D-7000). All HPLC operation was computer controlled with Hitachi software. Separation was carried out on an Agilent (Santa Clara, CA, USA) Zorbax EclipseXDB-C18 column with the following characteristics: 15 cm length, 2.1 mm diameter, and 5 μm average particle diameters. All extracts were injected at a volume of 20 μL using a fixed-volume

injection loop. HPLC fractions were collected in 2 mL sample vials with the aid of a Gilson fraction collector (model FC 20313).

2.3. Results and discussion

The investigated fibers were selected to cover a wide range of cloth materials such as acetate, polyester, cotton and nylon. Their respective reagent dyes were the following: Disperse Red 1, Disperse Red 4, Disperse Red 13, Basic Green 4, Basic Red 9, Basic Violet 14, Direct Blue 1, Direct Blue 71, Direct Blue 90, Acid Red 151, Acid Yellow 17, Acid Yellow 23 and Acid Green 27. These reagent dyes are commonly manufactured in the textile industry and fit into one of the following our categories: direct, disperse, basic and acid dyes. Direct dyes are those that have high affinity for cellulose materials such as cotton, rayon, etc. Disperse dyes are slightly soluble in water and typically used for synthetic fibers made of nylon, polyester, etc. Acid dyes are anionic dyes often applied from an acid dye-bath and basic dyes are cationic dyes characterized by their affinity for acrylic fiber and occasionally silk, wool or cotton.

2.4. General Extracting Solvent for Fluorescence Spectroscopy of Fibers

Numerous methods have been reported for isolating dyestuffs from fibers and for comparing dyes and dye mixtures with TLC. These include TLC systems for disperse, acid and basic dyes extracted from polyester, polyamide and acrylic fibers [67], for direct and reactive dyes extracted from cellulose fibers [68], for acid and metallized acid dyes from wool [7] and for disperse, acid and metallized dyes from polypropylene [69]. Some of these methods were compiled and presented as an analytical protocol in 1983 by the Trace Evidence Study Group of the California

Association of Criminalists [70]. This work was later extended to cotton and rayon fibers by Laing et al. [71]. Typically, the protocol involves three major steps: (a) Identification of the fiber type (usually involving microscopy); (b) selection and application of increasingly powerful extracting solvents to identify dye types; and (c) selection of appropriate TLC systems to discriminate extracted dyes. Although these procedures and their limitations pose few if any problems when large samples of fiber or fabric are available for comparison, they might present substantial difficulties in forensic comparisons with limited availability of fibers.

Under this prospective, we thought it would be valuable to propose a general extracting solvent for all the studied fibers. The investigated solvents were based on a literature review that revealed the predominance of the following four extracting solvents: 1:1 methanol – water (v/v), ethanol, 1:1 acetonitrile-water (v/v) and 57% pyridine - 43% water (v/v) [16, 64, 66, 72]. All measurements were made with threads collected from the top left corner of sample cloths, i.e. a cloth area arbitrarily selected with the sole purpose of consistency. Each investigated cloth was submitted to nine spectral runs recorded from three aliquots of three independent fiber thread extractions. For comparison purposes, all spectra were recorded with the same excitation (4nm) and emission (2nm) band-pass. Under these conditions, most of the studied fibers showed strong fluorescence in the four types of extracting solvents. For the few cases where relatively weak fluorescence was observed, further adjustment of excitation and emission band-pass was unsuccessfully attempted as weak fluorescence signals – i.e. barely distinguishable from the blanks - were still observed under 10nm excitation and emission band-passes. The signal intensities of the strongly fluorescent fibers measured with a 10nm excitation/emission band-pass fall beyond the upper linear limit (2 x 106 counts) of our instrument detection unit.

The spectral profiles and the fluorescence intensities of the studied samples varied with both the type of cloth and the chemical composition of the extracting solvent. Table 2.3 summarizes the extracting solvent with the highest fluorescence intensity for each type of studied fiber along with the maximum excitation and emission wavelengths of the extracts. Based on the strong fluorescence signals we consistently observed from all its fiber extracts, a 1:1 acetonitrile:water (v/v) mixture appeared to be the best choice for general extracting solvent. Figure 2.1, Figure 2.2

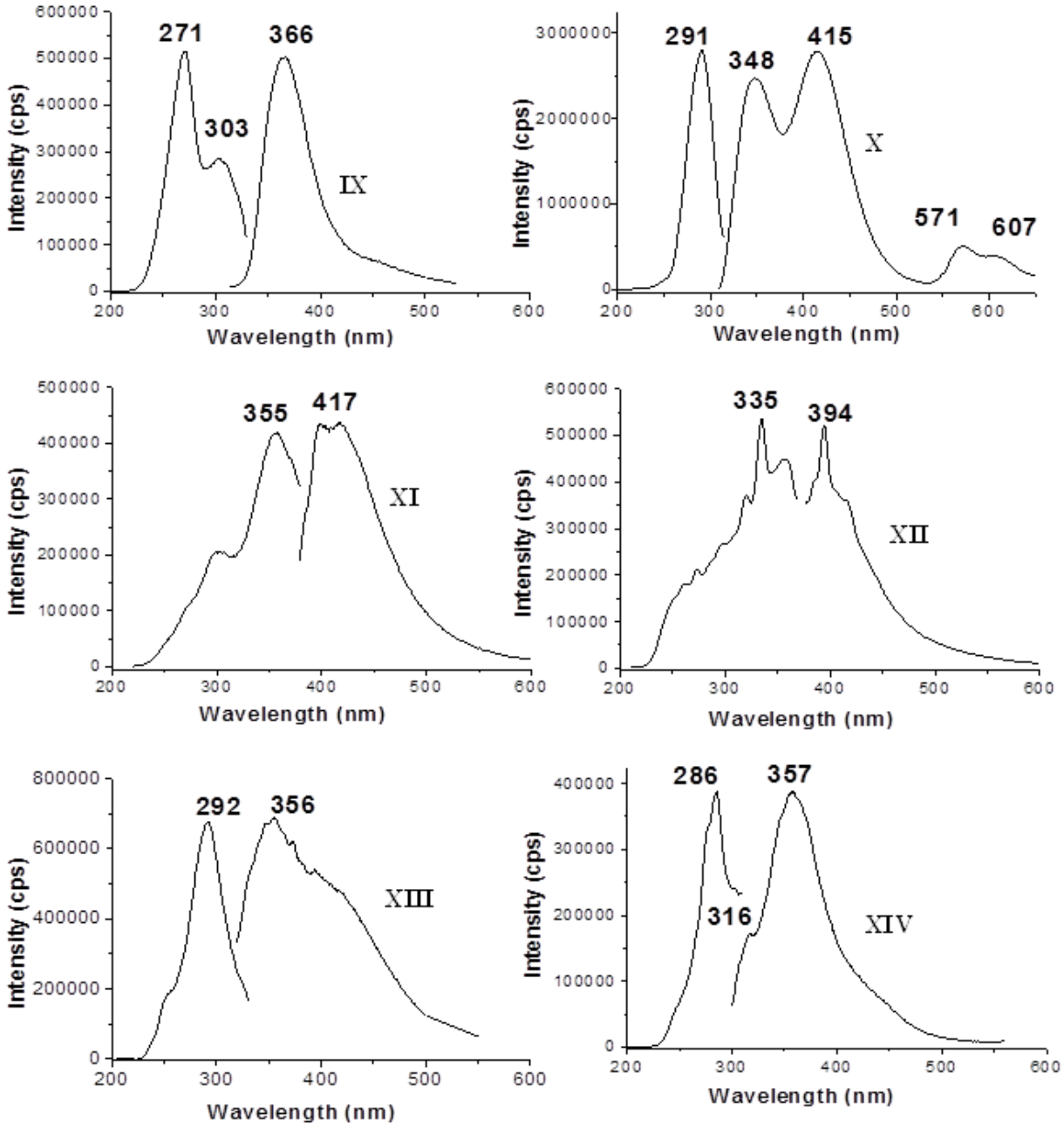

and Figure 2.3 compares the excitation and fluorescence profiles of the fourteen types of fibers extracted with this solvent. Fibers pre-dyed with Disperse Red 1, Direct Blue 1, Disperse Red 13 and Acid Green 27 showed extracts with similar excitation and fluorescence profiles. The same

is true for fibers pre-dyed with Basic Red 9, Basic Violet 14, Disperse Blue 56 and Acid Yellow 17. On the other end, fibers pre-dyed with Basic Green 4, Disperse Red 4, Direct Blue 71, Direct Blue 90, Acid Yellow 23 and Acid Red 151 showed distinct excitation and fluorescence spectra. Table 2.4 summarizes the maximum excitation and emission wavelengths of the studied fibers in 1:1 acetonitrile:water (v/v) extracts. Although the spectral comparison of fibers would certainly benefit from additional parameters of selectivity, the different excitation and fluorescence maxima still makes possible their visual discrimination on the basis of spectral profiles.

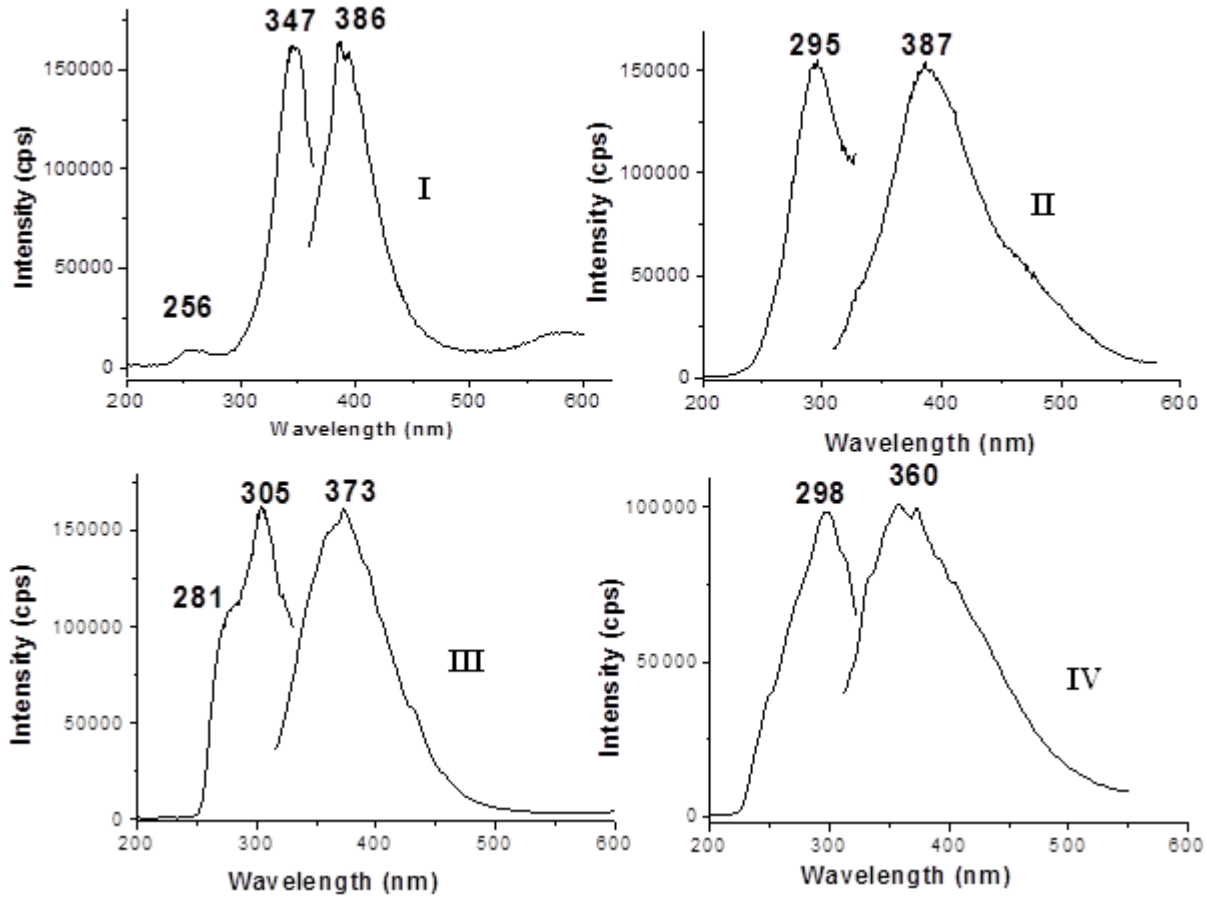

Figure 2.1. Excitation and fluorescence spectra of 1:1 acetonitrile/water (v/v) extracts collected from fiber threads of (I) Acetate pre-dyed with Disperse Red 1; (II) Cotton pre-dyed with Direct Blue 1; (III) Polyester pre-dyed with Disperse red 13; (IV) Nylon pre-dyed with Acid Green 27

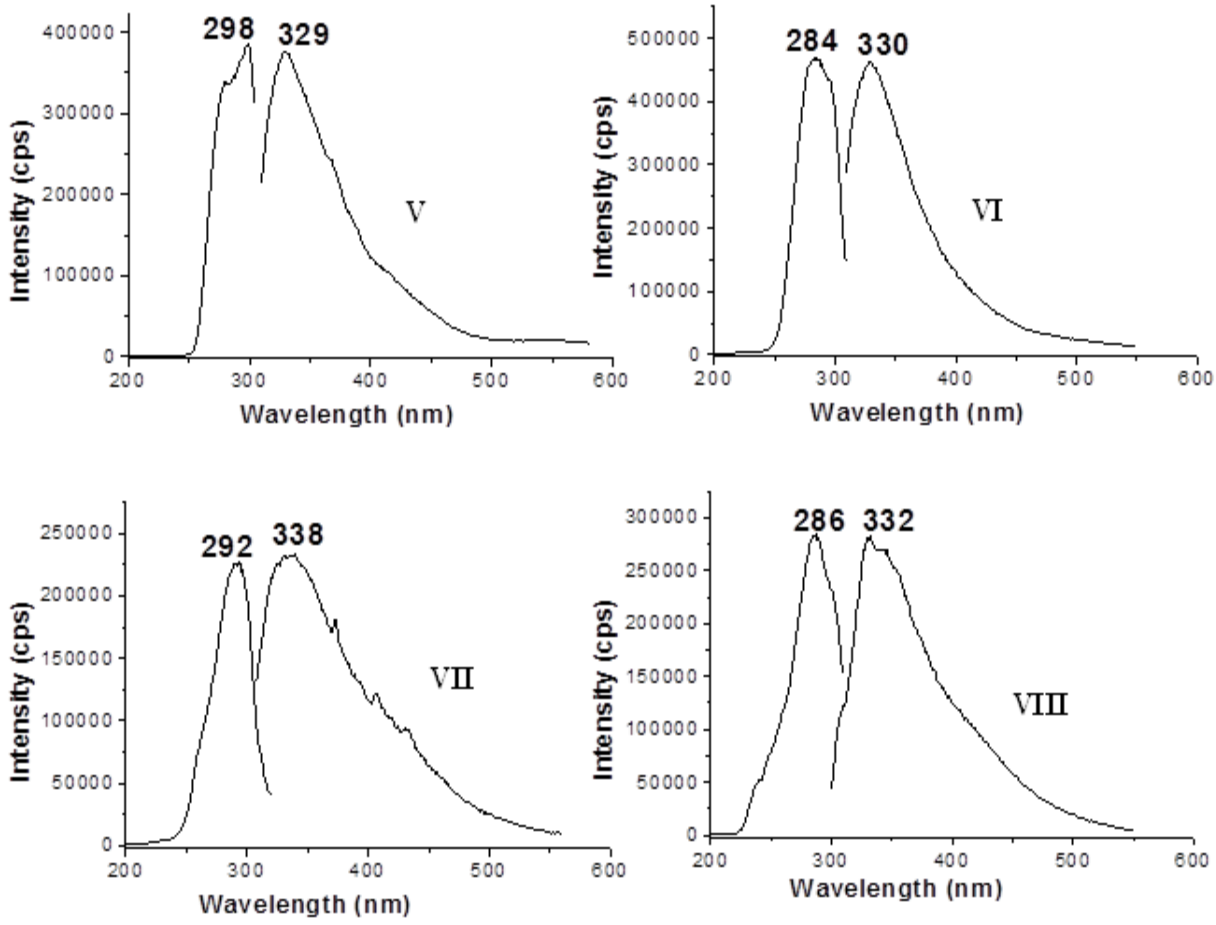

Figure 2.2. Excitation and fluorescence spectra of 1:1 acetonitrile/water (v/v) extracts collected from fiber threads of (V) Polyester pre-dyed with Basic Red 9; (VI) Polyester pre-dyed with Basic Violet 14; (VII) Polyester pre-dyed with Disperse Blue 56; (VIII) Nylon pre-dyed with Acid Yellow 17

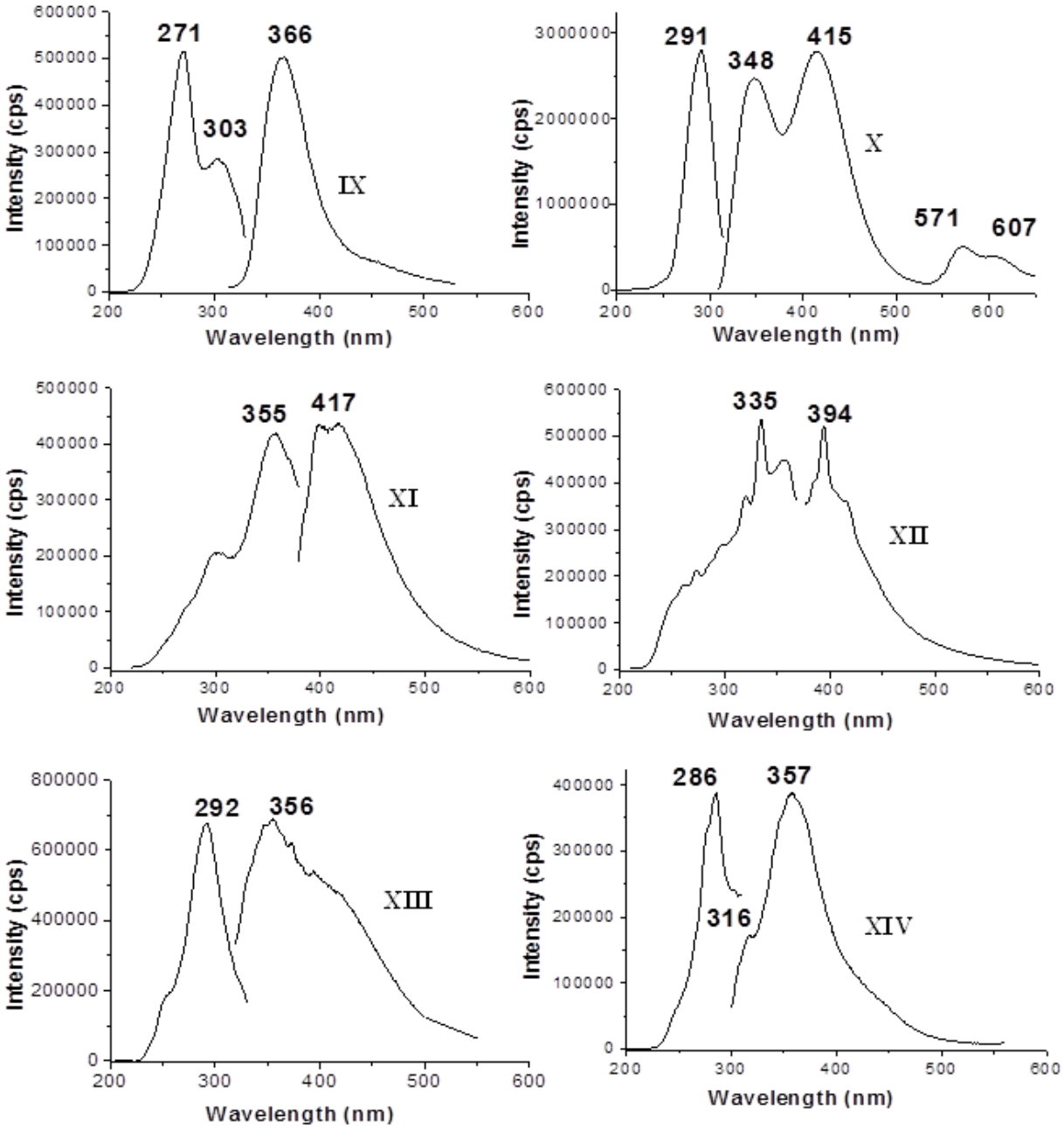

Figure 2.3. Excitation and fluorescence spectra of 1:1 acetonitrile/water (v/v) extracts collected from fiber threads of (IX) Poly-acrylic pre-dyed with Basic Green 4; (X) Polyester pre-dyed with Disperse Red 4; (XI) Cotton pre-dyed with Direct Blue 71; (XII) Cotton pre-dyed with Direct Blue 90; (XIII) Nylon pre-dyed with Acid Yellow 23; (XIV) Nylon pre-dyed with Acid Red 151

Table 2.3. Type of fiber with dye used to pre-dye fabric, the best extracting solvent for fluorescence and maximum excitation and fluorescence wavelengths of fiber extracts with the highest fluorescence intensity

Type of Fiber	*Respective Textile Dye*	*Solvent*	*Excitation Peaks (nm)*[a]	*Emission Peaks (nm)*[a]
Acetate 154	Disperse Red 1	1:1 acetonitrile/water (v:v)	256, 347	386
Polyester 777	Disperse Red 4	1:1 acetonitrile/water (v:v)	291	348, 415, 571, 607
Polyester 777	Disperse Red 13	ethanol	303	357, 404, 430
Polyester 777	Disperse Blue 56	4:3 pyridine/water (v:v)	319	385
Poly-acrylic 864	Basic Green 4	1:1 acetonitrile/water (v:v)	271, 303	366
Polyester 777	Basic Red 9	ethanol	295	350, 404, 430
Polyester 777	Basic Violet 14	1:1 acetonitrile/water (v:v)	284	330
Cotton 400	Direct Blue 1	ethanol	317, 333	373, 430
Cotton 400	Direct Blue 71	1:1 acetonitrile/water (v:v)	300, 355	417
Cotton 400	Direct Blue 90	4:3 pyridine/water (v:v)	335	406
Nylon 361	Acid Red 151	ethanol	305	358, 387, 406, 431, 459
Nylon 361	Acid Yellow 17	ethanol	287	338, 403, 430
Nylon 361	Acid Yellow 23	ethanol	289	345, 430
Nylon 361	Acid Green 27	1:1 methanol/water (v:v)	245, 303	412

[a] Wavelengths of maximum intensity are underlined

Table 2.4. Maximum excitation and fluorescence wavelengths of fiber extracts in 1:1 acetonitrile/water (v/v)

Type of Fiber	*Respective Textile Dye*	*Excitation Peaks (nm)*[a]	*Emission Peaks (nm)*[a]
Acetate 154	Disperse Red 1	256, 347	386
Polyester 777	Disperse Red 4	291	348, 415, 571, 607
Polyester 777	Disperse Red 13	281, 305	373
Polyester 777	Disperse Blue 56	292	338
Poly-acrylic 864	Basic Green 4	271, 303	366
Polyester 777	Basic Red 9	298	329
Polyester 777	Basic Violet 14	284	330
Cotton 400	Direct Blue 1	295	373, 430
Cotton 400	Direct Blue 71	300, 355	417
Cotton 400	Direct Blue 90	335	394
Nylon 361	Acid Red 151	286	316, 357
Nylon 361	Acid Yellow 17	286	332
Nylon 361	Acid Yellow 23	292	356
Nylon 361	Acid Green 27	298	360

[a] Wavelengths of maximum intensity are underlined

2.5. Reproducibility of Fluorescence Spectral Profiles

Considering reproducible spectra an essential characteristic for forensic fiber comparison, we next investigated the fluorescence spectral profiles of extracts obtained from single fibers belonging to the same piece of cloth. The reproducibility within the same area of cloth was investigated by recording spectral profiles from individual extracts belonging to adjacent fibers, i.e. single fibers located immediately next to each other. The spectral reproducibility within the entire cloth was investigated by recording spectral profiles form individual extracts of single fibers located in four different areas of the cloth. The four areas were arbitrarily chosen and corresponded to the top middle (TM), top corner (TC), bottom middle (BM) and bottom corner (BC) of the cloth.

Figure 2.4 compares the excitation and fluorescence spectra of fiber extracts collected from three single fibers located within the same area of cloth. The extracted fibers were right next to each other so that the first fiber was lying alongside (touching) the second fiber which was alongside the third fiber. Their spectral profiles are clearly reproducible with only a slight variation in intensity. Figure 2.5 shows the outstanding spectral reproducibility of single fiber extracts taken from different areas across the cloth. Other than a slight difference in intensity, which was within the reproducibility of measurements of the instrumental response, the spectral profiles are virtually the same. The same behavior was observed for all types of investigated cloths. This is also true for the four types of studied solvents (data not shown).

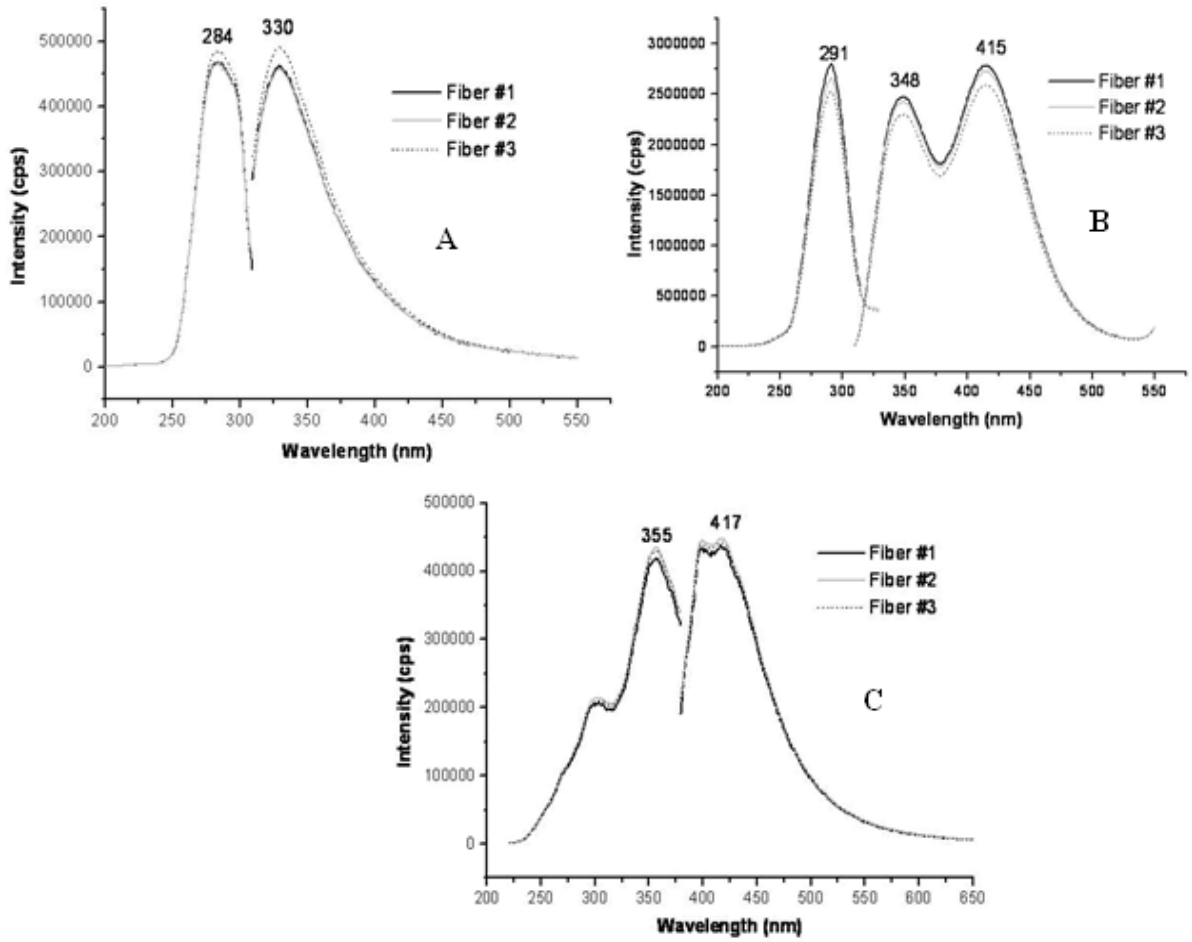

Figure 2.4. Excitation and fluorescence spectra of 1:1 acetonitrile/water (v/v) extracts collected from fiber threads of A) Polyester pre-dyed with Disperse Red 4; B) Polyester pre-dyed with Basic Violet 14 and C) Cotton pre-dyed with Direct Blue 71. Each spectrum corresponds to an extract from a single fiber thread. All fiber threads were adjacent to each other and located within the same area of cloth.

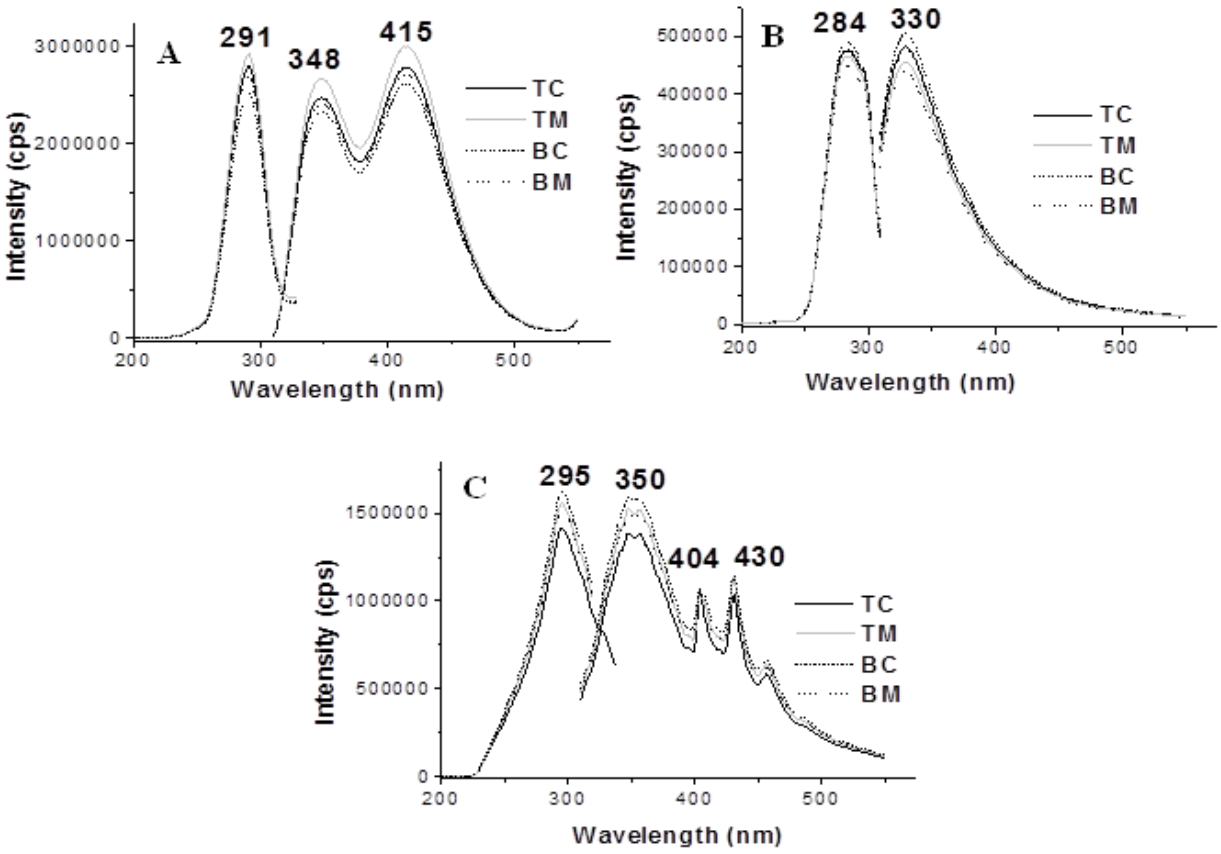

Figure 2.5. Excitation and fluorescence spectra of extracts collected in A) 1:1 acetonitrile/water (v/v) from polyester fibers pre-dyed with disperse red 4; B) 1:1 acetonitrile/water (v/v) from polyester fibers pre-dyed with basic violet 14 and C) Ethanol from polyester fibers pre-dyed with Basic Red 9. Each spectrum corresponds to an extract from a single fiber. All fibers were located at different areas within the same cloth.

2.6.Minimum Fiber Length for fluorescence Spectroscopy of Fiber Extracts

Extensive work in 1974 [73] showed that the average length of fibers transferred between clothing materials is approximately 5mm. Subsequent work in 1991 reemphasized the limited length and size distribution of retained transferred fibers in typical casework [19]. When removed eight hours after the transfer took place, the average recovered fiber had a length of less than 2 mm. Depending on the sensitivity of the instrumental technique, the short fiber length and the limited availability of sample could pose a significant challenge to forensic fiber protocols. We investigated this possibility for fluorescence spectroscopy with 1:1 acetonitrile:water (v/v) fiber extracts. .

Figure 2.6 compare fluorescence spectra of extracts obtained from single fibers with different lengths. As expected, the overall intensities of fluorescence spectra decreased with the lengths of the extracted fibers. However, fibers with 2 mm lengths still provided sufficient fluorescence to characterize the fibers on the basis of their spectral profiles. The same type of result was obtained for all fiber materials in Table 2.1.

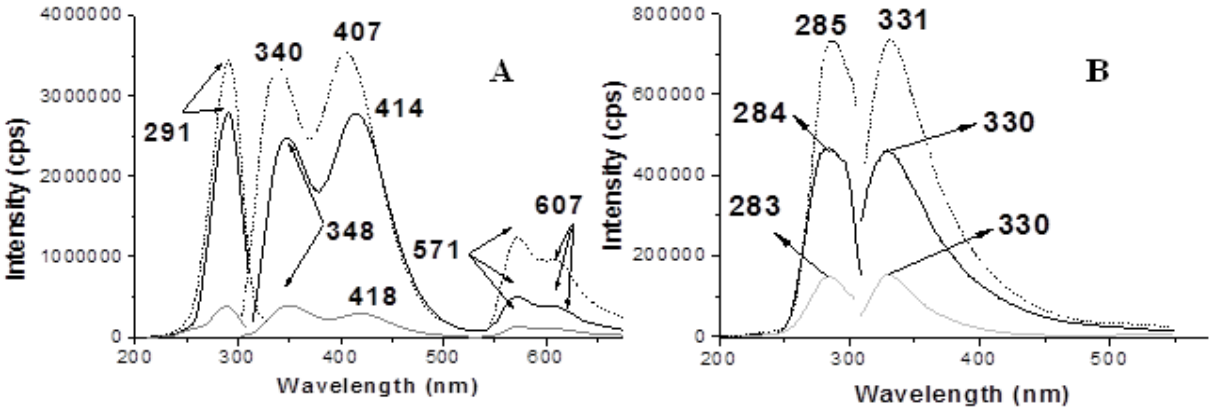

Figure 2.6. Excitation and emission spectra recorded on 1:1 acetonitrile/water (v/v) extracts collected from different lengths i.e. (---) 2cm (—) 1cm and (—) 2mm of A) Disperse red 4 fibers - emission spectra was recorded by exciting at 291 nm and excitation spectra by setting emission set at 415 nm and B) Basic Violet 14 fibers - emission spectra was recorded by exciting at 284 nm and excitation spectra by setting emission set at 330 nm. Slits were set at 4 and 2 nm band-pass for excitation and emission, respectively.

2.7. HPLC Analysis of Fiber Extracts

The spectral overlapping among fluorescence concomitants makes difficult to evaluate the number of components that contribute to the total fluorescence of the extract as well as their reproducibility for forensic fiber examination. A better insight on the individual reproducibility of fluorescence concomitants was obtained with the HPLC analysis of fiber extracts. Only five of the cloth materials in Table 2.1 were randomly selected for HPLC studies. Sample collection followed the same strategy as the one previously described in section 2.5. A minimum of three chromatographic runs were carried out per fiber extract. Each chromatographic run lasted a maximum of 40 minutes using a 1.5 mL/min flow rate and a water/methanol mobile phase. Separation was best achieved under the following gradient mobile phase conditions: 0 - 15 min = 70/30 water/methanol (v/v) to 30/70 water / methanol (v/v); 15 - 40min: 30/70 water / methanol

(v/v) to 100% methanol. The absorption, excitation and emission wavelengths selected for HPLC detection corresponded to the maximum wavelengths of the fiber extracts.

Table 2.5. Retention times of main peaks observed in absorption and fluorescence chromatograms of fiber extracts

Dye Extract	*Absorbance*	*Emission*[a]
Disperse Red 4	14.8	13.0, 14.2
Disperse Blue 56	n/a[b]	14.6, 20.9, 23.0
Acid Red 151	13.0	22.8, 28.9, 32.9
Acid Yellow 17	0.67	15.4, 19.1, 20.2
Acid Yellow 23	0.61	22.9, 29.0, 33.0

[a] Wavelengths of maximum intensity are underlined

Table 2.5 summarizes the retention times of the main chromatographic peaks observed in the absorption and fluorescence chromatograms. Each value represents the average of three chromatographic runs of the same extract. Typical relative standard deviations of retention times were lower than 5%. Table 2.5 compares the fluorescence chromatograms of fibers pre-dyed with Dispersed Red 4, Basic Green 4 and Acid Red 151. The agreement among the retention times and the fluorescence intensities of the four chromatograms for each type of fiber extract demonstrates the reproducible distribution of fluorescence components within fibers of the same piece of cloth.

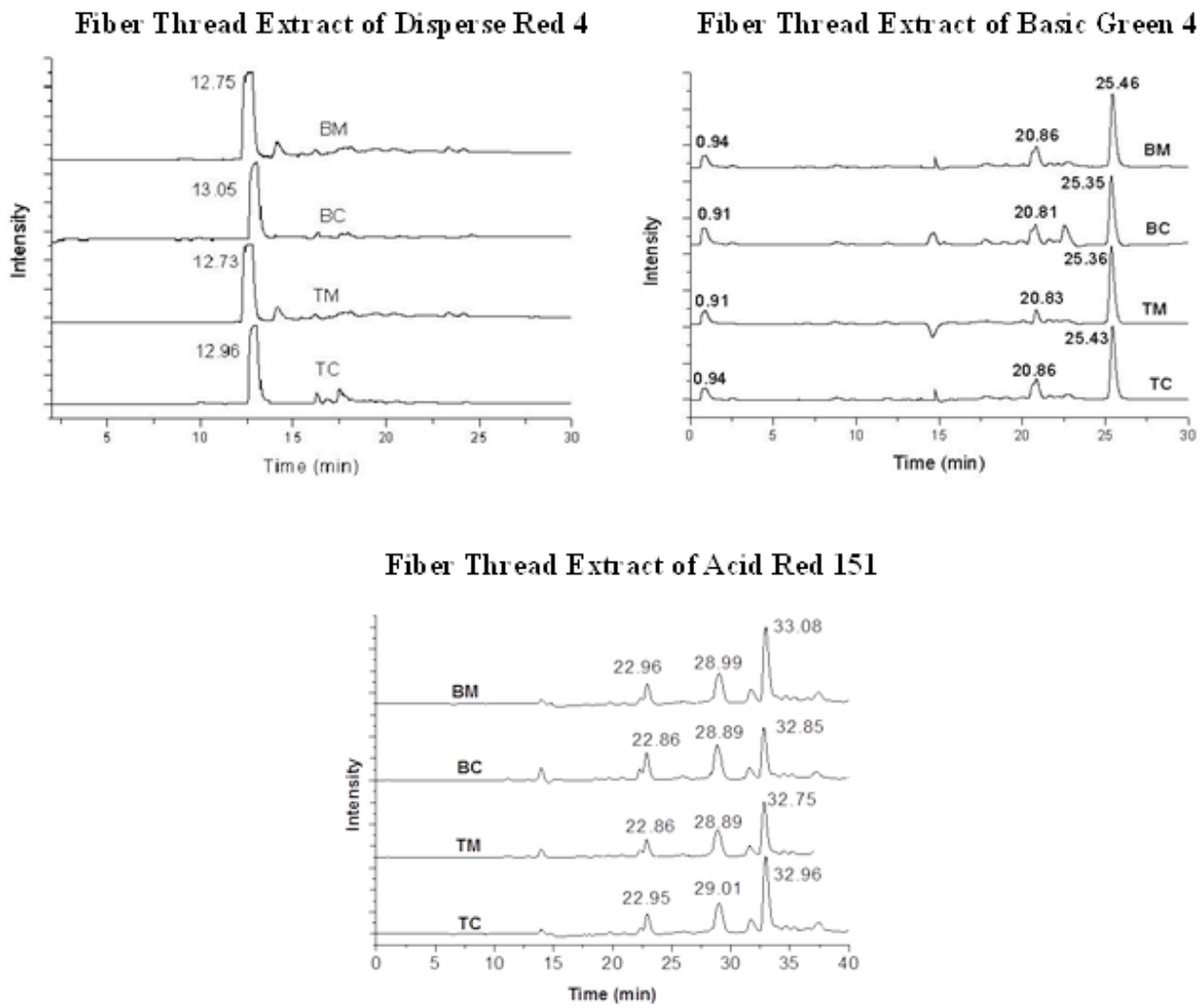

Figure 2.7. HPLC absorption chromatograms of fiber thread extracts. Excitation and fluorescence detection wavelengths were set as follows: 291/345nm (Disperse Red 4), 272/366nm (Basic Green 4) and 305/431nm (Acid Red 151)

2.8. Excitation-Emission Matrices

Recording two dimensional (2D) spectra - intensity versus wavelength - from a mixture with numerous fluorescence components only provides partial information on the total fluorescence of the sample. The resulting emission profile depends on the relative positions of the measuring excitation wavelength and the excitation maxima of the individual fluorescence components of the mixture. The relative contributions to the total fluorescence of the sample also depend on the fluorescence quantum yields of the individual components and possible quenching due to synergistic effects. The most appropriate data format to characterize the total fluorescence of a multi-fluorophor mixture is an excitation-emission matrix (EEM) [58]. Although EEM have been extensively applied to environmental [56], drug [57] and physiological [74-75] analysis, our literature search revealed no applications to the forensic analysis of fiber extracts. In this section, we demonstrate their potential for the forensic examination of fibers.

Table 2.6. Profile comparison of 2D RT-excitation and fluorescence spectra and RTF-EEM recorded from dye reagents and fiber extracts

Type of Fiber	*2D-Excitation*	*2D-Fluorescence*	*EEM*
Disperse Red 4	different	different	different
Disperse Blue 56	*very similar*	*very similar*	different
Basic Green 4	*very similar*	*very similar*	different
Basic Red 9	different	different	different
Acid Red 151	different	different	different
Acid Yellow 17	different	different	different
Acid Yellow 23	different	different	different
Acid Green 27	different	different	different

Eight types of textiles fibers were investigated via EEM spectroscopy. For the purpose of comparison, EEMs were also recorded from Sigma-Aldrich dye standards. A comparison of the

dye reagents used by Testfabrics to pre-dye the investigated fibers was not possible due to our difficulties in obtaining the matching reagent dyes. Table 2.6 provides a visual comparison of the spectral profiles obtained via 2D and EEM spectroscopy. The fact that Disperse Blue 56 and Basic Green 4 fiber extracts provide very similar 2D spectral profiles to those recorded from their respective standards indicates insufficient selectivity of the 2D data format for the forensic differentiation of fibers. Our statement takes into consideration the possible variations that often exist in the chemical composition of dye reagents from different commercial sources and/or variations that may also exist within dye reagent batches from the same commercial source.

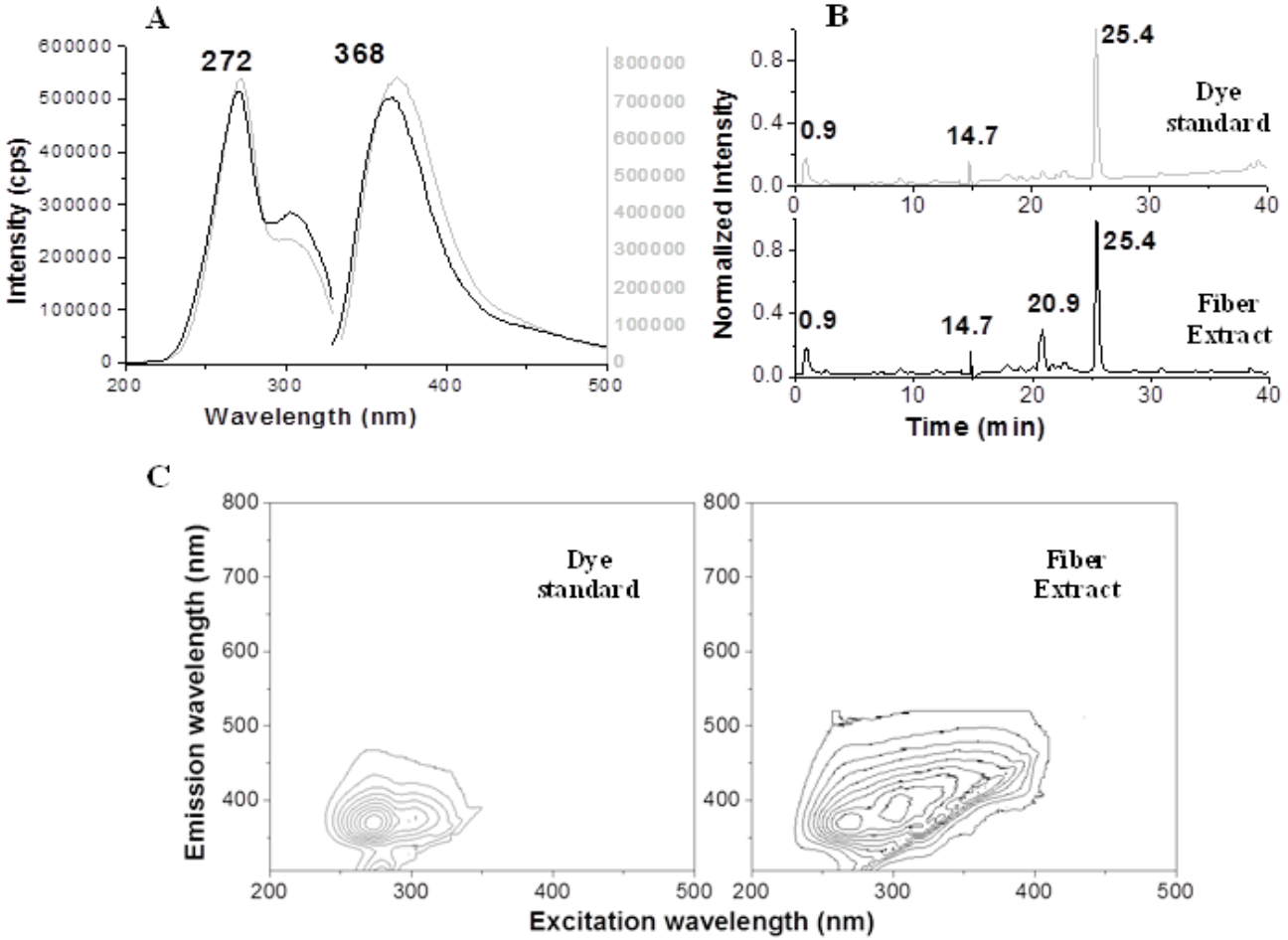

Figure 2.8. Comparison of basic green 4 (—) fiber extract and (—) Sigma-Aldrich dye standard recorded at excitation and emission wavelengths of 271 nm and 366 nm respectively A) 2D- excitation and fluorescence spectra; B) Fluorescence chromatograms; C) 3D- excitation-emission matrices

Figure 2.8A compares the 2D spectra of the fiber extracts pre-dyed with Basic Green 4 to those recorded from the Sigma-Aldrich standard. The spectral profiles are virtually the same, which makes differentiation of these two samples not possible. Figure 2.8B compares the fluorescence chromatograms of the fiber extract and the standard recorded at the maximum excitation and emission wavelengths of their 2D spectra. Upon excitation at 271nm, the total fluorescence of the dye standard and the fiber extract at 366 nm results from the contribution of three and four fluorescence concomitants, respectively. The similarity of the 2D spectral profiles in fig. 5A does not reflect the presence of an additional component in the fiber extract. The equivalent retention times of the other three peaks suggests that the three remaining fluorophors are the same in both samples. A clear difference exists between the EEM data formats of the two samples Figure 2.8C. The presence of additional fluorophors in the extract with excitation above 350 nm makes possible the visual differentiation of the two samples. The same is true for the EEMs of Disperse Blue 56 fiber extract and its respective Sigma-Aldrich standard (Figure 2.9. Comparison of disperse blue 56 (—) fiber extract and (—) Sigma-Aldrich dye standard A) 3D-excitation emission matrices; B) Fluorescence chromatograms recorded at 583nm and 660 nm of excitation and emission wavelengths respectively for Sigma-Aldrich dye standard and 320 nm and 385 nm of excitation and emission wavelengths respectively for fiber extracts.

The fluorescence chromatogram of the dye standard recorded at 583 nm (excitation) and 660 nm emission (Figure 2.9 B) reveals the presence of six fluorescence components that are absent in the fiber extract. The main reason the EEM data formats are able to differentiate among these two extracts and the standard is their ability to convolute the contribution of all the fluorescence components to the total fluorescence of the sample.

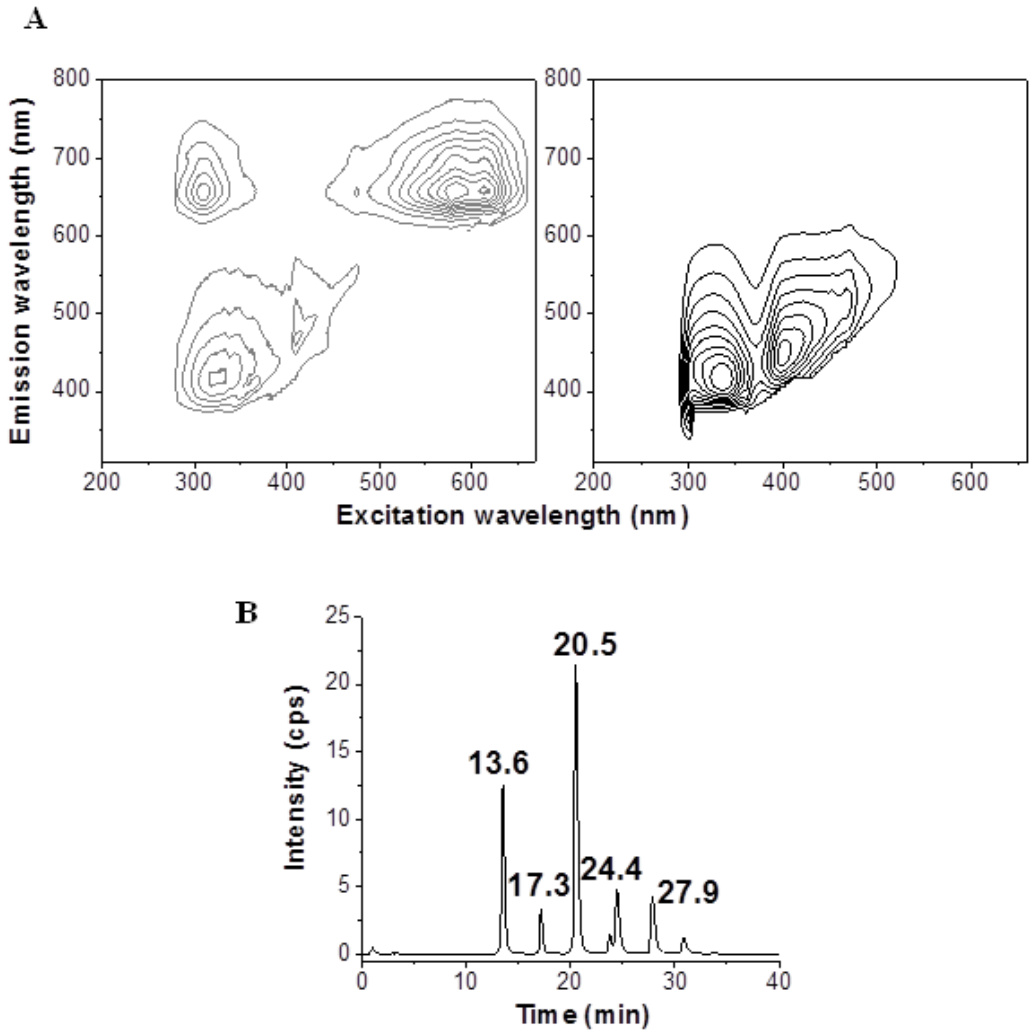

Figure 2.9. Comparison of disperse blue 56 (—) fiber extract and (—) Sigma-Aldrich dye standard A) 3D- excitation emission matrices; B) Fluorescence chromatograms recorded at 583nm and 660 nm of excitation and emission wavelengths respectively for Sigma-Aldrich dye standard and 320 nm and 385 nm of excitation and emission wavelengths respectively for fiber extracts.

2.9. EEM Comparison of Visually Indistinguishable Fibers

Large amounts of textile materials are produced each year in replicate fiber types and colors. There are cases where it is not possible to discriminate between two fibers that have been dyed with highly similar dyes. This is not an uncommon situation. Many hundreds of commercial dyes with indistinguishable colors exist as the result of minimal structural variations encouraged by the patent process and commercial competition. Acid Yellow 17 and Acid Yellow 23 fall into this category. When used to color Nylon 361 fibers, these dyes provide visually indistinguishable fibers. Comparison of Figure 2.2 (VIII) and Figure 2.3 (XIII) shows the possibility to visually differentiate the two types of fibers on the basis of 2D fluorescence spectra. Further differentiation was then investigated via EEM spectroscopy. Ten single fibers of each type of material were individually extracted and an EEM was recorded from each extract. Reproducible EEM contours were obtained for the ten fibers of each type of material. Figure 2.10, Figure 2.11 and Figure 2.12 provide typical EEMs recorded from the two types of fiber extracts. EEM contours were generated in the post-acquisition mode with Origin software. Origin finds the maximum and minimum fluorescence intensity values from the spreadsheet data set and calculates the increment that is required to create the desired number of levels in the contour plot. The contour plot displays intensity values in the form of levels with maximum intensities arranged towards the center of the contour. Independent of the number of levels, clear differences are observed among the EEM contours of the two fiber extracts.

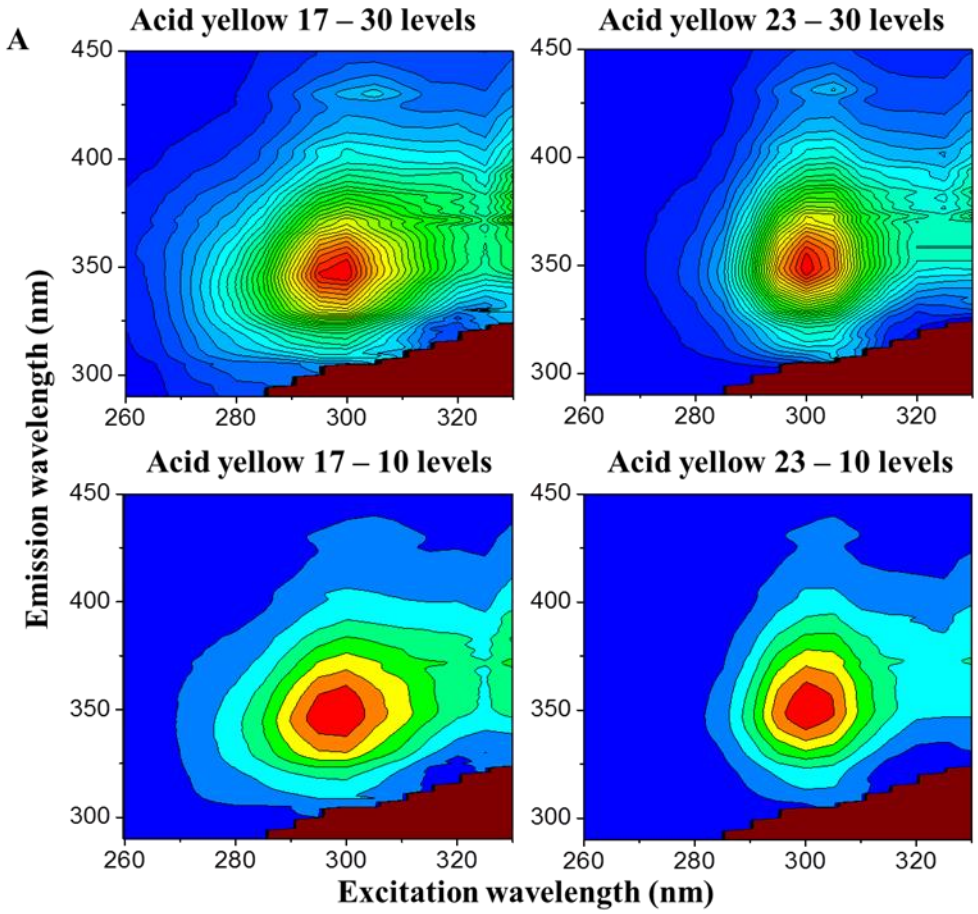

Figure 2.10. Comparison of excitation-emission matrices of acid yellow 17 and acid yellow 23 fiber extracts with different contour levels at excitation wavelength range of 260 to 330 nm and emission wavelength range of 290 to 450 nm

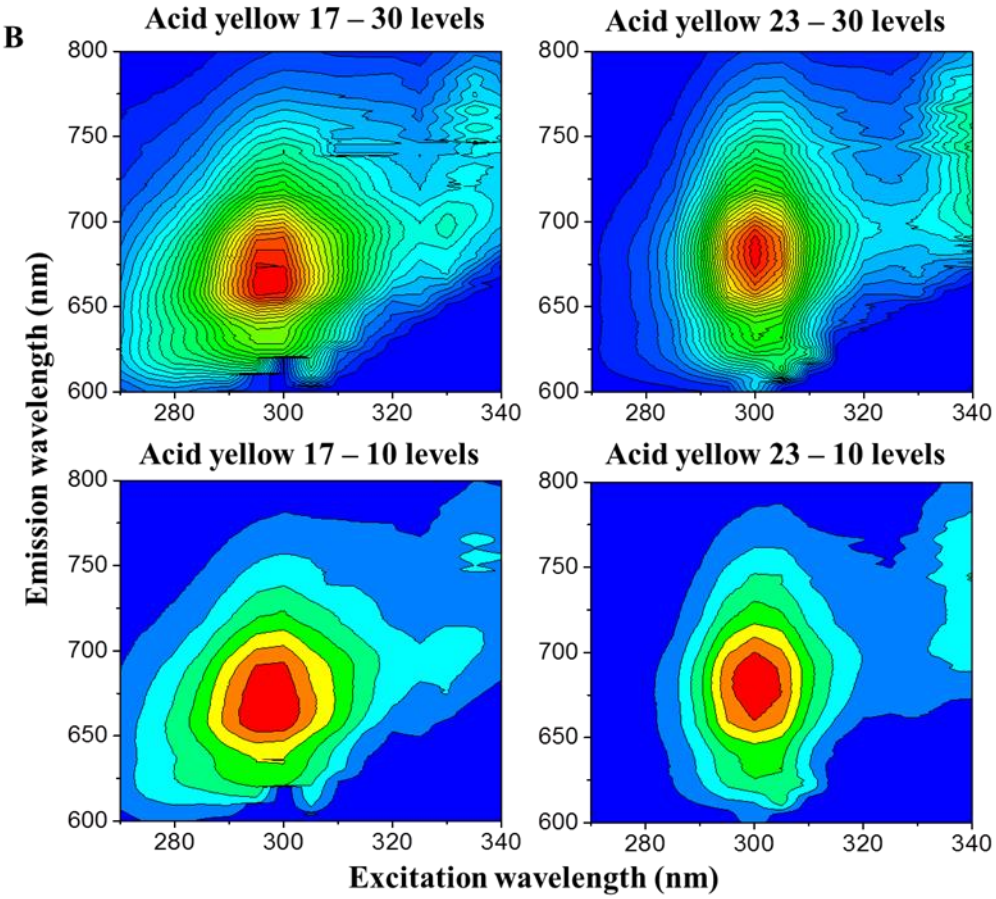

Figure 2.11. Comparison of excitation-emission matrices of acid yellow 17 and acid yellow 23 fiber extracts with different contour levels at excitation wavelength range of 270 to 340 nm and emission wavelength range of 600 to 800 nm

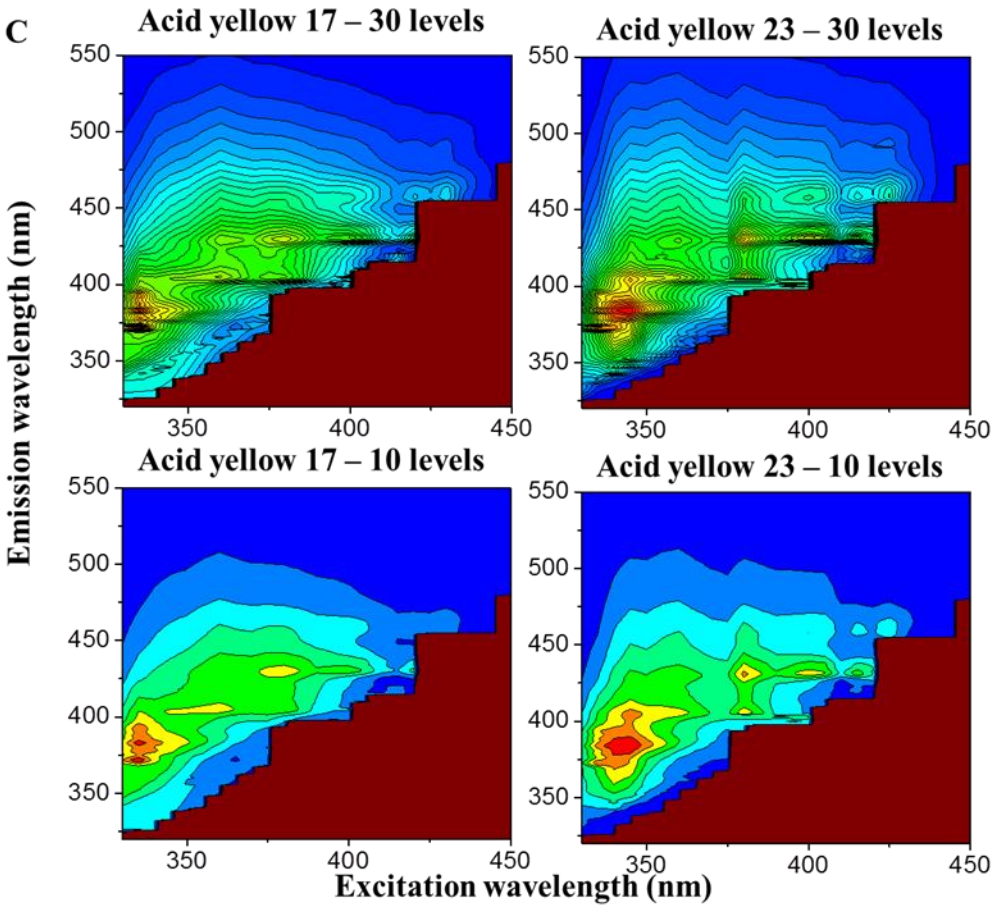

Figure 2.12. Comparison of excitation-emission matrices of acid yellow 17 and acid yellow 23 fiber extracts with different contour levels at excitation wavelength range of 325 to 450 nm and emission wavelength range of 320 to 550 nm

2.10. Conclusions

We have presented the first thorough investigation of the potential of fluorescence spectroscopy for the forensic analysis of fiber extracts. A 1:1 acetonitrile:water (v/v) mixture appears to be a well-suited extracting solvent for the fluorescence of fibers from acetate, polyester, cotton and nylon materials pre-dyed with direct, disperse, basic and acid dyes. The comparison of the fourteen types of fiber extracts showed three distinct groups of excitation and fluorescence profiles. Acetate 154/ Disperse Red 1, Cotton 400/ Direct Blue 1, Polyester 777/Disperse Red 13 and Nylon 361/ Acid Green 27 fibers showed extracts with similar excitation and fluorescence profiles. The same is true for Nylon 361/ Acid Yellow 17 fibers and Polyester 777 fibers pre-dyed with Basic Red 9, Basic Violet 14 and Disperse Blue 56. On the other end, Cotton 400 fibers pre-dyed with Direct Blue 71 and Direct Blue 90, Nylon 361 fibers pre-dyed with Acid Yellow 23, Acid Green 27 and Acid Red 151, Poly-acrylic 864/ Basic Green 4 and Polyester 777/ Disperse Red 4 fibers showed unique excitation and fluorescence spectra. Although the comparison of fibers within the first two groups should benefit from additional selectivity, the different excitation and fluorescence maxima still makes possible their visual discrimination on the basis of spectral profiles. In all cases, the strong fluorescence of 1:1 acetonitrile:water (v/v) extracts made possible the analyses of fibers with 2 mm length.

In all cases, outstanding reproducibility of spectral profiles with minimum variations in fluorescence intensities was observed from individual extracts belonging to adjacent fibers – i.e. single fibers located immediately next to each other –within the same area of cloth - and from single fibers located in four different cloth areas. The comparison of fluorescence chromatograms from extracts of fibers collected from different areas of a cloth confirmed the

reproducibility of individual fluorescence concomitants within the same piece of cloth. In comparison to 2D spectra, EEM appear to be a better data format for forensic fiber comparison. This advantage results from an intrinsic characteristic of EEMs, which is their ability to convolute the contribution of all fluorescence concomitants to the total fluorescence of fiber extracts. The clear differences of EEM contours recorded from fiber extracts of Nylon 361 fibers pre-dyed with Acid Yellow 17 and Acid Yellow 23 provide the foundation to further develop this approach for the forensic comparison of visually indistinguishable fibers.

CHAPTER 3: INSTRUMENTAL SET-UP FOR NON-DESTRUCTIVE ANALYSIS OF TEXTILE FIBERS VIA ROOM-TEMPERATURE FLUORESCENCE SPECTROSCOPY

3.1. Introduction

A few reports exist on the fluorescence spectroscopy for forensic fiber examination. Parker[76] was the first to report on the fluorescence spectra of textile fibers using a microscope interfaced to a spectrophosphorimeter equipped with a chopper arrangement. Only one type of fiber (a dyed woolen fiber) was examined to illustrate the potential of emission microscopy in forensic science. Hartshorne and Laing[50-51, 77] utilized a modified micro-spectrophotometer to record fluorescence spectra from single fibers with the purpose of discriminating fluorescence brighteners and fluorescent red dyestuffs. Because sample excitation was accomplished with band-pass filters, the main limitation of the micro-spectrophotometer was its inability to record excitation spectra and fluorescence spectra as a function of single excitation wavelengths. Despite this instrumental limitation, the authors concluded that - for the examined red dyestuffs and fluorescence brighteners – micro-spectrofluorimetry provided higher fiber discrimination than microscopy and micro-spectrophotometry.

In a recent article, Nakamura and co-workers[78] reported on the nondestructive dye analysis of Shosoin textiles by excitation-emission matrix (EEM) fluorescence spectroscopy. The EEM data formats were recorded directly from the fibers with the aid of a reflectance fiber optic probe and a commercial spectrofluorimeter. Among the five investigated dyestuffs - namely *kihada* yellow, *kariyasu* yellow, *ai* blue, *akane* red and *shikon* purple - the authors[78] were able to distinguish *kihada* yellow and *akane* red. While the distinction of *kariyasu* yellow was impaired by scattering, EEM spectroscopy gave no information about *ai* blue and *shikon* purple.

In this chapter, we describe an instrumental approach with the ability to record excitation and fluorescence spectra, as well as excitation-emission matrixes (EEMs) from single textile fibers. Our approach requires affordable equipment that probably already exists in many forensic science laboratories, namely a basic spectrofluorimeter and an epi- fluorescence microscope. The behavior of both fluorescence intensity and signal-to-background ratio were evaluated as a function of pinhole size, excitation-emission band-pass and fluorophor concentration with the aid of dye standards in the ultraviolet and visible spectral regions. The new instrument was then used to investigate the reproducibility of fluorescence spectra within the length of fiber threats and among fiber threats from the same garment. The fiber extract studies presented in chapter 2 do not provide information on the distribution of fluorescence impurities and/or dyes within the length of fibers. If the distribution of fluorescence impurities and/or dyes within a fiber happens to be heterogeneous, the spectral profiles recorded directly from the fiber might show some dependence with the fiber area probed under the microscope. Possible spectral variations within a fiber might have detrimental implications in the forensic comparison of known and questioned fibers.

3.2.Experimental

3.2.1. Instrumentation

The spectrofluorimeter (FluoroMax-P, Horiba Jobin-Yvon) used in these studies was equipped with a continuous 100 W pulsed xenon lamp emitting broadband illumination from 200 to 2000 nm. Excitation and fluorescence spectra were recorded with two spectrometers holding the same reciprocal linear dispersion (4.2 $nm \cdot mm^{-1}$) and accuracy (±0.5 nm with 0.3 nm

resolution). Both diffraction gratings had the same number of grooves per unit length (1200 grooves·mm^{-1}) and were blazed at 330nm (excitation) and 500nm (emission). A photomultiplier tube (Hamamatsu, model R928) with spectral response from 185 to 650 nm was used for fluorescence detection operating at room temperature in the photon-counting mode. Commercial software (DataMax) was used to computer-control the instrument. All recorded spectra and intensities were un-corrected for instrumental response.

The epi-fluorescence microscope (Olympus BX-51) was connected to the spectrofluorimeter with commercially available fiber optic bundles (Horiba Jobin-Yvon). Excitation and collection efficiency between the fiber optic bundles and the spectrofluorimeter was optimized with a fiber optic platform (Horiba Jobin-Yvon) placed in the sample compartment of the spectrofluorimeter. Figure 3.1 shows a schematic diagram with the main components of the microscope and the fiber optic platform. The two concave mirrors located on the fiber optic platform directed light from the excitation monochromator of the spectrofluorimeter into the excitation bundle and reflected the fluorescence from the emission bundle into the emission monochromator of the spectrofluorimeter.

Excitation and emission radiation were separated with the aid of two 50/50 dichromatic beam splitters, one for the ultraviolet (UV) and the other for the visible (VIS) wavelength range. A turret placed immediately above the microscope objective and aligned with both the excitation and the emission optical paths facilitates the use of either one of the two beam splitters. The turret can accommodate up to six optical components. A pinhole plate was located between the 50/50 beam splitter and the moving mirror that directed fluorescence emission either into to the CCD camera (iDS UI-1450SE-C-HQ USB camera) of the microscope or the emission fiber

bundle of the spectrofluorimeter. The role of the pinhole is to isolate the illuminated area while rejecting light scattered from the sample.

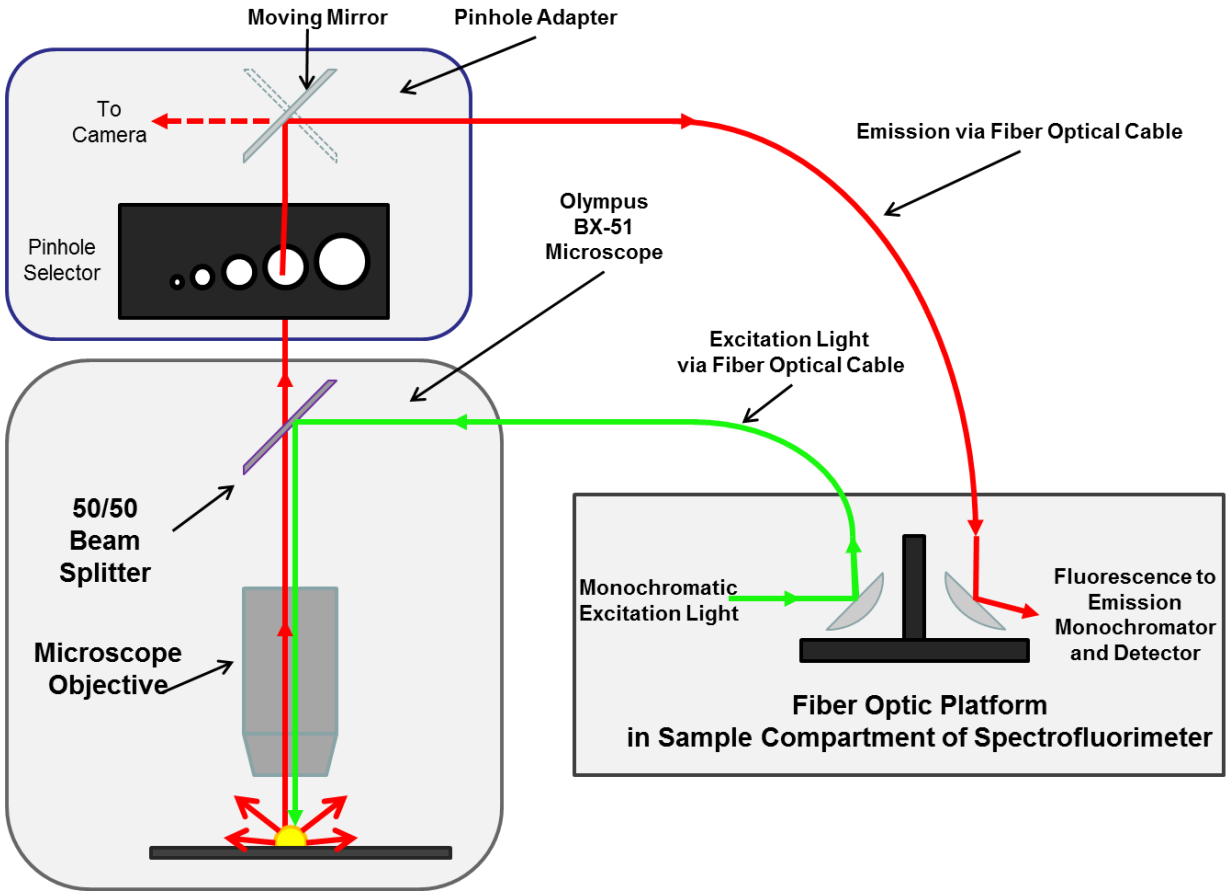

Figure 3.1. Schematic diagram showing microscope connected to fiber optic mount of spectrofluorimeter via fiber optic bundles

3.2.2.Chemicals and supplies

Rhodamine-6G and BPBD-365 dyes were purchased from Exciton. Disperse red 4 powdered dye at reagent grade purity was purchased from Sigma-Aldrich at the highest available purity. HPLC grade methanol was acquired from Fischer scientific. Nano-pure water obtained from a Barnstead nano-pure infinity water purifier was used throughout. OFR-LMU-10x-UVB

and UMPlanFl-10x objectives were acquired from Olympus to use in the UV and visible regions, respectively.

3.3. Results and discussion

3.3.1. Instrumental performance

The initial selection of microscope objectives followed the recommendation of Olympus representatives. Evaluation of instrumental performance was carried out using "standard samples" consisting of sealed capillary tubes (250 micro-meters internal diameter; 3 cm long) filled with micro-litter volumes of dye solutions. The two selected dyes had high fluorescence quantum yields with maximum excitation and fluorescence wavelengths ($\lambda_{ex}/\lambda_{em}$) in the working wavelength ranges of the microscopic objectives (BPBD-365, $\lambda_{ex}/\lambda_{em}$ = 327/373nm and Rodhamine 6G, $\lambda_{ex}/\lambda_{em}$ = 527/561nm). Methanolic solutions of standard dyes were prepared at specified concentrations (27μM solution of Rhodamine-6G and 1.59mM solution of BPBD-365) and diluted with methanol accordingly. The relative positions between the capillary tube and the microscope lens were held constant by placing the capillary within the groove of an in-house built microscope stage plate (see Figure 3.2).

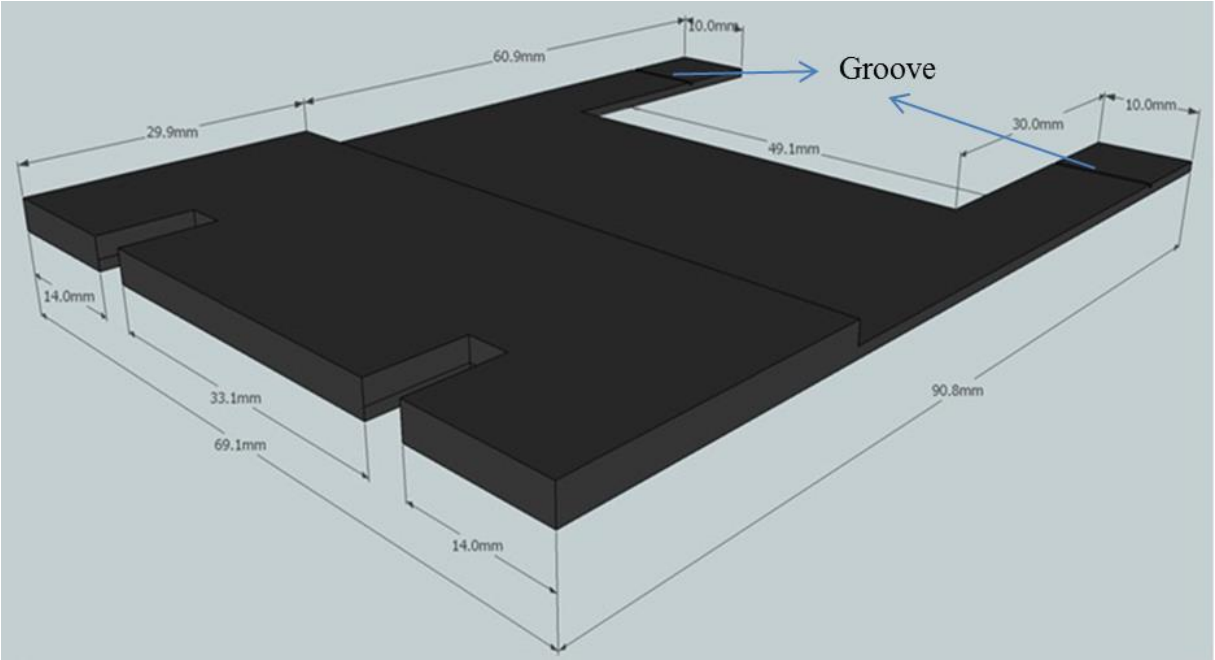

Figure 3.2. 3D-image of an in-house built microscopic stage plate for holding capillary tube

3.3.2. Pinhole size and excitation-emission band-pass.

Figure 3.3 shows images recorded from the visible "standard sample" and a textile fiber thread pre-dyed with Disperse Red 4. The size of the pinhole correlates well to the size of the illuminated area in the sample. The image of the fiber therad was recorded with no pinhole. For size comparison purposes, the small circle located at the center of the thread corresponds to the area of the 100 micro-metter (μm) pinhole diameter.

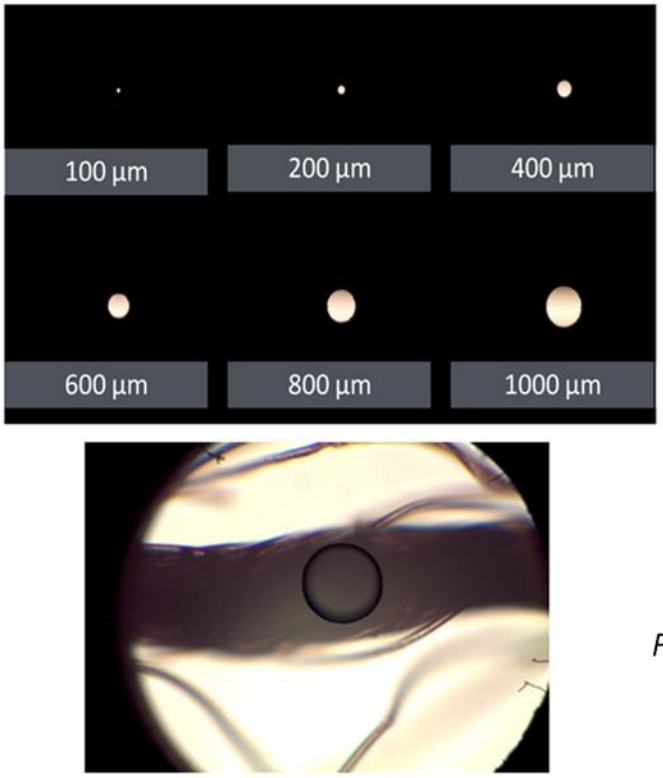

Figure 3.3. Comparison of pinhole sizes using images of a 250 micro-meters internal diameter capillary tube filled with a metnaolic solution of Rhodamine 6G and a Disperse Red 4 fiber thread.

Figure 3.4 overlays several excitation and fluorescence spectra recorded from the visible standard sample. All spectra in "A" were recorded with the same excitation and emission band-pass (5nm). As expected, the intensity of spectra decreases with the size of the pinhole. All spectra in "B" were recorded with the same pinhole diameter but with different excitation and emission band-pass. As expected, the intensity of spectra decreases with the slit-widths of the spectrofluorimeter. The same trend was observed in the ultraviolet spectral region (see Figure 3.5).

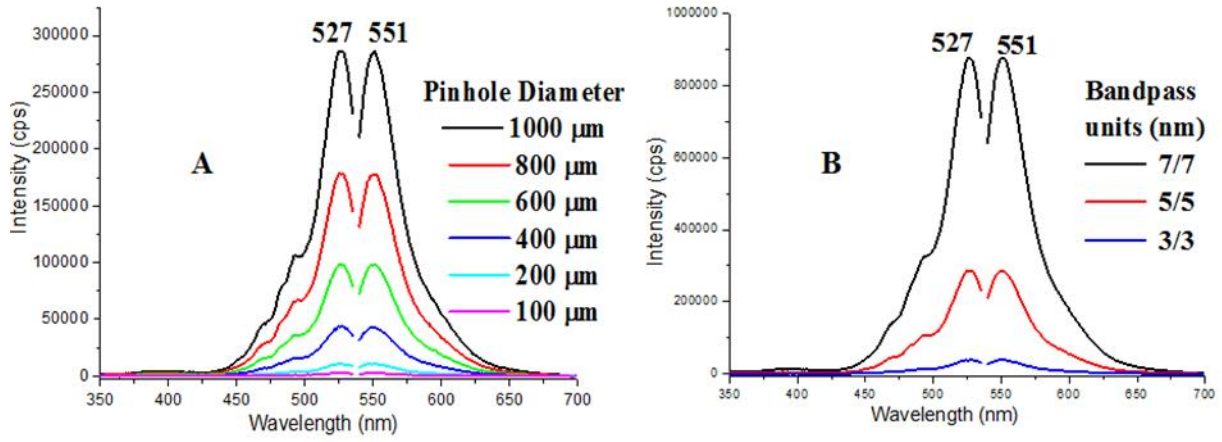

Figure 3.4. Excitation and fluorescence spectra recorded from the visible standard sample. Spectra were recorded at: (A) various pinhole diameters with constant (5nm) excitation and emission band-pass; (B) various excitation/emission bandpass with constant pinhole diameter (1000 micro-metters)

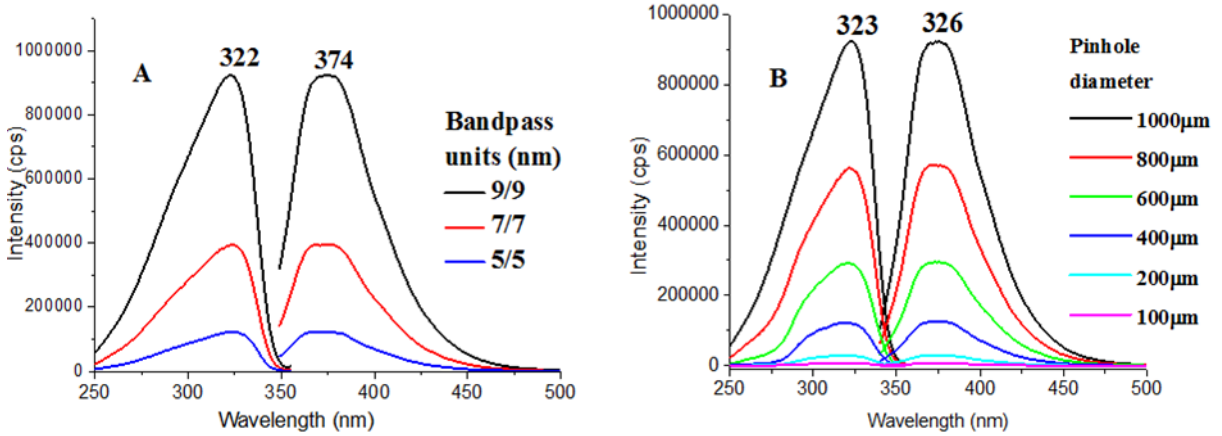

Figure 3.5. Excitation and fluorescence spectra recorded from the ultraviolet standard sample. Spectra were recorded at: (A) various excitation/emission bandpass with constant pinhole diameter (1000 micro-metters); (A) various pinhole diameters with constant (9nm) excitation and emission band-pass

3.3.3. Fluorescence intensity as a function of fluorophor concentration

Figure 3.6 shows the calibration curves recorded from several standard samples prepared with various concentrations of BPBD-365 and Rhodamine 6G in methanol. Each signal plotted in the calibration graph corresponds to the average fluorescence intensity of three individual measurements made from three capillaries filled with the same dye concentration. Blank measurements were made from pure methanol encapsulated in capillary tubes of 250 µm internal diameter.

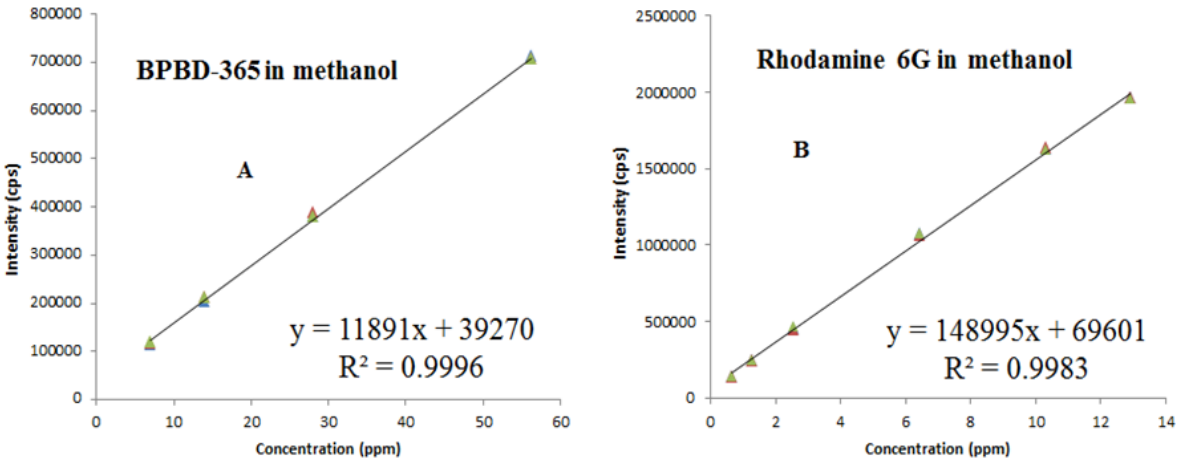

Figure 3.6. Calibration curves of methanolic solutions of A) BPBD-365 recorded at λex/ λem = 310/373nm with 11/11 nm band-pass using 10x-UV objective; B) Rhodamine-6G recorded at λex/ λem = 528/549 nm with 9/9nm bandpass using the 10x-Visible objective.

The same trend was observed with Disperse Red 4 (see Figure 3.7), a reagent dye commonly used in the textile industry. The excellent linear behavior of the calibration curves demonstrates proper instrumental functioning and reproducibility of measurements.

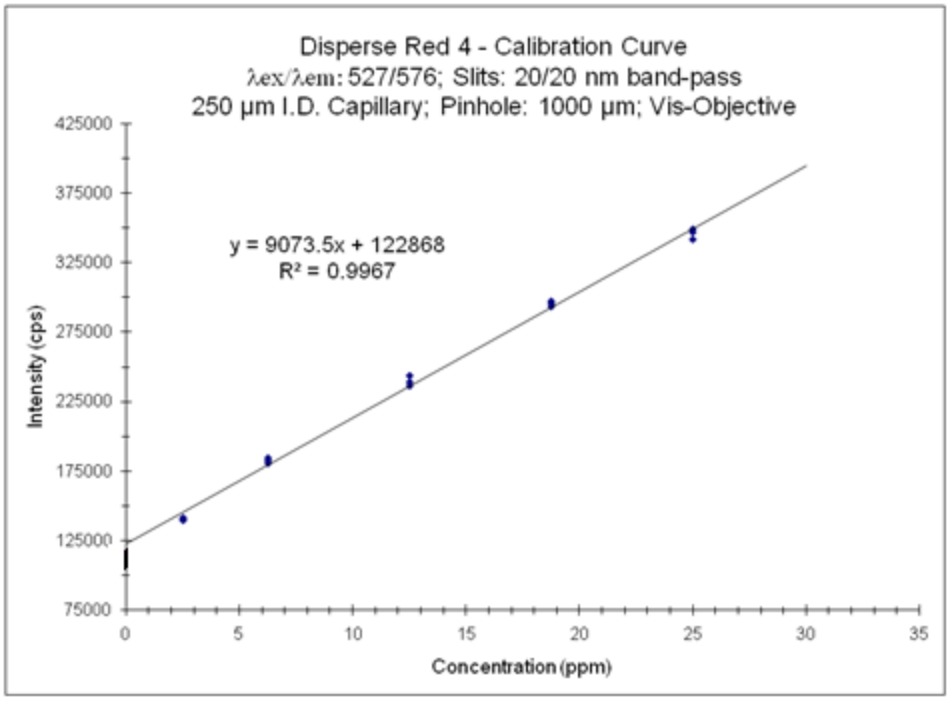

Figure 3.7. Calibration curve of methanolic solution of disperse red 4 recorded at λex/ λem = 509/576 nm with 20/20 nm bandpass using the 10x-Visible objective

3.3.4.Signal-to-background ratio

Figure 3.8 and Figure 3.9 show the general trend we observed on the signal-to-background (S/B) ratio of Disperse Red 4 (visible) and the ultraviolet standard sample (BPDB-365) as a function of excitation/emission band-pass and pinhole size. For any given set of excitation and emission band-pass, the value of the S/B ratio of the visible sample increases with the pinhole size. The same is true for the S/B ratio of the ultraviolet sample when recorded with 100µm and 400µm pinhole sizes. When using the 1000mm pinhole, the fluorescence signals recorded with the 7 and 9nm excitation/emission band-pass have the same intensity. This is the result of the detector's saturation at 9nm excitation/emission band-pass with a 1000 µm pinhole

size. Comparing the trend of the fluorescence signals recorded with 9/9 band-pass (see non-linear trend of blue dots) to those recorded with 3/3nm (see linear trend of green dots), detector saturation with the 9/9 nm band-pass appears to start with the 400µm pinhole. Detector's saturation should be avoided because it would lead to distorted spectra.

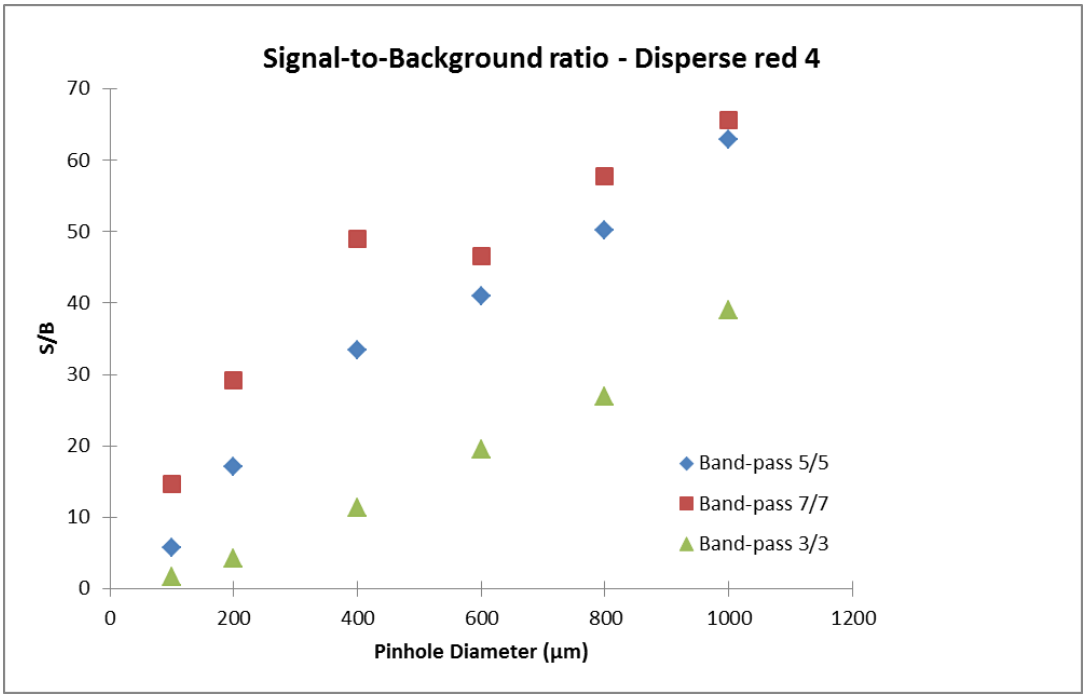

Figure 3.8. Signal-to-background ratio of Disperse Red 4 as a function of pinhole size and excitation/emission band-pass (nm).Plotted ratios correspond to average values of triplicate measurements. Measurements made with the 10x-Visible objective.

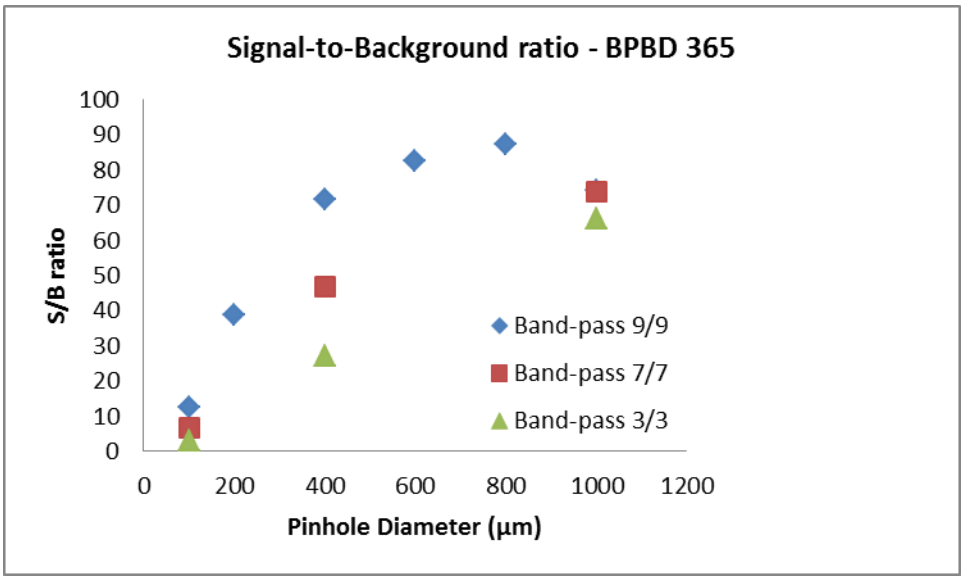

Figure 3.9. Signal-to-background ratio of BPDB-365 as a function of pinhole size and excitation/emission band-pass (nm).Plotted ratios correspond to average values of triplicate measurements. Measurements made with the 10x-UV objective

3.3.5. Spectral Reproducibility within the Length of a Fiber Thread

The investigated fibers were removed from the garments listed in Table 2.1. Threads, 4cm in length, were removed from four different regions of the cloth according to Figure 3.10. Excitation and emission spectra were collected at three different areas of the fiber thread with the aid of the stage plate in Figure 3.2 and fiber holder shown in Figure 3.11. The latter was made in house with the purpose of providing reproducible positioning of fibers under the microscope. It was painted matte black to minimize the measurement of possible reflection and scatter of light. The 3-mm inner diameter holes located at the fiber holder facilitate the reproducible positioning of the microscope objective with respect to the fiber. The reproducible positioning of single fibers with respect to the microscope objective was made possible with the aid of two visible grooves on the back of the fiber holder. Grooves were 4cm apart from each other. Spectra were

collected by placing the microscope objective at three different locations (α, β and γ) within each 3-mm hole.

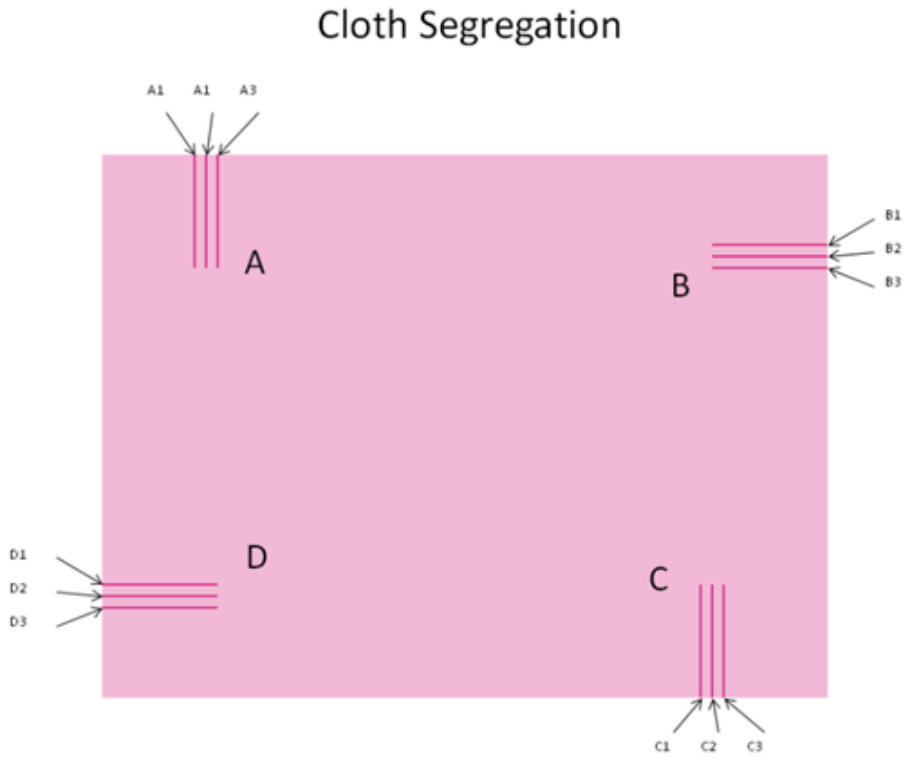

Figure 3.10. Cloth segregation for the analysis of fibers. “Cloth regions” are denoted by capital letters A, B, C and D. Subscripts under capital letters refer to single fiber threats collected within the same cloth area

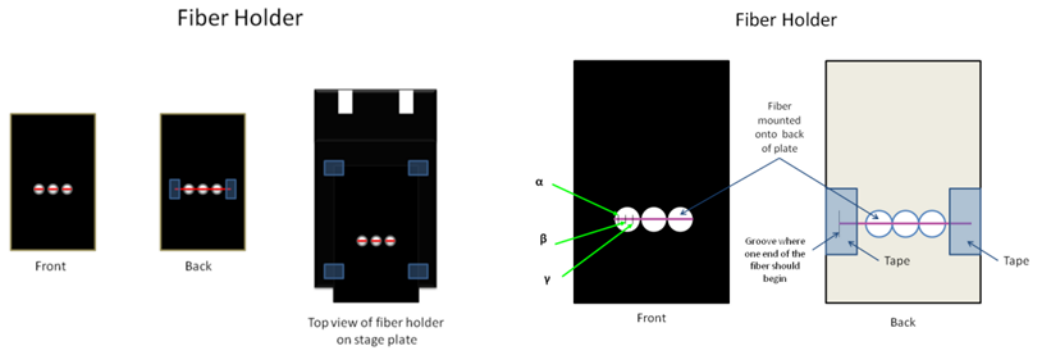

Figure 3.11.Fiber holder for reproducible fiber positioning under the microscope objective

Examples of the type of data we have generated is illustrated with Disperse Red 4. Figure 3.12 presents an overlay of spectra collected from three spots on threads A1, A2 and A3 isolated from region A. Each spectrum in the figure is an average of 9 spectral runs. Similar types of data recorded on threads B1, C1 and D1 is shown in Figure 3.13. Tables embedded in the figures present an average intensity of all the measurements made on each thread with their relative standard deviation values (RSD). The RSD values calculated for these spectra are within the reproducibility of measurements usually observed with fluorescence spectroscopy. Appendix C shows similar type of data from threads of regions B, C and D.

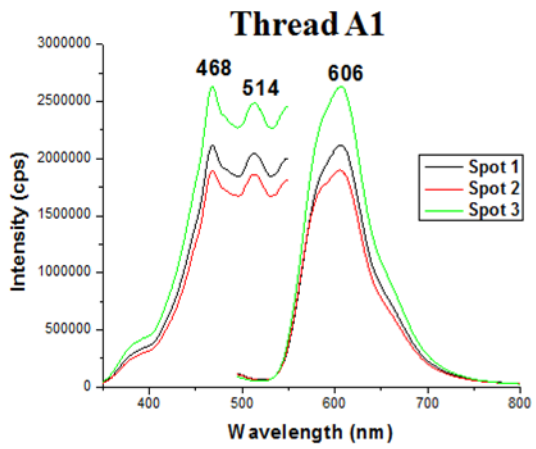

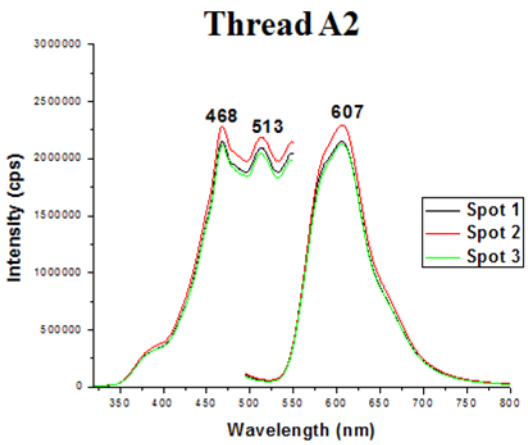

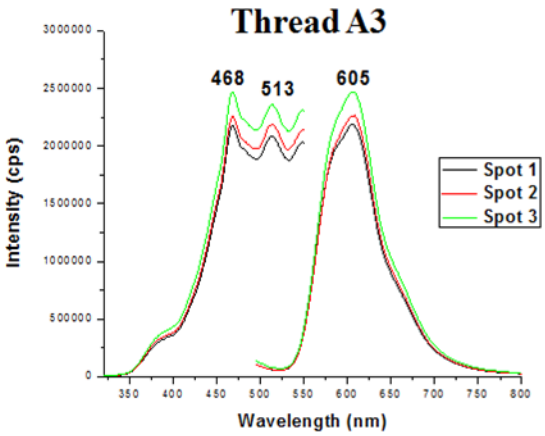

Thread	Average ± S.D*	R.S.D**
A1	2161990 ± 115766	5.35 %
A2	2190603 ± 50014	2.28 %
A3	2305901 ± 82734	3.58 %
A	**2196495 ± 73235**	**3.33 %**

*S.D = Standard deviation
**R.S.D = Relative standard deviation

Figure 3.12. Over lay of spectra collected from different spots on a threads from region A. Spectra were collected with excitation-emission monochromator bandpass of 12 nm under a 1000 µm pinhole diameter

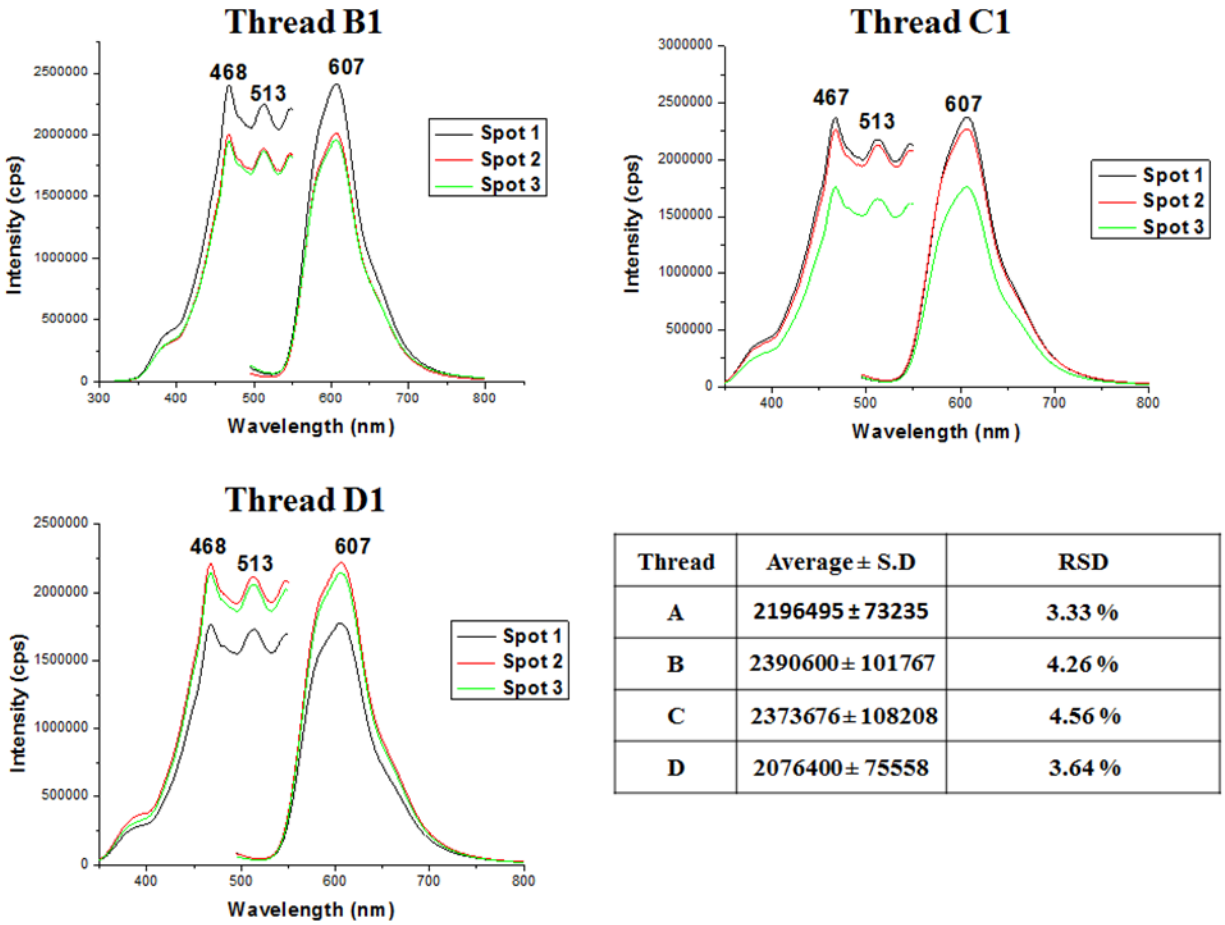

Thread	Average ± S.D	RSD
A	2196495 ± 73235	3.33 %
B	2390600 ± 101767	4.26 %
C	2373676 ± 108208	4.56 %
D	2076400 ± 75558	3.64 %

Figure 3.13. Over lay of spectra collected from different spots on threads from region B, C and D. Spectra were collected with excitation-emission monochromator bandpass of 12 nm under a 1000 µm pinhole diameter

3.4. Conclusion

An instrumental set-up was successfully developed for fluorescence microscopy of fibers. The intensity of fluorescence spectra showed a direct correlation with the microscope pinhole diameter the excitation/emission band-pass of the spectrofluorimeter. A linear correlation was observed between fluorescence intensity and fluorophor concentration. Excellent reproducibility of measurements was obtained in both the ultraviolet and visible spectral regions. Within the linear range of the detector, the value of the S/B ratio increased with the pinhole size. Reproducible spectral profiles were observed along the length of a fiber thread and among threads of the same garment. The possibility to adjust the diameter of the microscope pinhole and the excitation and emission band-pass of the spectrofluorimeter should allow the analyst to record fluorescence data from single fibers. Under this prospective, further evaluation of the S/B ratio as a function of pinhole diameter for sample areas smaller than the projected pinhole areas might prove useful.

CHAPTER 4:EVALUATION OF MICROSCOPE OBJECTIVES FOR NON-DESTRUCTIVE ANALYSIS OF TEXTILE FIBERS

4.1. Introduction

The main goal of this chapter is to evaluate various microscope objectives for collecting fluorescence signal from single fibers. Experiments in Chapter 3 were conducted with 10xUV and 10x-visible objectives. These objectives have relatively low numerical apertures, which limit the amount of emitted light being collected from the fiber. The numerical aperture of an objective provides an indication of the amount of light that the objective can collect i.e. collection efficiency (CE) and can be obtained from the following equation[79]

$$Numerical\ aperture\ (NA) = n(sin\theta)$$

Where, n is the refractive index the medium between objective and the coverslip and θ is half of the angular aperture (A) of the objective (see Figure 4.1).

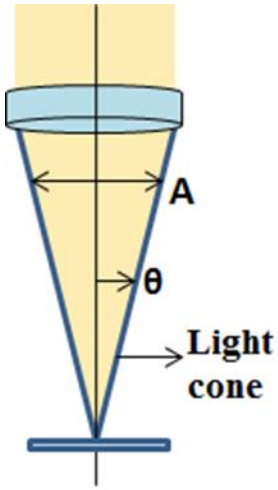

Figure 4.1. Schematic illustrating angular aperture (A) of an objective; θ = A/2

The CE of a microscope objective correlates with its NA via the equation[80]

$$CE = \sin^2[\arcsin(NA/n)/2]$$

In our case, the refractive index of the surrounding medium is approximately 1.

4.2.. Experimental:

4.2.1. Materials:

4.2.1.1. Microscope objectives:

Based on the availability of objectives in our lab, a total of five objectives were chosen for this study. Commercial sources, type of objectives and working ranges of the objectives are provided in the Table 4.1.

Table 4.1. List of microscope objectives evaluated in this study

Objective	**Commercial source**	**Working wavelength range**	**Objective type**	**CE (%)**
LMU-40x-UVB	OFR	UV	Dry	6.7
UPlanSApo-20x/0.75; ∞/0.17/FN26.5	Olympus	Visible	Dry	16.9
UPlanSApo-20x/0.85 Oil; ∞/ - /FN26.5	Olympus	Visible	Oil	9.1
UPlanSApo 40x/0.90	Olympus	Visible	Dry	28.2
UPlanFL N 40x/1.30	Olympus	Visible	Oil	26.2

4.2.1.2. Methods:

The performance of each objective was evaluated recording spectra and measuring the signal-to-background ratio of fibers in Table 2.1. The tested fibers were selected according to their excitation and emission maxima to cover – as best as possible - the entire ultraviolet and visible spectral regions. Fabric samples were received in sealed packages and were stored in dark to prevent contamination and possible deterioration due to exposure to light. Threads and fibers were isolated from the fabric using scissors and tweezers pre-cleaned with methanol. Quartz slides and coverslips were used to hold the fiber samples for experiments in UV-region and for visible region glass slide and cover slips were used. Signal measurements were made at the maximum excitation and emission wavelengths of fibers placed on quartz (ultraviolet measurements) or glass (visible measurements) slides. The maximum wavelengths were obtained from two dimensional spectra recorded either in the ultraviolet or visible regions. Background signals were collected at the maximum wavelengths of fibers placing a quartz (ultraviolet measurements) or glass (visible measurements) slide under the microscope objective.

4.3. Results and Discussion:

4.3.1. Evaluation of UV objectives:

A full description of the two UV objectives tested in these studies is provided in Table 4.2.

Table 4.2.Comparison of 10x- and 40x- UV objectives

Objective	Working distance	Numerical aperture	Theoretical collection efficiency
LMU-UVB 10x	15mm	0.25	1.6%
LMU-UVB 40x	1mm	0.50	6.7%

The type of results we obtained with the UV objectives is summarized in Figure 4.2-Figure 4.4. Fibers pre-dyed with basic red 9 are among the weakest fluorescence fibers in Table 2.1. Using the 10x-UV objective, the diameter of the circular area of fiber probed under the microscope with a 200μm pinhole approximately matches the width of the fiber (see top right image in Figure 4.2). With this pinhole size diameter, the spectral features of the fiber are indistinguishable from the spectral features of the background (see top left image in Figure 4.2). As shown at the bottom spectra in Figure 4.2, the use of larger pinholes sizes increases the intensity of both the fluorescence signal (S) from the fiber and the background (B) signal. S increases with the size of the pinhole because of the excitation of larger areas of fiber. Similarly, the background signal increases as a result of the co-irradiation of larger areas of microscope slide. The variation of S and B as a function of pinhole size is shown in Figure 4.3. Because the enhancement rate of S as a function of pinhole size diameter is larger than the enhancement rate of B, the spectral features recorded from the fiber improve as the pinhole size diameter increases.

Although the best spectral features from the fiber are recorded with an open pinhole, examination of the bottom left spectra in Figure 4.2 still shows a strong background contribution to the fluorescence spectrum of the fiber.

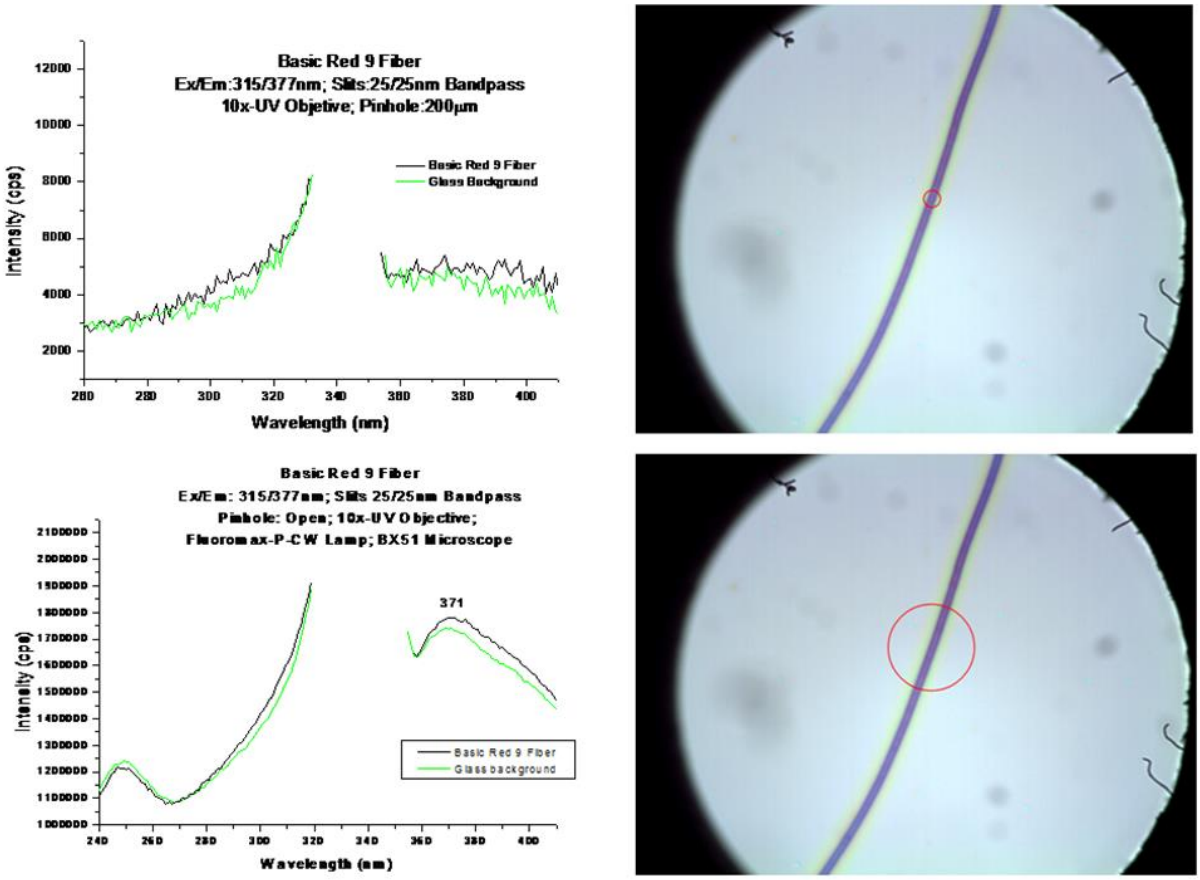

Figure 4.2. Data recorded from a single fiber pre-dyed with Basic Red 9 using a 10XUV microscope objective. Left: Excitation and fluorescence spectra recorded with a 200 µm pinhole size diameter (top) and open pinhole (bottom). Right: images of single fiber. The red circle represents the area of fiber probed with a 200 µm (top) and a 1000 µm (bottom) pinhole size diameter

Pinhole (µm)	Signal (S, cps)	Background (B, cps)	S-B (cps)
200	5383	4625	758
400	19619	17450	2169
600	41480	39800	1680
800	74050	62810	11240
1000	112970	99280	13690
Open	1800000	1700000	100000

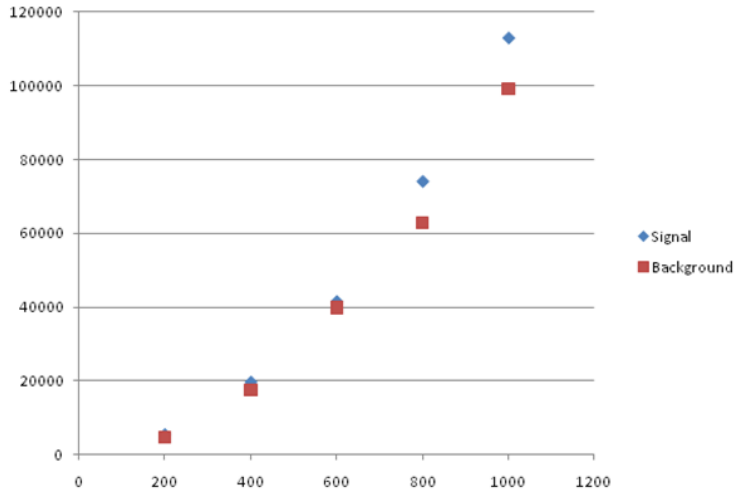

Figure 4.3. Data recorded from a single fiber pre-dyed with Basic Red 9 using a 10XUV microscope objective. Table at the top summaries the signal (S) and the background (B) intensities recorded at the maximum excitation and fluorescence wavelengths of the fiber. The graph plots the S and B values as a function of pinhole diameter (200-1000µm)

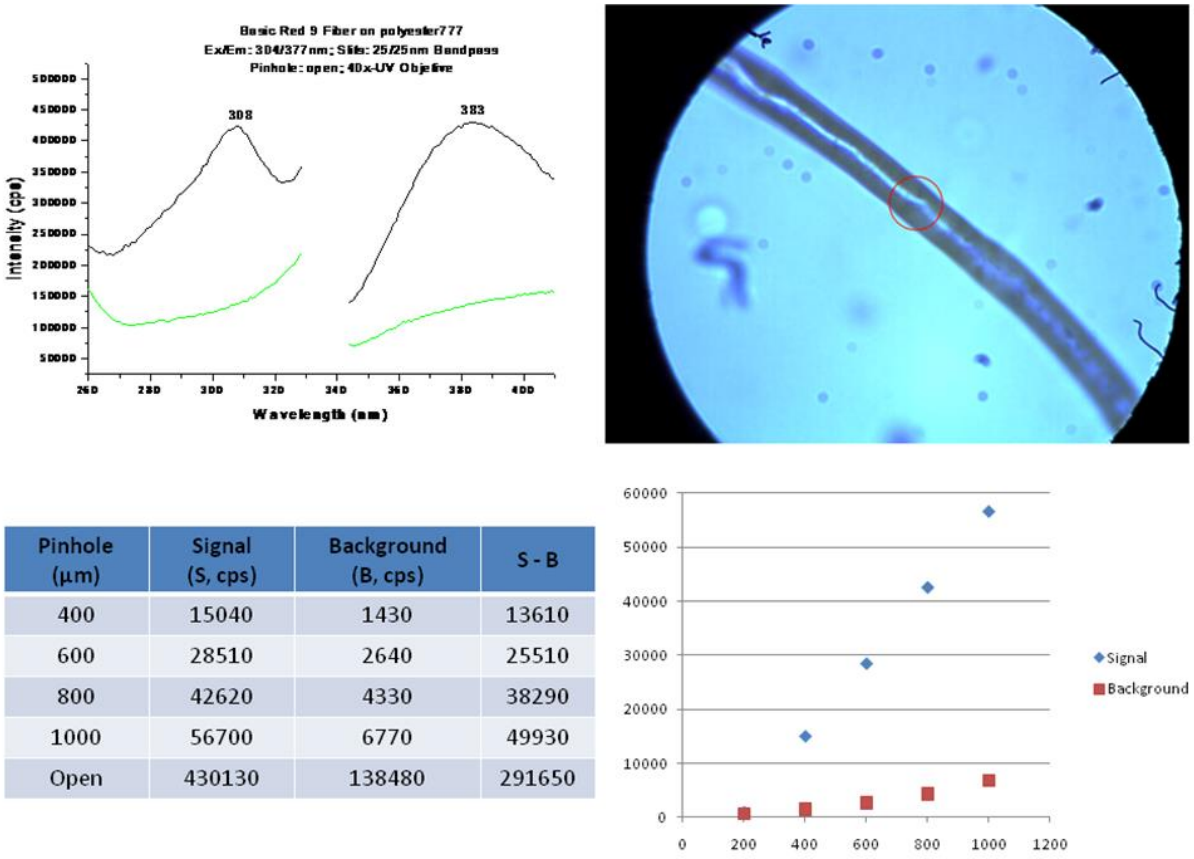

Pinhole (µm)	Signal (S, cps)	Background (B, cps)	S - B
400	15040	1430	13610
600	28510	2640	25510
800	42620	4330	38290
1000	56700	6770	49930
Open	430130	138480	291650

Figure 4.4. Data recorded from a single fiber pre-dyed with basic red 9 using a 40XUV microscope objective. Top Left: Excitation and fluorescence spectra recorded with the open pinhole. Top Right: image of single fiber. The red circle represents the area of fiber probed with a 600µm pinhole size diameter. Table at the bottom summaries the signal (S) and the background (B) intensities recorded at the maximum excitation and fluorescence wavelengths of the fiber

Figure 4.4 reports data recorded from the same fiber but with the 40x-UV objective. The fiber spectra collected with an open pinhole present distinct features when compared to the background spectra. When compared to the enhancement of B, the enhancement of S as a function of pinhole diameter occurs at a faster rate with the 40x-UV objective than with the 10x-UV objective (compare graphs in Figure 4.3 and Figure 4.4). Opposite to the 10x-UV objective, the use of an open pinhole with the 40x-UV objective makes possible to differentiate the spectral features of the fiber from background emission.

Figure 4.5 compares signals and background intensities of the investigated fibers using 10x-UV and 40x-UV objectives. An open pinhole was employed with both objectives.

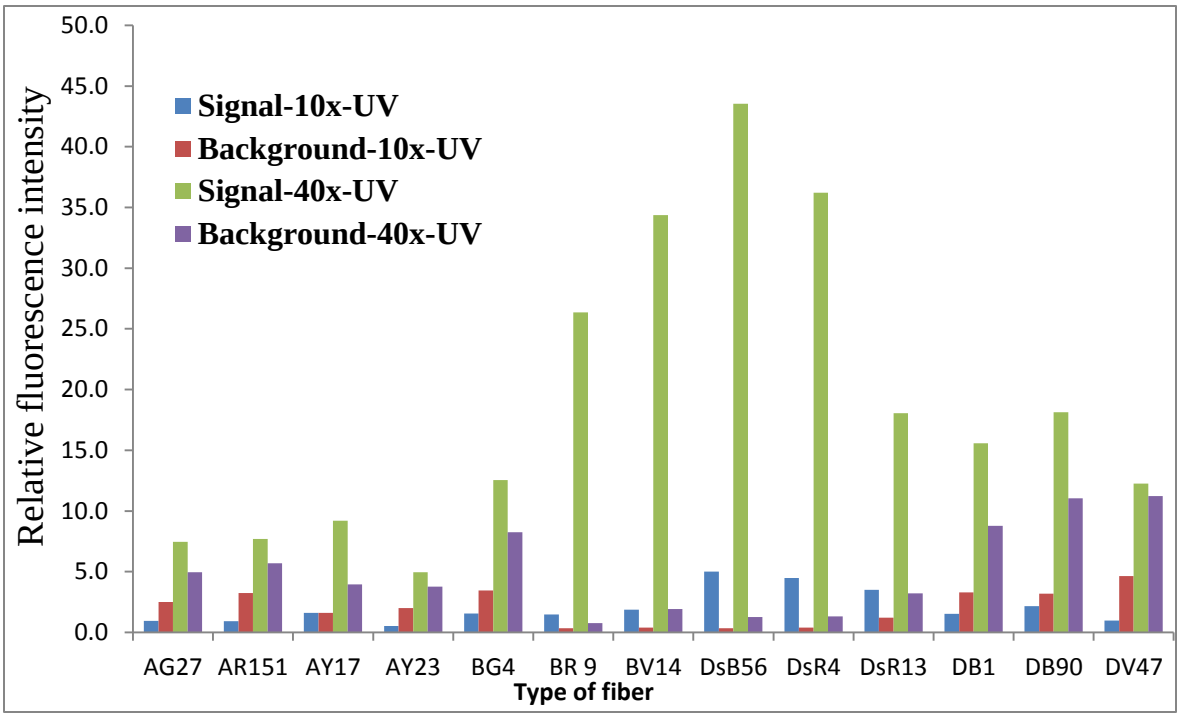

Figure 4.5. Comparison of intensities of signal and noise at λ_{max} recorded using 10x- and 40x- UV objectives

All S and B intensities recorded with the 40x-UV objective are higher than those recorded with 10x-UV objective. This fact results in part from the better CE (~6.5x) of the 40x-UV objective over the 10x-UV objective (CE ~ 1%). In some cases, the B values recorded with 10x-UV objective are higher than the S value. The same is not true for the 40XUV objective, which shows higher S than B values in all cases. This is probably due to the field of view of each objective. With the 10x-UV objective, the open pinhole diameter corresponds to a 600μm (0.6mm) diameter field of view. With the 40x-UV objective, the open pinhole diameter corresponds to a 150μm (0.15mm) diameter field of view. It should be noted that both fields of view make possible to analyze fibers considerably shorter than the ~2mm fiber length typically encountered in crime scenes.

4.3.2.. Evaluation of visible objectives:

Table 4.3 summarizes the specifications of the visible objectives tested in these studies.

Table 4.3. Specifications of visible microscope objectives evaluated in this study

Objective*	**Working distance**	**NA**	**CE (%)**
UPlanSApo 20x	0.60 mm	0.75	16.93
UPlanSApo 20x Oil	0.17 mm	0.85	9.08
UPlanSApo 40x	0.18 mm	0.90	28.2
UPlanFl 40x Oil	0.20 mm	1.30	26.2

* PlanSApo = lens corrected for curvature of field, chromatic and spherical aberrations.

Table 4.4 and Table 4.5 summarize the results obtained with 20x-Vis and 40x-Vis objectives, respectively. Comparison of values in Table 4.4 at all emission wavelengths shows better S/B with the oil immersion objective. Although it has a low numerical aperture than the

20x- dry objective, the oil immersion objective presents the advantage of minimizing radiation losses at optical interfaces. The same trend was not observed with 40x-Vis objectives. The S/B ratio appears to depend on the wavelength of excitation and fluorescence emission. This might be the result of differences on the type of lenses. The 40x-dry objective is an apochromatic lens and 40x-oil immersion objective is a fluorite type. Fluorite lenses are corrected for aberrations only at red and blue wavelengths whereas apochromatic lenses are corrected at blue, green and red wavelengths of light.

Table 4.4. Signal-to-background ratios for 20x- dry and 20x- oil visible objectives

Type of fiber	**λ_{ex}^{*}(nm)**	**λ_{em}^{*}(nm)**	**20x-Dry**			**20x-Oil**		
			S	**B**	**S/B**	**S**	**B**	**S/B**
Acid green 27	582	713	1.12×10^{6}	5.0×10^{5}	2.21	1.65×10^{6}	4.99×10^{5}	3.31
Acid yellow 17	465	547	1.65×10^{6}	2.81×0^{5}	5.88	1.69×10^{6}	2.45×10^{5}	6.91
Basic green 4	617	699	9.22×10^{5}	$6.00E+0^{4}$	15.37	1.32×10^{6}	3.20×10^{4}	41.29
Direct blue 1	585	714	1.47×10^{6}	9.39×10^{4}	15.65	2.08×10^{6}	9.80×10^{4}	21.22
Disperse blue 56	586	675	9.57×10^{5}	9.61×10^{4}	9.96	1.89×10^{6}	1.07×10^{5}	17.65
Disperse red 4	467	605	1.26×10^{6}	7.30×10^{3}	172.53	1.46×10^{6}	4.55×10^{3}	320.88

λ_{ex}^{*} = Maximum excitation wavelength

λ_{em}^{*} = Maximum emission wavelength

Table 4.5. Signal-to-background ratios for 40x- dry and 40x- oil visible objectives

Type of fiber	**λ_{ex} (nm)**	**λ_{em} (nm)**	**40x-Dry**			**40x-Oil**		
			S	**B**	**S/B**	**S**	**B**	**S/B**
Acid green 27	582	713	7.20 x 105	1.86×10^5	3.86	1.32×10^6	3.38×10^5	3.92
Acid yellow 17	465	547	6.04×10^5	8.16×10^4	7.41	1.58×10^6	6.26×10^5	2.53
Basic green 4	617	699	1.01 x 106	4.18×10^4	24.25	2.21×10^6	4.87×10^4	45.44
Direct blue 1	585	714	1.21 x 106	2.52×10^4	48.03	1.80×10^6	1.57×10^5	11.42
Disperse blue 56	586	675	7.95 x 105	4.44×10^4	17.92	1.15×10^6	1.89×10^5	6.06
Disperse red 4	467	605	6.45 x 105	5.32×10^3	121.21	5.18×10^5	3.52×10^3	147.13

λ_{ex}^{*} = Maximum excitation wavelength

λ_{em}^{*} = Maximum emission wavelength

4.4. Conclusions:

Two UV objectives were tested for the analysis of single fibers. Based on the better results we observed with all the investigated fibers, all future studies in the ultraviolet region were carried with the 40x-UV objective. Between the 20x objectives tested in the visible region, the best results were observed with the 20x-oil immersion objective. The S/B with the 40x objectives showed dependence on the wavelength of emission. The best results alternated between dry and oil objectives. The best objective for each type of fiber in the visible region is listed in Table 4.6. Among these three objectives, the main deciding factor in favor of the 40x-visible dry objective was the fact that the dry objective avoids fiber immersion a potentially extracting medium that could remove fluorescence impurities from the fiber.

Table 4.6. Microscope objective that provided the best S/B ration in the visible spectral range

Type of fiber	**Excitation/emission maximum (nm)**	**Type of objective**
Acid green 27	582/713	40x-oil
Acid yellow 17	465/547	40x-dry
Basic green 4	617/699	40x-oil
Direct blue 1	585/714	40x-dry
Disperse blue 56	586/675	40x-dry
Disperse red 4	467/605	20x-oil

CHAPTER 5: EXCITATION AND FLUORESCENCE SPECTRA RECORDED FROM SINGLE FIBERS

This chapter presents a systematic study of the fluorescence spectral profiles recorded from eleven types of fibers listed in Table 2.1.

5.1. Excitation-fluorescence spectra of single fibers in UV-region:

According to the type of garment, fibers in Table 2.1 can be divided into four types, namely nylon 361, cotton 400, poly-acrylic 864 and polyester 777 fibers. Nylon 361, cotton 400 and poly-acrylic 864 did not show fluorescence in the UV-region. Spectra recorded from these three types of pre-dyed and un-dyed fibers showed no distinct features or intensity differences from that of the background. Considering the fact that many of the studied dyes showed fluorescence in liquid solutions, the lack of fluorescence emission in their respective pre-dyed fibers can be attributed to quenching effects occurring within the fiber. Pre-dyed and un-dyed polyester 777 fibers, on the other hand, presented spectral features considerably different from background emission. Irrespective of the dye present on the fiber, all polyester 777 fibers presented similar spectra with maximum of excitation at ~305nm and maximum of emission at ~375 nm. This fact suggests that observed fluorescence results from the major contribution of the garment itself (polyester 777). Excluding basic violet 14 fibers, excitation and fluorescence spectra of all pre-dyed polyester 777 fibers showed lower fluorescence intensity than un-dyed fibers. This phenomenon arises likely because the dye present on the fiber absorbs part of the excitation reaching the fiber and the fluorescence emitted by polyester 777. All reagent dyes in liquid solutions presented absorption within the excitation and emission ranges of polyester 777.

Basic violet 14 fibers exhibited similar fluorescence intensity as that of un-dyed fibers. Typical spectra are shown in Figure 5.1. The entire set of spectra are gathered in appendix D.

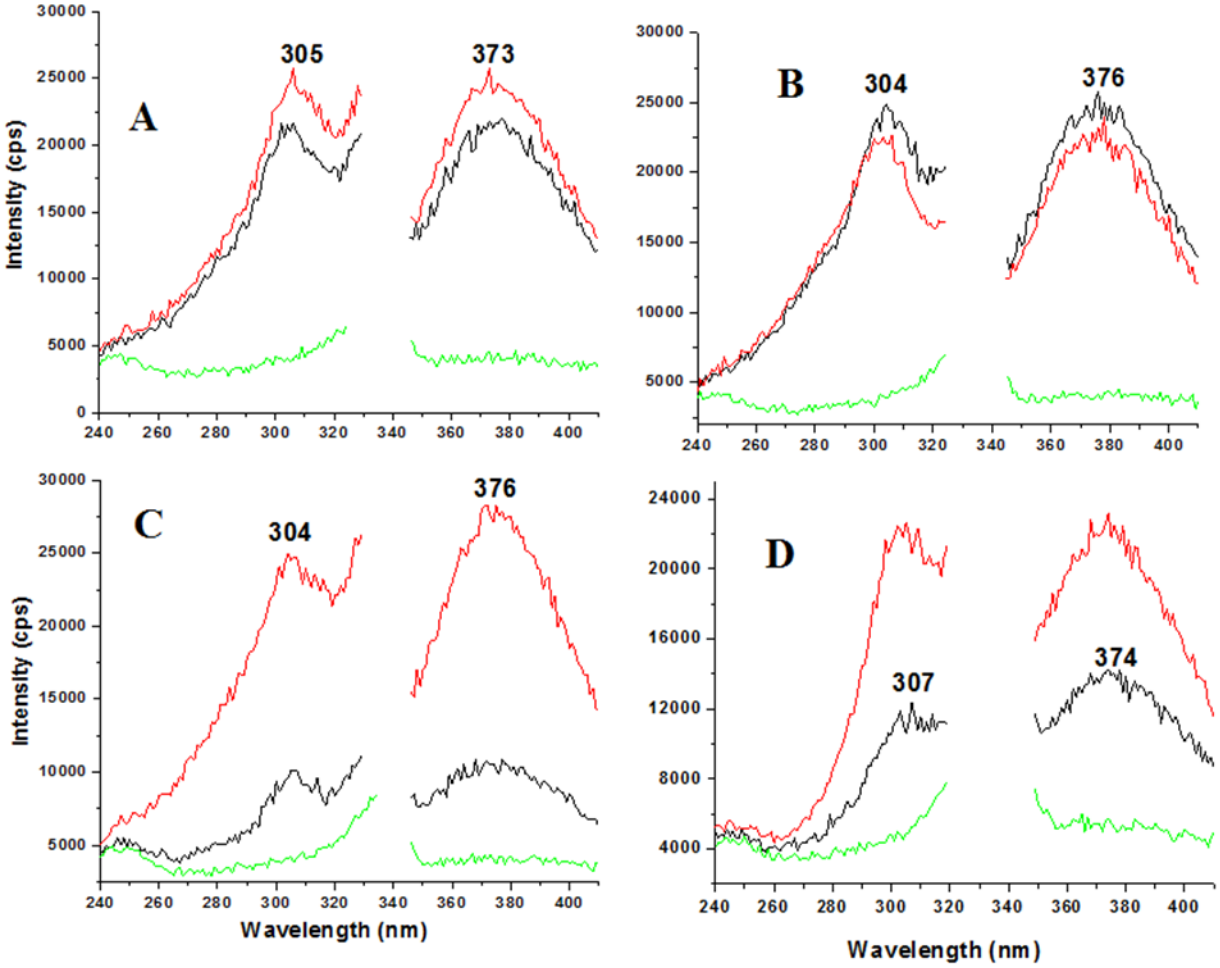

Figure 5.1. Overlay of excitation-emission spectra of background (___), undyed polyester 777 fibers (___) and polyester 777 fibers pre-dyed (___) with A) Basic red 9; B) Basic violet 14; C) Disperse red 13; D) Disperse red 4.

5.2. Excitation-fluorescence spectra of fibers in visible region:

5.2.1.Nylon 361 fibers:

Unlike in the UV-region, un-dyed nylon 361 fibers exhibited fluorescence in the visible region of the spectrum. Acid green 27 and acid yellow 17 fibers showed fluorescence spectral profiles distinctly different than that of un-dyed fibers. Spectra profiles recorded from acid yellow 23 fibers were similar and less intense to that of un-dyed fibers, suggesting that the fluorescence of the un-dyed fiber is a major contributor to the total fluorescence of the pre-dyed fiber. A similar statement can be made for pre-dyed fibers with acid red 151. The main difference between these yellow 23 and acid red 151 fibers is that the fluorescence of acid yellow 23 fibers was slightly higher than the background emission. The fluorescence from red 151 fibers was almost identical to background emission. Their excitation and emission spectra are shown in Figure 5.2.

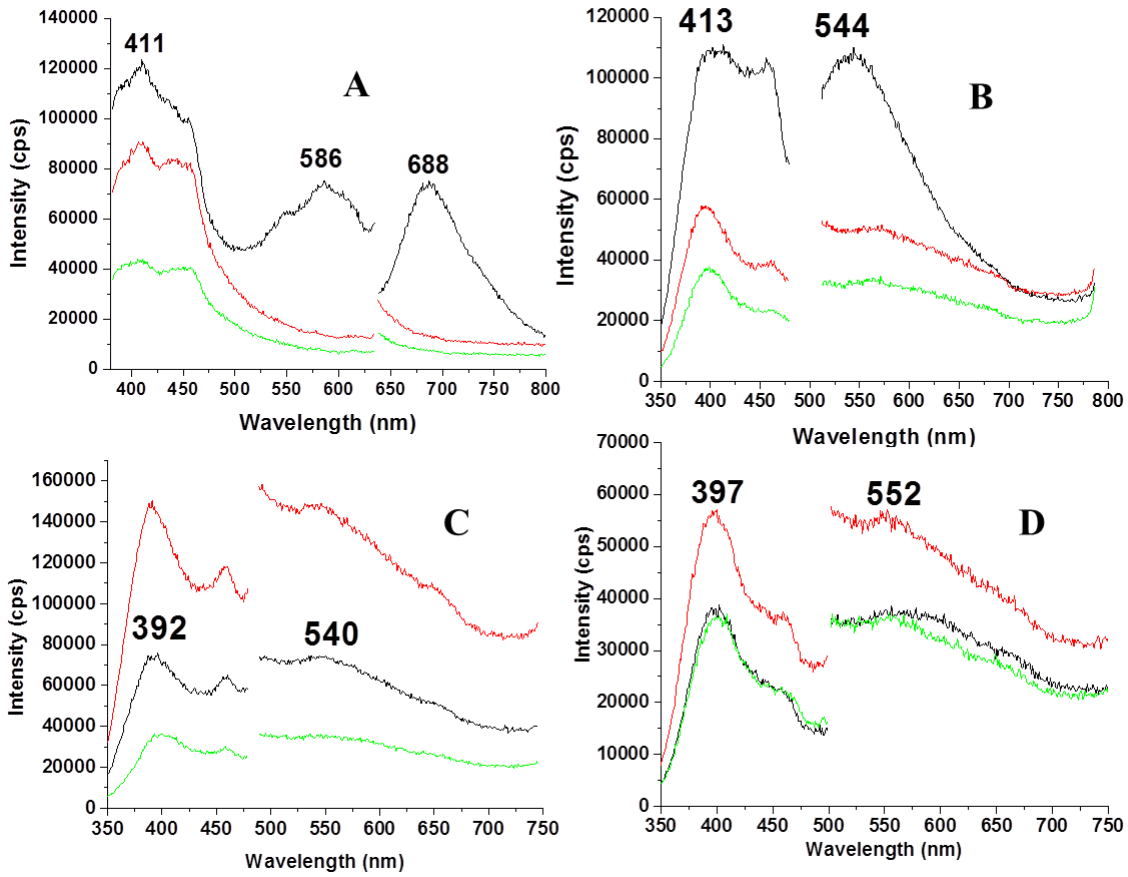

Figure 5.2. Overlay of excitation-emission spectra of background (___), undyed nylon 361 fibers (___) and nylon 361 fibers pre-dyed (___) with A) Acid green 27; B) Acid yellow 17; C) Acid yellow 23; D) Acid red 151

5.2.2.Cotton 400 fibers:

Pre-dyed and undyed cotton 400 fibers exhibited fluorescence in visible spectral region. Their spectral profiles are shown in Figure 5.3. Irrespective of the dye present on the fiber, pre-dyed cotton 400 fibers exhibited similar spectral profiles to that of the un-dyed material. Apparently, the fluorescence recorded from fibers pre-dyed with direct blue 1 or direct blue 90 is mainly due to the emission of cotton 400.

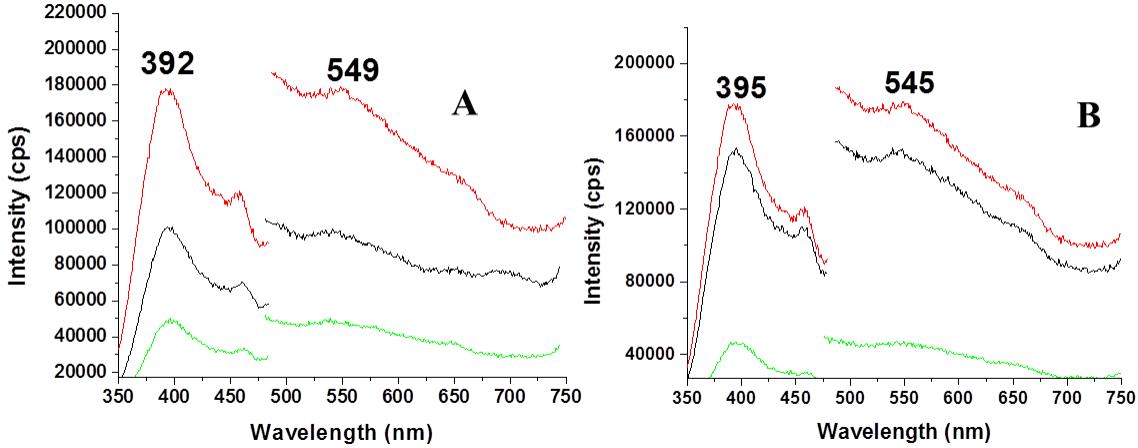

Figure 5.3. Overlay of excitation-emission spectra of background (___), undyed cotton 400 fibers (___) and cotton 400 fibers pre-dyed (___) with A) direct blue 1 (λ_{ex}/ λ_{em}=397/548nm) and direct blue 90 (λ_{ex}/ λ_{em}=397/548nm) reagent dyes

5.2.3. Poly-acrylic 864 fibers:

Excitation and fluorescence spectra of poly-acrylic 864 fibers pre-dyed with basic green 4 are shown in Figure 5.4. The excitation spectrum of pre-dyed fibers present two maximum peaks at 420 nm and 615 nm. Upon excitation at 615nm, the fluorescence contribution of the un-dyed garment is negligible. This fact suggests that the excitation peak at 615 nm and emission peak at 670 nm is likely from the dye present on the fiber.

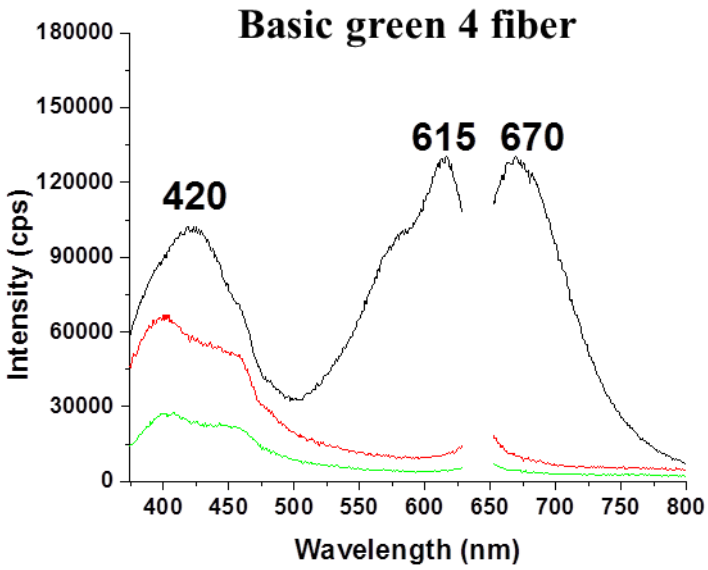

Figure 5.4. Overlay of excitation-emission spectra of background (___), undyed poly-acrylic 864 fiber (___) and poly-acrylic 864 fiber pre-dyed (___) with basic green 4 reagent dye. Emission spectra recorded upon excitation at 615nm.

5.2.4. Polyester 777 fibers:

Excitation and fluorescence spectra recorded on un-dyed and pre-dyed polyester 777 fibers are presented in Figure 5.5. The intensity of the spectral profile recorded form fibers pre-dyed with disperse red 13 is considerably lower to that of the un-dyed fiber. Synergistic processes due to the presence of the dye probably cause quenching of the fluorescence emitted by polyester

777. Disperse red 4 fibers exhibited strong fluorescence with negligible contribution from the garment material. Similarities in the spectral features of disperse red 4 fibers and the reagent dye solution (see appendix E-11B) discloses major fluorescence contribution of dye to the total fluorescence spectrum of the dyed fiber.

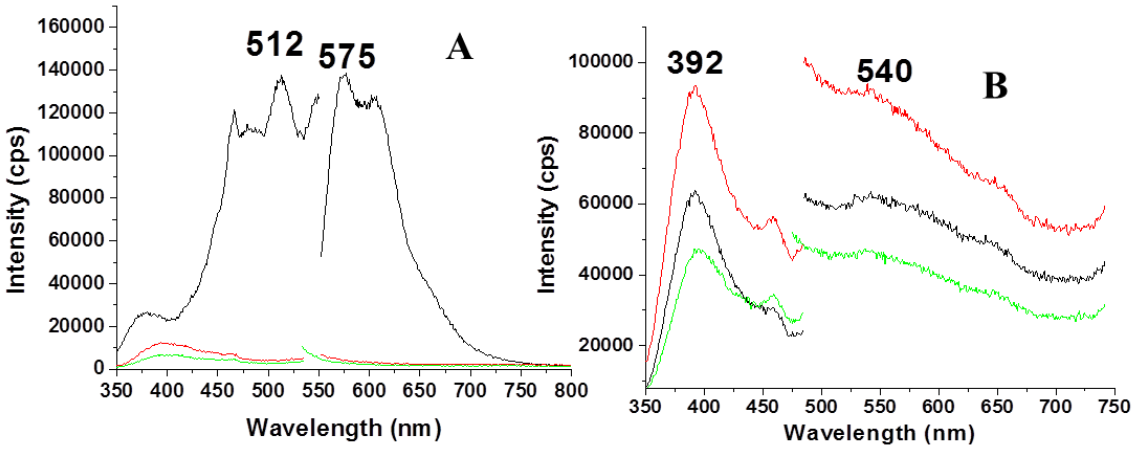

Figure 5.5. Overlay of excitation-emission spectra of background (___), undyed nylon 361 fibers (___) and nylon 361 fibers pre-dyed (___) with A) Disperse red 4 ($\lambda_{ex}/\lambda_{em}$=513/575 nm); B) Disperse red 13 ($\lambda_{ex}/\lambda_{em}$=397/548 nm)

5.3.Conclusions:

Comparison of spectral data recorded within the ultraviolet and visible regions shows that most of the studied fibers present fluorescence within the visible spectral region. With the exception of fibers pre-dyed with acid green 27 and disperse red 4, comparison of the fluorescence characteristics of pre-dyed fibers to those recorded form their respective dye reagents in liquid solutions (see chapter 2 and appendix E) show that a straightforward correlation is not possible. Spectral differences likely arise from the fluorescence contribution of the fiber material and/or synergistic effects between the dye-reagent and the fiber material.

Based on the spectral characteristics obtained from single fibers in visible region, pre-dyed fibers can be classified into 4 types. Type I include fibers that do no present fluorescence. Nylon 361 fibers pre-dyed with acid red 151 belong to this type. Spectra obtained from these dyed fibers are similar in intensity with that of background. Acid yellow 23, direct blue 1, direct blue 90 and disperse red 13 fibers belong to type II, which include fibers that show fluorescence predominantly from the fiber material (nylon 361, polyester 777 or cotton 400) with negligible contribution from the dye. Type III fibers include fibers pre-dyed with acid yellow 17 and basic green 4. Although these dye reagents are the main contributors to the total fluorescence of the fibers, their spectral profiles in liquid solutions do not match the spectral profiles of the pre-dyed fibers. Type IV fibers include fibers pre-dyed with acid green 27 and disperse red 4. Their spectral profiles match those form the dye reagents in liquid solutions.

Figure 5.6 summarizes the spectral features of the pre-dyed fibers investigated in this chapter. With the exception of acid red 151 fibers, all the other fibers showed excitation and fluorescence spectra with higher intensities than background emission. The similarities among the spectral profiles of different types of fibers challenge the use of this methodology for forensic purposes. However, it should be noted that all spectra in Figure 5.6 were recorded at the maximum excitation and emission wavelengths of the fibers. Unlike EEM data formats, two-dimensional spectra do not take advantage of the total fluorescence of the sample.

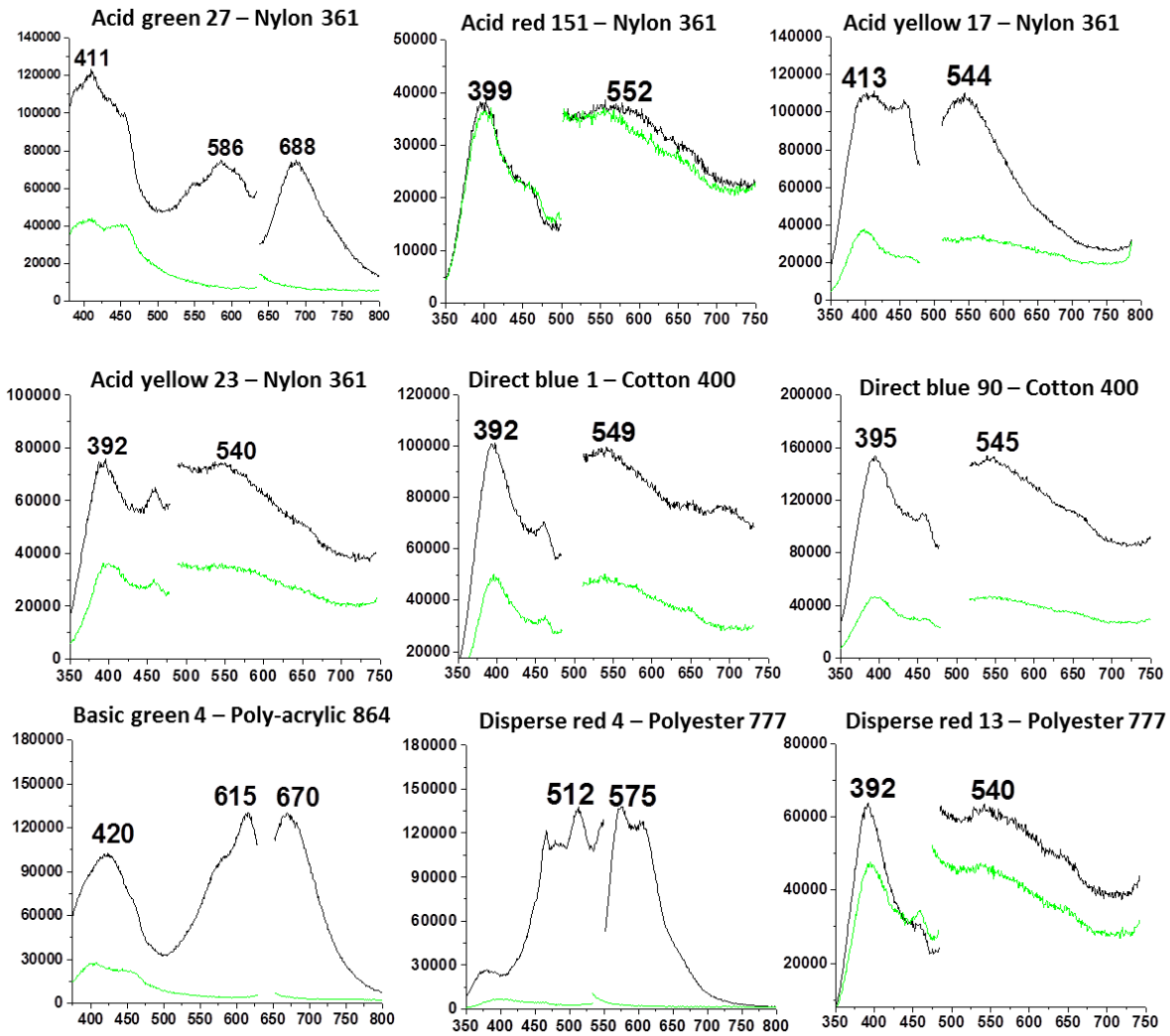

Figure 5.6. Overlay of excitation-emission spectra recorded from background (___) and pre-dyed single fibers

CHAPTER 6: NON-DESTRUCTIVE ANALYSIS OF SINGLE DYED TEXTILE FIBERS VIA ROOM TEMPERATURE FLUORESCENCE SPECTROSCOPY AND PRINCIPAL CLUSTER ANALYSIS

6.1. Introduction

The development of analysis methods for the identification of dyes in textile fibers has become increasingly important for samples of historical,[81] archeological,[82-83] or forensic[84] investigations. For each case, analysis is optimally conducted from a single fiber, either because the sample is precious or a bulk sample is unavailable to investigators. Currently, many methods for the analysis of dyes in fibers have been developed for cases when the material composition of the fiber does not provide exclusive identifying information (e.g. cotton, wool and other natural fibers are ubiquitous). Highly sensitive and selective methods of single fiber-dye analysis include electrospray ionization mass spectrometry,[85-86] surface enhanced Raman spectroscopy,[87-89] and capillary electrophoresis.[90] In the above cases, single fiber analysis is possible, but pretreatment[87] or extraction techniques[85, 90] are required that can potentially damage the precious fiber sample. Single fiber analysis without pretreatment has been reported by Markstrom and coworkers[91] using liquid crystal tunable filter microspectrophotometer, acquiring visible absorbance spectra with only the fixture of a fiber on a glass slide. Fiber identification using this method may be approached by comparison of spectra, provided that the two-dimensional absorbance data are sufficiently distinct. As discussed by Huang et al, such distinction may not always be attained using only absorbance spectra.[86]

Single fiber identification can be substantially enhanced by acquiring data of higher dimensionality than that obtained by absorbance spectra, as well as the inclusion of statistical methods of classification. This chapter describes the non-destructive acquisition of 3-

dimensional excitation-emission luminescence using a the instrumental set-up described section 3.2.1. Two pairs of pre-dyed fibers that are indistinguishable by eye and have similar absorbance spectra (Figure 6.1and Figure 6.2) were used for the purposes of identification.

Even with higher dimensionality data provided by the excitation emission matrixes, comparison of spectra for purposes of fiber identification requires a statistical figure of merit. A variety of approaches to classification of fibers by classification have been published. Palmer and coworkers[92] developed a system of dividing fibers into classes based on perceived color of the source garment, followed by visual evaluation of absorbance spectra using terms such as "trough," "peak," "shoulder," and "noise." This approach may be useful for rapid and preliminary comparison, but lacks statistical rigor. More recently, statistical analysis methods have been employed in forensic evaluations with success in a variety of areas. Barret and coworkers investigated the application of hierarchical cluster analysis, principal component analysis (PCA) and discriminant analysis (DA) in in classifying dyed hair specimens.[93] Yu et al.[94] reported the evaluation of Entellan New fiber mount using PCA. Recent innovative application of statistical analysis to forensic samples have been reported by and Sikirzhytski et al.[95] and Bueno et al.[96] in the Lednev group. In those cases, a variety of multivariate statistical methods were applied to the analysis of Raman data for the forensic identification body fluid traces[95] and gunshot residue.[96] Herein, we report the use of principal component cluster analysis for the identification of visually indistinguishable single dyed fibers. Multiple spots along the fiber were sampled to provide a training set for comparison to other fibers, threads and regions of fabric. Statistical figures of merit for correct identification of fiber dyes are described so that

matching single evidential fibers to other single fibers, threads, or bulk materials may be accomplished with 95-99% confidence.

6.2.Materials and Methods:

6.2.1.Reagents and Materials

Two pairs of indistinguishable fibers were chosen namely acid blue 25 and acid blue 41 dyed on nylon 361; direct blue 1 and direct blue 53 dyed on cotton 400. Their corresponding dyes were purchased from Sigma-aldrich (excluding acid blue 41 which was purchased from acros organics) at reagent grade level. Percent composition of dye in the reagent standard and the type of fabric used in dying process is provided in Table 6.1. Purchased dyes were supplied to Testfabrics, inc (West Pittson, PA) for dying. Pre-dyed and undyed fabric was received and stored in sealed packages to avoid possible environmental contamination. HPLC grade methanol, purchased from Fischer scientific and nanopure water obtained from a Barnstead nanopure infinity water purifier was used to make solutions for absorbance measurements and fluorescence measurements. Tweezers, blades and scissors used for isolating the fibers from fabric were cleaned with methanol and were visually examined under UV-light (254 nm) to check the presence of fluorescence impurities.

Table 6.1. Commercial sources and purity of dyes along with the corresponding type of fibers used for the dyes

Dye	Commercial source	% purity of dye	Fiber type
Acid blue 25	Sigma	45%	Spun nylon 361
Acid blue 41	Acros organics	N/A	Spun nylon 361
Direct blue 1	Sigma	N/A	Cotton 400
Direct blue 53	Sigma	N/A	Cotton 400

6.2.2. Instrumentation

Absorbance measurements were made with quartz micro-cuvettes (1-cm path length and 2-mm width) that can hold a maximum of 700µL. A single beam spectrophotometer (model Cary 50, Varian) equipped with a 75W xenon pulsed lamp, 20 nm fixed band-pass and a maximum scan rate of 24,000 $nm.min^{-1}$ was used to record the absorbance. Fluorescence measurements were made as described in chapter 3 under using optimum pinhole diameter and excitation and emission band-pass of 20 nm.

6.2.3.Room temperature fluorescence spectroscopy

Two pairs of fabric (8”x10”) were chosen for the experiments: Acid blue 25 and 41, and Direct blue 1 and 53. Fibers isolated from each pair are found to be indistinguishable when compared under white light (see Figure 6.2). Two dimensional – excitation emission spectra recorded on single textile fiber isolated from these indistinguishable pairs is presented in appendix F. Excitation Emission Matrixes (RTF-EEM) was collected with excitation wavelength ranging between 350 and 675 nm at 5nm increments and emission wavelength ranging between

430 and 800 nm at 1 nm increments using cut-off filters. Three fabric elements were sampled with EEM data: single: single fibers, single threads, and fibers from different bulk regions of fabric. To acquire EEM data within a fiber, a single fiber pulled from a thread was fixed against the hole of the sample holder (see Figure 3.11) using tape so that an approximately 3mm of the length of the fiber can be used for measurements. A quartz slide and cover slip were used with the sample holder. EEMs were collected on five randomly chosen spots on the fiber, then the sample holder was inverted so the reverse side of the fiber could be sampled and EEMs were collected from five spots on the other side of the fiber. Similarly, individual threads (composed of 10 fibers) were also sampled by pulling a thread from each fabric. Ten EEMs were collected from each of the 10 fibers isolated from the thread. Finally, individual spectra from different fibers collected from separate bulk regions of fabric were collected to evaluate variation in spectra from different regions. Reproducibility of these EEMs is presented in appendix B. In case of direct blues, collecting EEMs was confined to 10 spots on a fiber.

6.2.4.Comparison of EEMs

Training set EEM data (10 spectra from different spots on an individual fiber) were collected for each dyed fiber. To identify the excitation wavelength at which the emission spectra showed the maximum deviation, the training spectra were averaged and, for a given dye pair (e.g. acid blue 25 and acid blue 41) the averaged training spectra were subtracted and the residuals calculated for points in the matrix. The residuals were squared and plotted, as shown in Figure 6.4 and Figure 6.5. The excitation wavelength that generated the greatest difference in the emission spectra were identified from the maxima in the residuals plots.

6.2.5.Data Analysis

Emission spectra of maximum deviation between dye pairs were identified by scrutinizing the maxima in the residuals plots in Figure 6.4 and Figure 6.5, and the excitation wavelength corresponding to the highest points in the residuals plots were used for cluster analysis. Data were pretreated by baseline correction and normalization prior to calculation of principal component eigenvectors. A data matrix containing the training set spectra was created with the intensity of a given spot on the training fiber contained on a row, and each wavelength in a different column. Each spot on the training set was represented as a row in the original data matrix. A square covariance (Z) matrix was calculated:

$$Z = D^T D$$

Eigenvectors (Q_0), a set of orthonormal vectors describing the wavelength variation in the D-matrix, and the diagonal matrix of eigenvalues (λ_0) were calculated by diagonalizing the Z matrix:

$$Q_0{}^T Z Q_0 = \lambda_0$$

The majority of vectors in the eigenvector matrix describe noise contained in the data matrix, while only a small number of eigenvectors with the largest eigenvalues contain the majority of the variance in the spectra. Malinowski[97] has developed a rigorous test to determine the number of principle components and exclude eigenvectors that describe only noise, using a Fischer's F-ratio of reduced eigenvalues. To calculate reduced eigenvalues, the eigenvalues are normalized and weighted according to their distribution so that the reduced eigenvalue is proportional to the variance in the data. The equation for the F-ratio calculation is:

$$F(1, s-n) = \frac{\sum_{j=n+1}^{s}(r-j+1)(c-j+1)}{(r-n+1)(c-n+1)} \frac{\lambda_n}{\sum_{j=n+1}^{s}\lambda_j^0}(s-n)$$

This equation calculates the F-ratio for an eigenvalue to the next smallest eigenvalue to test the null hypothesis. If there are r rows and c columns in the data matrix resulting in s eigenvalues (λ), the nth eigenvalue is being tested for significance. The F-ratio is calculated with s-n degrees of freedom.

Based on the F-test of reduced eigenvalues of the direct blue data set, two eigenvectors were required to describe 99.9% of the variance in the data set, and according to the reduced eigenvalue F-test, the null hypothesis is rejected for two eigenvectors using an F-ratio with 99% confidence. Similarly, acid blue principle components required only two eigenvectors according to the F-test with two eigenvectors to accounting for 99.4% of the variance in the training set. Accordingly, the eigenvector matrix was truncated to exclude noise vectors.

Principle component scores were calculated for each spectrum in the training set by multiplying the data matrix by the truncated eigenvector matrix. The scores were mean centered, normalized, and plotted to evaluate the clusters formed by the individual dyes in the training set. The shapes of the clusters were elliptical, so equations describing the shapes of the ellipses were determined. First, the center of mass for each cluster was calculated by averaging the x- and y-coordinates for each point in a training cluster. The angle of the skew of the ellipses was determined by fitting the training data to a best fit line, the slope of which is equal to the tangent of the skew angle. The radii of the ellipses were calculated from the training set clusters by calculating the distance of each point from the center of each ellipse, equivalent to the standard deviation in each direction, along the axis of the skew angle. The standard deviation of the

training cluster along the axis perpendicular to the skew angle was also calculated. The standard deviations of the training set points along the angle of rotation were used to determine the boundaries of an ellipse, centered at a point (h,k) representing the center of mass of the training cluster and rotated by angle,α. The equation for a rotated ellipse with center (h,k) is given by:

$$\left(\frac{cos^2\alpha}{a^2}+\frac{sin^2\alpha}{b^2}\right)(x-h)^2+2cos\alpha sin\alpha\left(\frac{1}{a^2}-\frac{1}{b^2}\right)(x-h)(y-k)+\left(\frac{sin^2\alpha}{a^2}+\frac{cos^2\alpha}{b^2}\right)(y-k)^2=1$$

In this equation, a is the standard deviation and the major axis of the ellipse along angle α, and b is the standard deviation and minor axis perpendicular to the rotation angle.

Boundaries of ellipses within three standard deviations of the center of the training cluster are shown in Figure 6.6 and Figure 6.7. Unambiguous assignment of some fibers, threads, and regions within the cluster within three standard deviations of the center is, in some cases, quite apparent. However, the scatter outside the boundary of three standard deviations requires additional statistical characterization, as described in the following.

An F-test was utilized to compare the variance of the training cluster ellipse to the distance of a given questionable point (representing a fiber, thread or region) from the ellipse. It was important to consider the direction of the point from the center of the cluster, since the distance from the boundary of the ellipse to its center depends upon the direction in which the boundary is measured. An equation for a line formed by the point in question and the center of the ellipse was solved simultaneously with the equation for the ellipse to determine the point on the boundary in the direction of the questionable point, and subsequently the distance from the

center of the cluster to the boundary. The F-ratio for the variance of the point (d_i) and the boundary of the cluster ($d_{ellipse}$) was given by

$$F = \frac{d_i^2}{d_{ellipse}^2}$$

To classify a fiber, thread, or region as belonging to a given training set, the F-ratio must be less than the critical F-value. With 99% confidence, the critical F-value is 10.56.

6.3. Results and Discussion

6.3.1. Absorbance spectra of reagent dye solutions:

Reagent dye molecular structures are presented in appendix A. Aldrich Handbook of Stains, Dyes and Indicators[98] has absorption spectra of many dyes documented in it. Among different solvent systems used to make dye standard solutions, 50% v/v methanol-water was the most commonly used solvent system in the handbook. Reagent solutions prepared in 50% methanol/water was used for absorbance measurements. Figure 6.1 provides an overlay of normalized absorption spectra recorded from reagent dye standard solutions. As shown in Figure 6.1, highly similar absorption spectral profiles are observed for each pair of reagent dye solutions. Bright field images of single textile fiber pairs presented in Figure 6.2 show that the differentiation of these fibers is not possible when observed under white light.

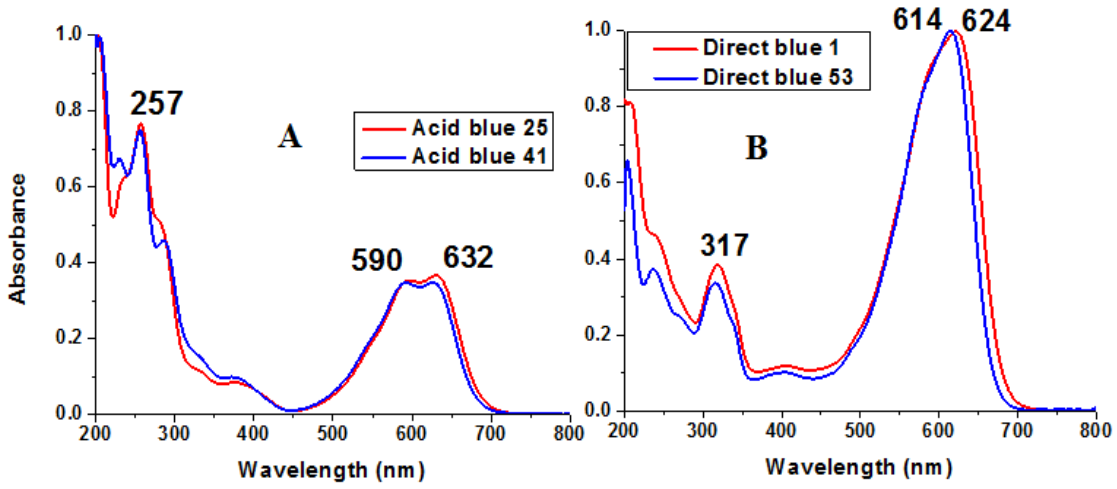

Figure 6.1. Normalized absorbance spectra of A) Acid blue 25 and 43; B) Direct blue 1 and 53

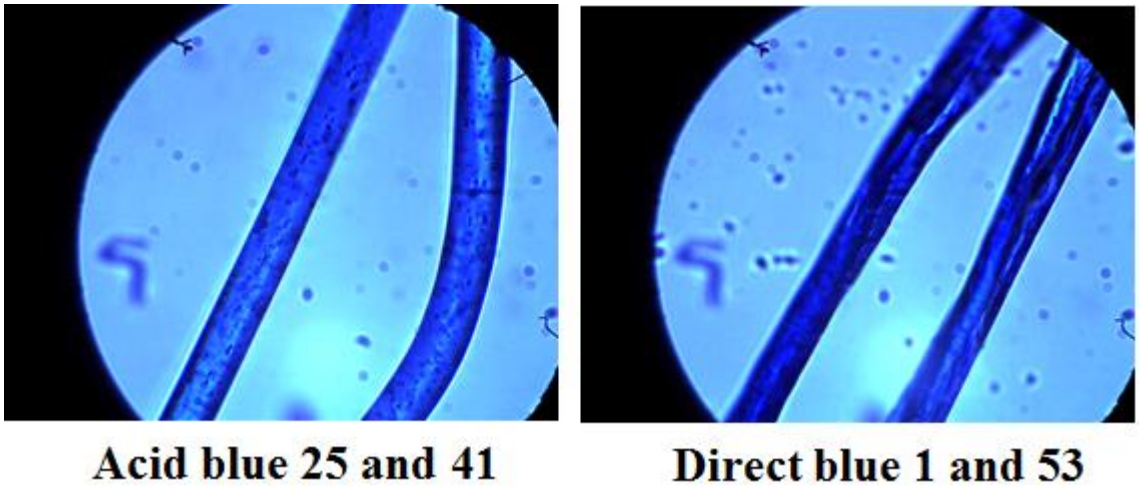

Figure 6.2. Bright field images of indistinguishable pair of fibers

6.3.2. Fluorescence measurements on single textile fibers:

Non-destructive identification of single fibers by comparison of EEM data requires statistical figures of merit, particularly in cases where dye characteristics, such as spectra, are similar. Determination of principal component scores from training spectra - acquired from a single fiber - facilitated comparison of other single fibers with the same composition and the same or similar dyes. Principal component scores were calculated from emission spectra at an excitation wavelengths showing the maximum residual sum of squares between emission spectra (see Figure 6.4 and Figure 6.5). In the case of acid blue dye pair (Figure 6.4), the greatest residual in emission occurred with an excitation wavelength of 560 nm (Figure 6.3). In the case of direct blue (Figure 6.5), two maxima in the residuals plots were observed at 580 and at 420 nm excitation. For principal component analysis, the emission at 580 was selected because the noise in this region of the spectrum was diminished relative to that at 420 (Figure 6.3)..

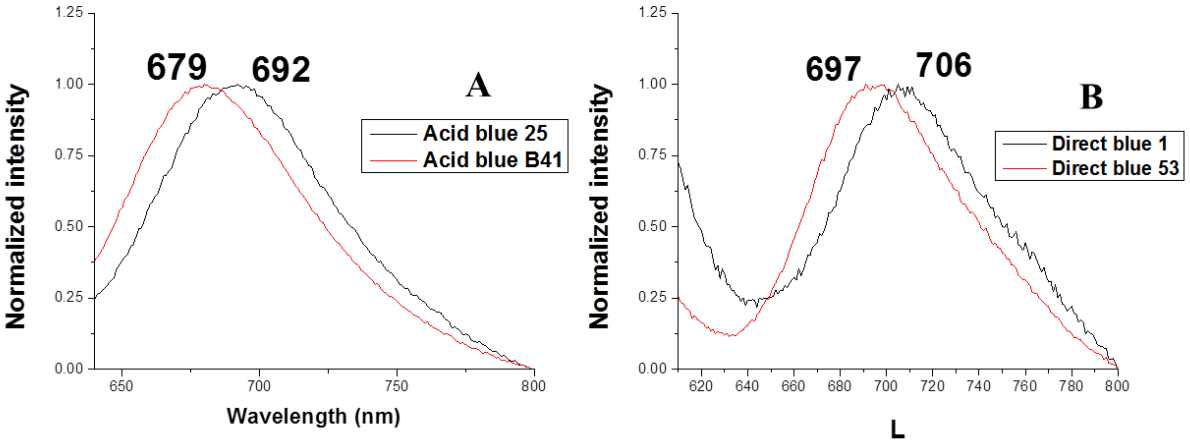

Figure 6.3. Normalized emission spectra of A) acid blue fibers – λ_{em} = 560 nm; B) Direct blue fibers - λ_{em} = 580 nm

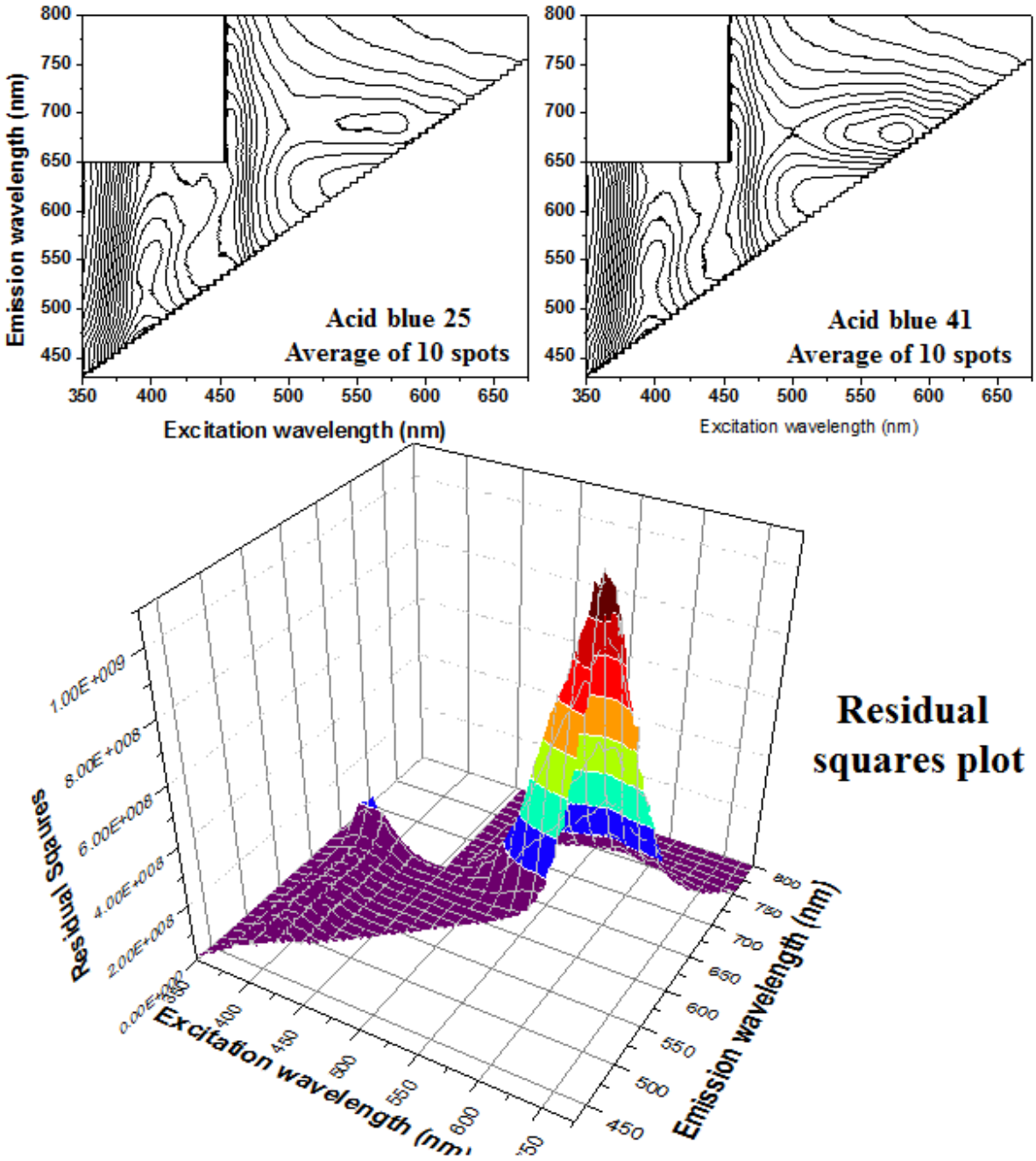

Figure 6.4. Average of 10 EEMs recorded within the fiber and residual squares plot for acid blue fibers

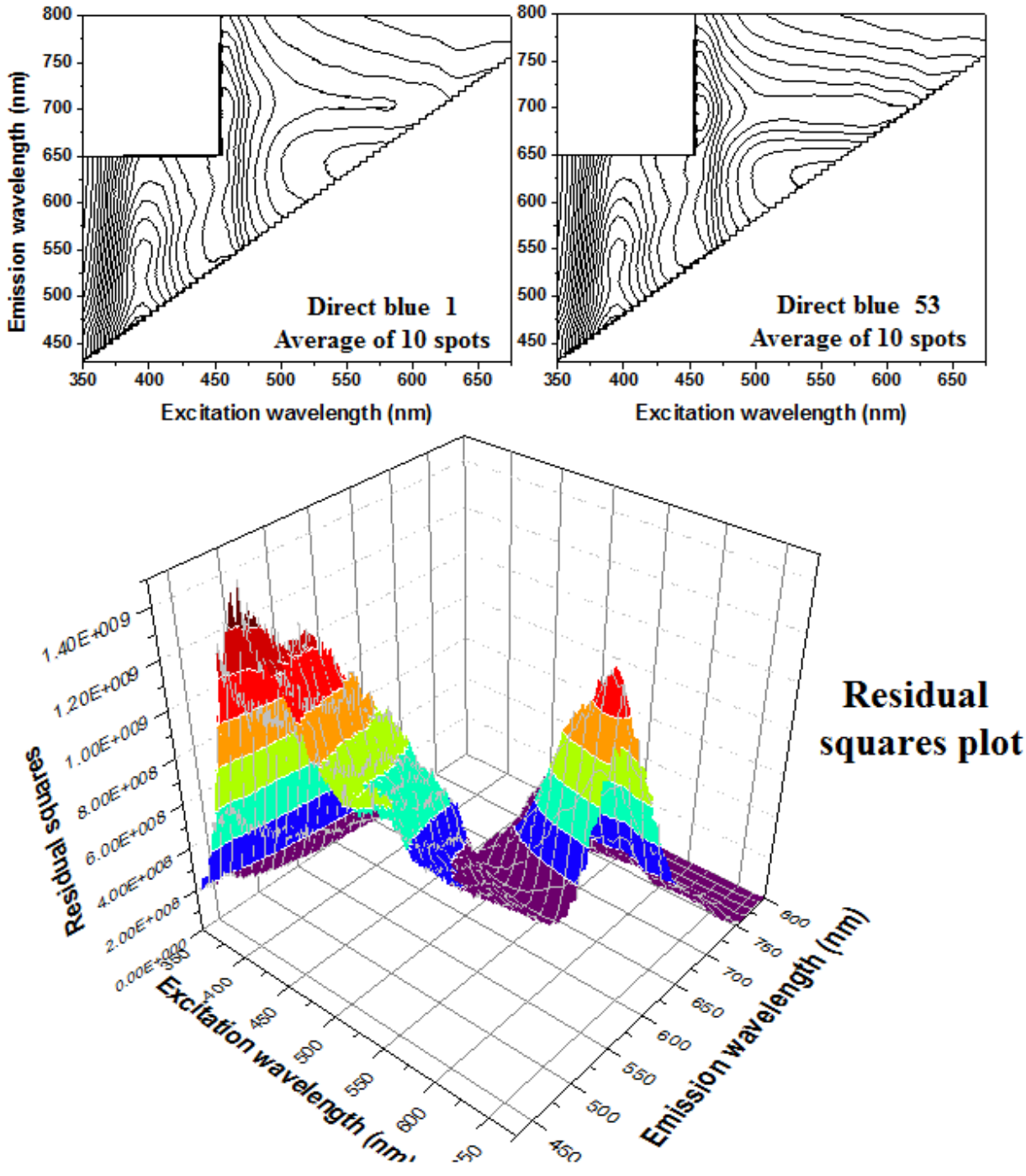

Figure 6.5. Average of 10 EEMs recorded within the fiber and residual squares plot for basic green fibers

Principal component scores cluster plots for similar dye pairs are shown in Figure 6.6 and Figure 6.7, where the radii of the ellipses drawn around the cluster correspond to three times the standard deviation, or elliptical radii, of each training cluster. In many cases, the line demarcating three standard deviations indicates that the fibers, threads, and regions belong to the cluster with the correct dye identity. In some cases, scores from a given fiber fall outside the three standard deviation boundary, yielding false negative results. Hence, an additional statistical test using F-ratios for the variances of the training clusters was employed (see appendix G). The accuracy and rate of false positive and false negative identification of a given fiber based on the F-test are shown in Table 6.2.

Principal component scores from acid blue 25 fibers and threads were tested for correct classification using the F-test. With 99% confidence, all were classified correctly and none were misidentified as acid blue 41. Similarly, for the acid blue 41 validation set containing fibers, threads and regions, all except a single thread was classified correctly at the 99% confidence level. The thread excluded from the acid blue 41 cluster was a false negative, but was not classified as acid blue 25 dye.

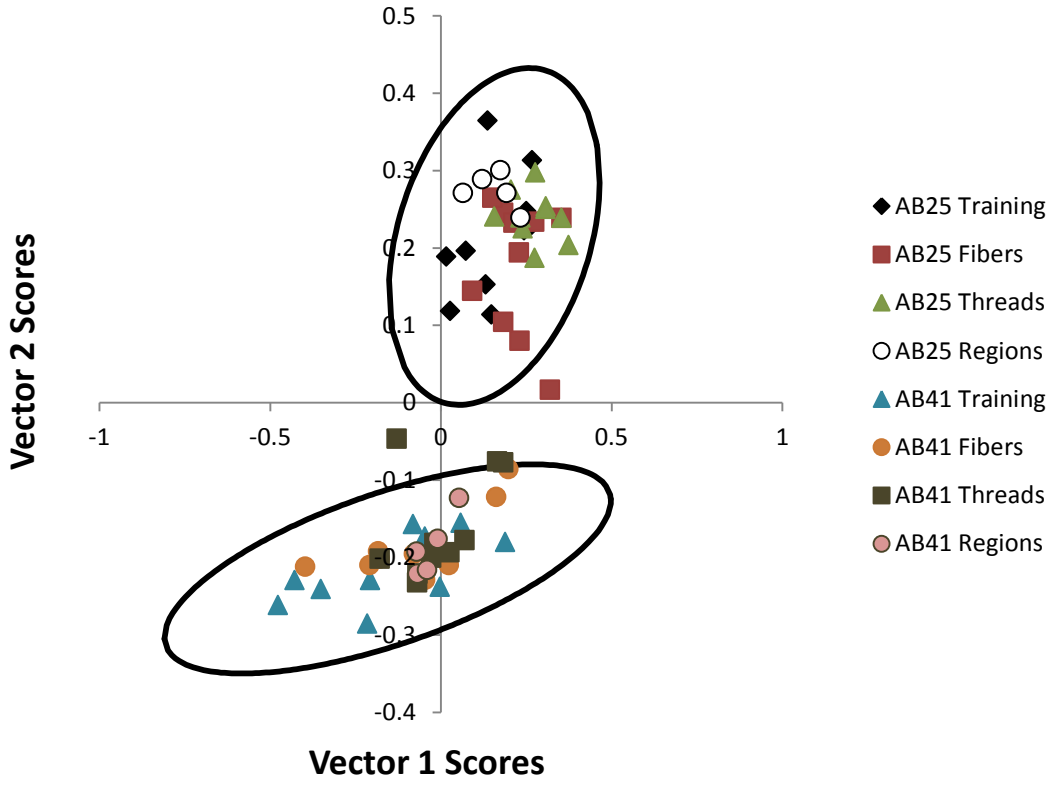

Figure 6.6. Principal component scores cluster plot of acid blue 25 (AB25) and acid blue 41 (AB41)

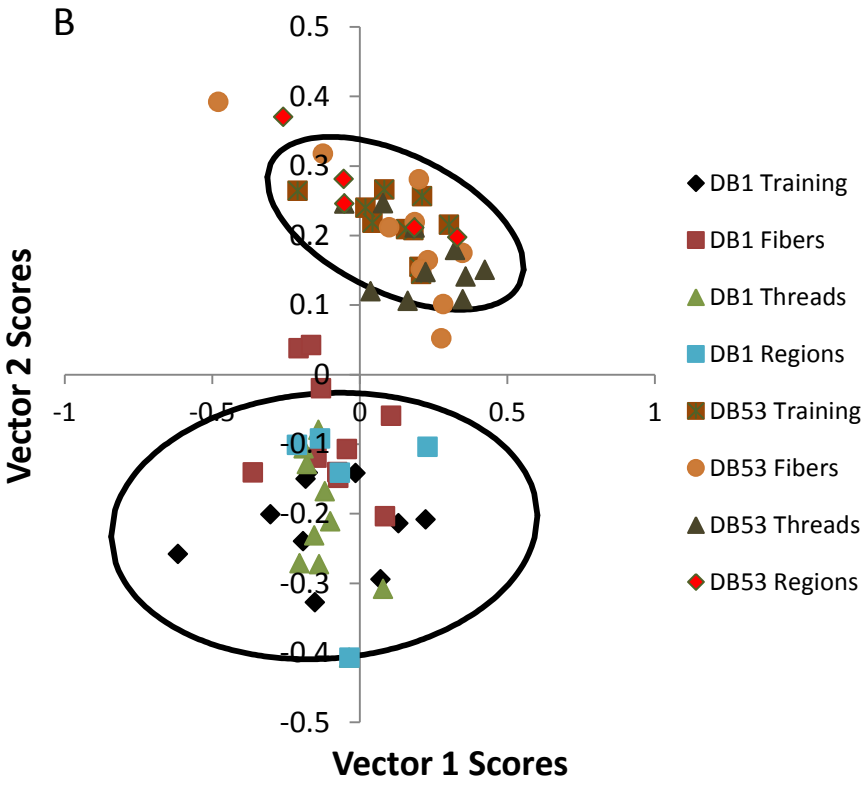

Figure 6.7. Principal component scores cluster plot of direct blue 1 (DB1) and direct blue 53 (DB53)

Table 6.2. Classification based on proximity (within three times the radii of cluster ellipse) to the center of the training cluster with 99%confidence level

Type	Accuracy (%)			False positive (%)			False negative (%)		
	Fibers	**Threads**	**Regions**	**Fibers**	**Thread**	**Regions**	**Fibers**	**Thread**	**Regions**
Acid blue 25	100%	100%	100%	0%	0%	0%	0%	0%	0%
Acid blue 41	100%	90%	100%	0%	0%	0%	0%	10%	0%
Direct blue 1	80%	100%	100%	0%	0%	0%	20%	0%	0%
Direct blue 53	90%	100%	80%	0%	0%	0%	10%	0%	20%

For the case of direct blue 1, 80% of the fibers were correctly classified, with two false negatives, but their distance from the direct blue 53 cluster excluded false positive identification. All the threads and regions dyed with direct blue 1 were correctly identified at 99% confidence. In the case of direct blue 53 fibers, dyes and threads, 90% of fibers, 100% of threads, and 80% of regions were correctly identified as dyed with direct blue 53. No fibers, threads or regions were incorrectly classified as direct blue 1.

The false exclusion of fibers, threads or regions from training clusters reflects the limitations of obtaining a training set from only a single fiber, for which small differences in spectra might result in exclusion of the sample from correct identification. These false negative results could be diminished if larger training sets were obtained from threads or regions, rather than a single fiber. For a forensic investigation scenario in which this fiber identification scheme could be employed, false positive identification (i.e. concluding that fibers match when they do not) is more destructive than a false negative result. Given the hazards of incorrectly matching fibers, the results presented here indicate that 99% confidence levels could be employed, which only yielded false negatives and no false positive identification fibers resulted from the analysis.

6.4. Conclusion

The acquisition of excitation-emission matrixes for nondestructive analysis of dye in single textile fibers can provide valuable identification information. The coupling of two commercially available instruments enhances the luminescence capabilities above that of the individual instruments, allowing the acquisition of a complete training set for fiber dye identification from an individual fiber. Accounting for the variance of the EEM spectra at different regions along the

length of the fiber provides a useful training set that can be used as the basis for principal component cluster analysis. The statistical approach to identification was demonstrated using challenging dyes with similarities both in two-dimensional absorbance spectra and in three-dimensional EEM data. By limiting the criteria for identification to 99% confidence level, no false positive identification events are observed. This may be of particular import when fibers possess forensic importance with and inaccurate identification has legal repercussions.

CHAPTER 7: OVERALL CONCLUSION

This dissertation presents a comprehensive investigation of the room-temperature fluorescence of textile fiber. Considering the disadvantages associated to selecting the best solvent for fiber extraction prior to RTF spectroscopy in forensic comparisons, we propose a 1:1 acetonitrile:water (v/v) mixture as the common extracting solvent for the fluorescence of fibers from acetate, polyester, cotton and nylon materials pre-dyed with direct, disperse, basic and acid dyes. The comparison of the fourteen types of fiber extracts showed three distinct groups of excitation and fluorescence profiles. Acetate 154/ Disperse Red 1, Cotton 400/ Direct Blue 1, Polyester 777/Disperse Red 13 and Nylon 361/ Acid Green 27 fibers showed extracts with similar excitation and fluorescence profiles. The same is true for Nylon 361/ Acid Yellow 17 fibers and Polyester 777 fibers pre-dyed with Basic Red 9, Basic Violet 14 and Disperse Blue 56. On the other end, Cotton 400 fibers pre-dyed with Direct Blue 71 and Direct Blue 90, Nylon 361 fibers pre-dyed with Acid Yellow 23, Acid Green 27 and Acid Red 151, Poly-acrylic 864/ Basic Green 4 and Polyester 777/ Disperse Red 4 fibers showed unique excitation and fluorescence spectra. Although the comparison of fibers within the first two groups should benefit from additional selectivity, the different excitation and fluorescence maxima still made possible their visual discrimination on the basis of spectral profiles. In all cases, the strong fluorescence of 1:1 acetonitrile:water (v/v) extracts made possible the analyses of fibers with 2mm length.

Outstanding reproducibility of spectral profiles with minimum variations in fluorescence intensities was observed from individual extracts belonging to adjacent fibers – i.e. single fibers located immediately next to each other –within the same area of cloth - and from single fibers located in four different cloth areas. The comparison of fluorescence chromatograms from

extracts of fibers collected from different areas of a cloth confirmed the reproducibility of individual fluorescence concomitants within the same piece of cloth. In comparison to 2D spectra, EEM appeared to be a better data format for forensic fiber comparison. The clear differences of EEM contours recorded from fiber extracts of Nylon 361 fibers pre-dyed with Acid Yellow 17 and Acid Yellow 23 provide the foundation to further develop this approach for the forensic comparison of visually indistinguishable fibers.

The non-destructive analysis of fibers was accomplished with an instrumental set-up combining a basic spectrofluorimeter and an epi- fluorescence microscope. The behavior of both fluorescence intensity and signal-to-background ratio were evaluated as a function of pinhole size, excitation-emission band-pass and fluorophor concentration with the aid of dye standards encapsulated in capillary tubes. Seven microscope objectives were evaluated for collecting fluorescence spectra from single textile fibers in the ultraviolet and visible spectral regions. Satisfactory fluorescence signals and spectral profiles were obtained using open pinholes and 40X objectives in both the ultraviolet and visible spectral regions. With the 40X objectives, the open pinhole diameter corresponds to a 150μm (0.15mm) fiber length. This fiber length is considerably shorter than the ~2mm fiber length typically encountered in crime scenes. From this prospective, the combination of an open pinhole and a 40X objective appears to be well suited for the non-destructive analysis of fibers.

Comparison of spectral data recorded from single fibers in the ultraviolet and visible regions showed the strongest fluorescence in the visible wavelength range. Based on the spectral characteristics obtained from single fibers in visible region, pre-dyed fibers can be classified into 4 types. Type I include fibers that do no present fluorescence. Nylon 361 fibers pre-dyed with

acid red 151 belong to this type. Spectra obtained from these dyed fibers are similar in intensity with that of background. Acid yellow 23 and direct blue 1fibers belong to type II, which include fibers that show fluorescence predominantly from the fiber material (nylon 361, polyester 777 or cotton 400) with negligible contribution from the dye. Type III fibers include fibers pre-dyed with acid yellow 17 and basic green 4. Although these dye reagents are the main contributors to the total fluorescence of the fibers, their spectral profiles in liquid solutions do not match the spectral profiles of the pre-dyed fibers. Type IV fibers include fibers pre-dyed with acid green 27 and disperse red 4. Their spectral profiles match those form the dye reagents in liquid solutions.

The similarities observed among the spectral profiles of different types of fibers challenge the use of excitation and fluorescence spectra for forensic purposes. EEM data formats directly recorded from single fibers were then investigated for the discrimination of indistinguishable fiber pairs. Similar to two-dimensional spectra recorded from single fibers, EEMs showed to be reproducible within the bulk of the fabric. Figures of merit from the statistical comparison of EEMs with principal component cluster analysis made possible the discrimination of visually indistinguishable fibers pairs. No false positives were found at 99% confidence levels for the studied fibers.

Future studies in our lab will investigate spectral changes that might occur in textile fibers as a result of exposure to environmental conditions such as laundering, exposure to cigarette smoke and weathering. With the examination of these effects through comparison of fibers, we expect to gain a better understanding of textile physical, chemical and spectral changes that might affect fiber comparison via fluorescence microscopy. In collaboration with Dr. Sigman's

research group, we will explore the statistical comparison of EEM and micro-spectrophotometry data for the analysis of forensic fibers.

APPENDIX A: MOLECULAR STRUCTURES OF REAGENT DYES

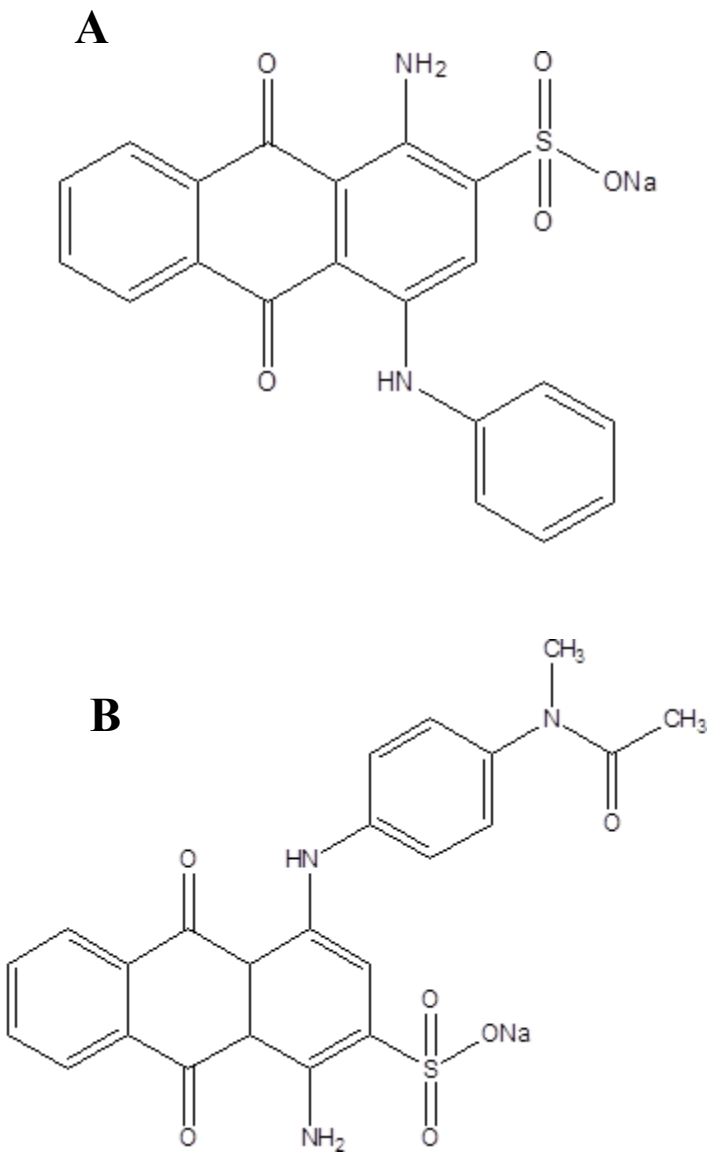

Figure A.1. Molecular structure of indistinguishable pair of fibers – A) Acid blue 25; B) Acid blue 41 reagent dye

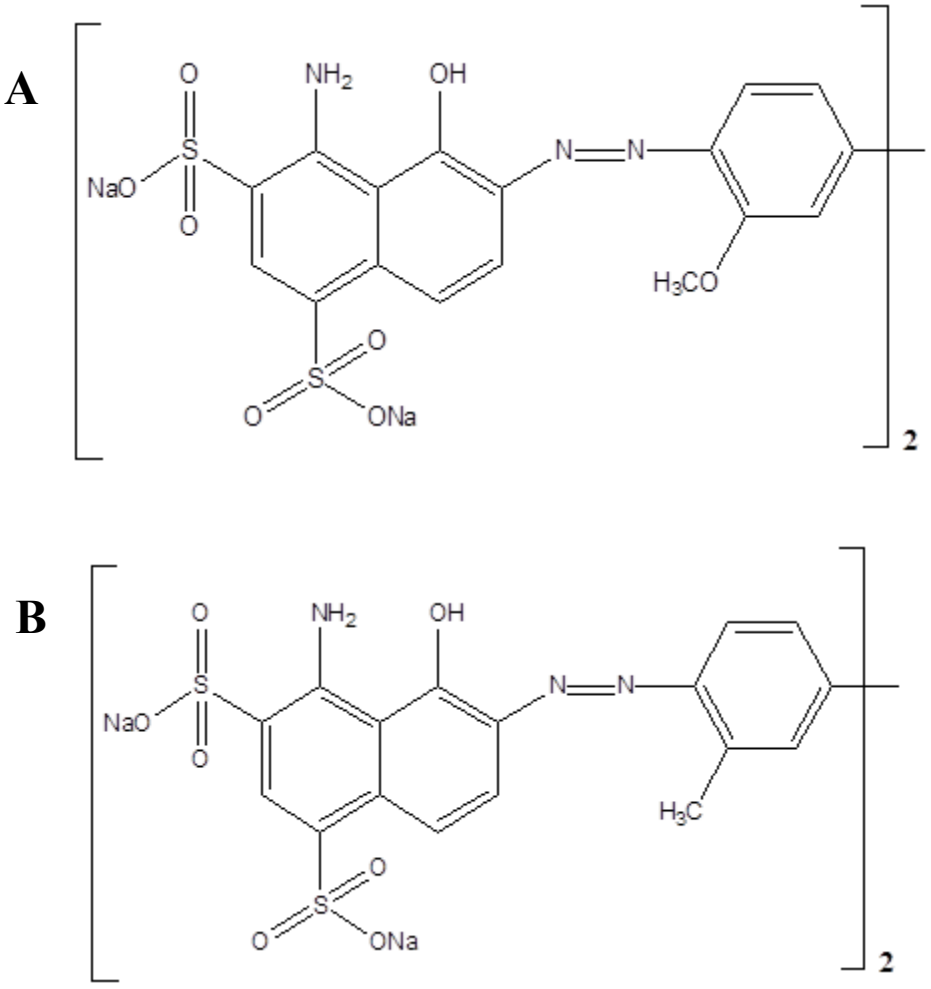

Figure A.2. Molecular structure of indistinguishable pair of fibers – A) Direct blue 1; B) Direct blue 53 reagent dye

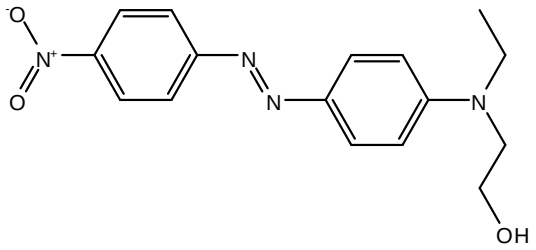

Disperse red 1

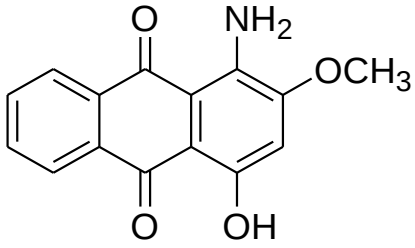

Disperse red 4

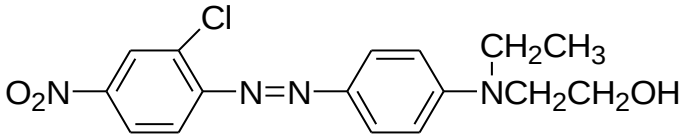

Disperse red 13

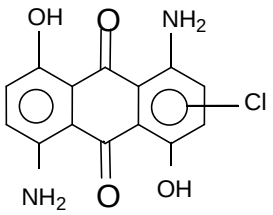

Disperse blue 56

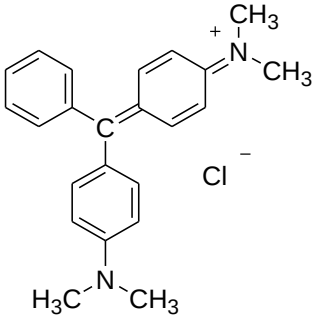

Basic green 4

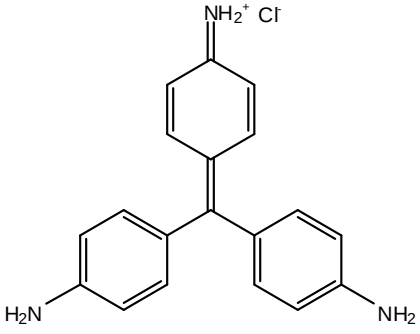

Basic red 9

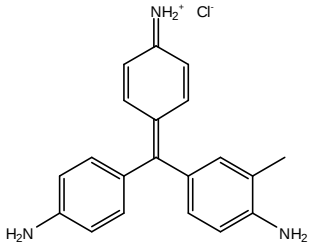

Basic violet 14

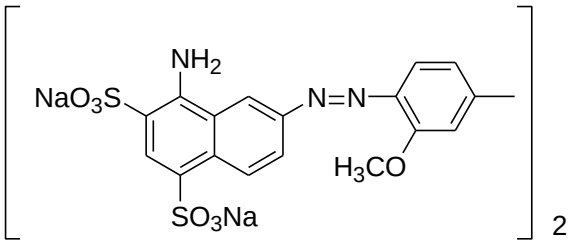

Direct blue 1

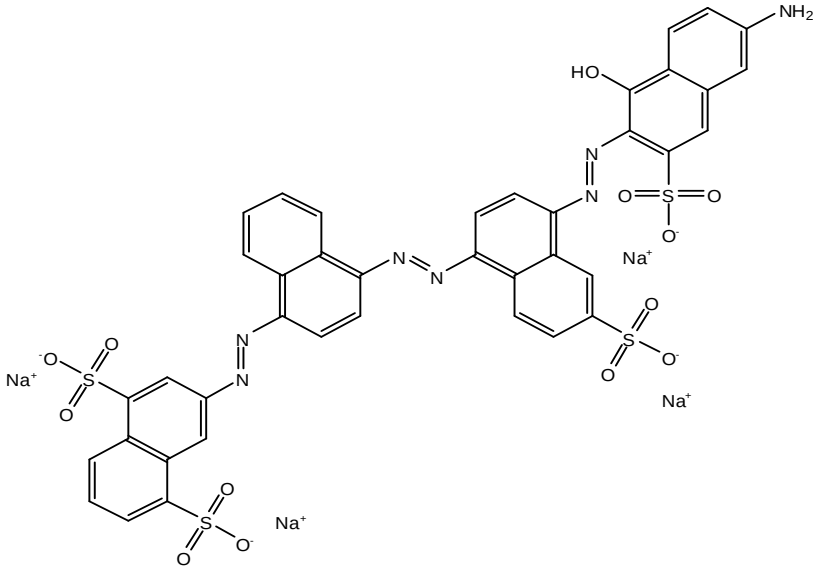

Direct blue 71

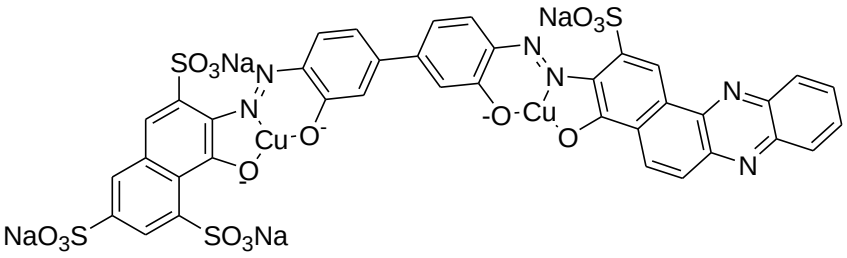

Direct blue 90

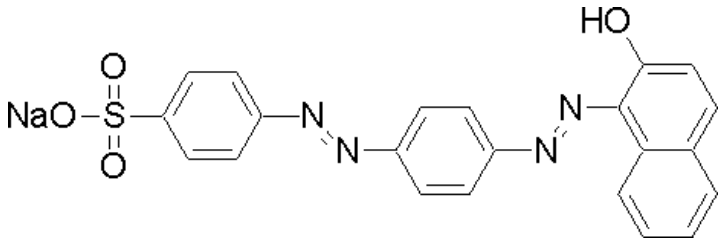

Acid red 151

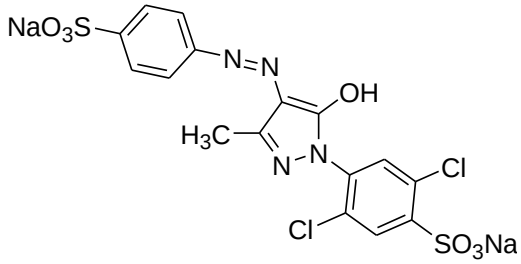

Acid yellow 17

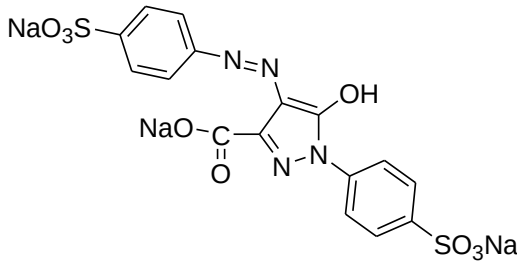

Acid yellow 23

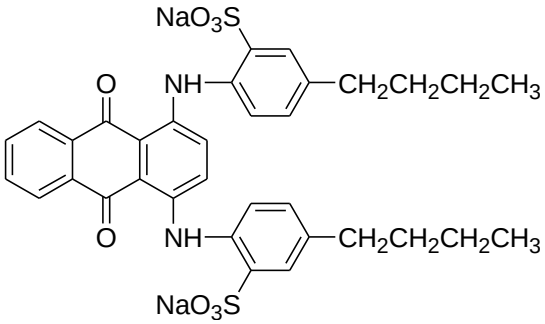

Acid green 27

APPENDIX B: REPRODUCIBILITY OF EXCITATION-EMISSION MATRICES RECORDED ON SINGLE TEXTILE FIBERS

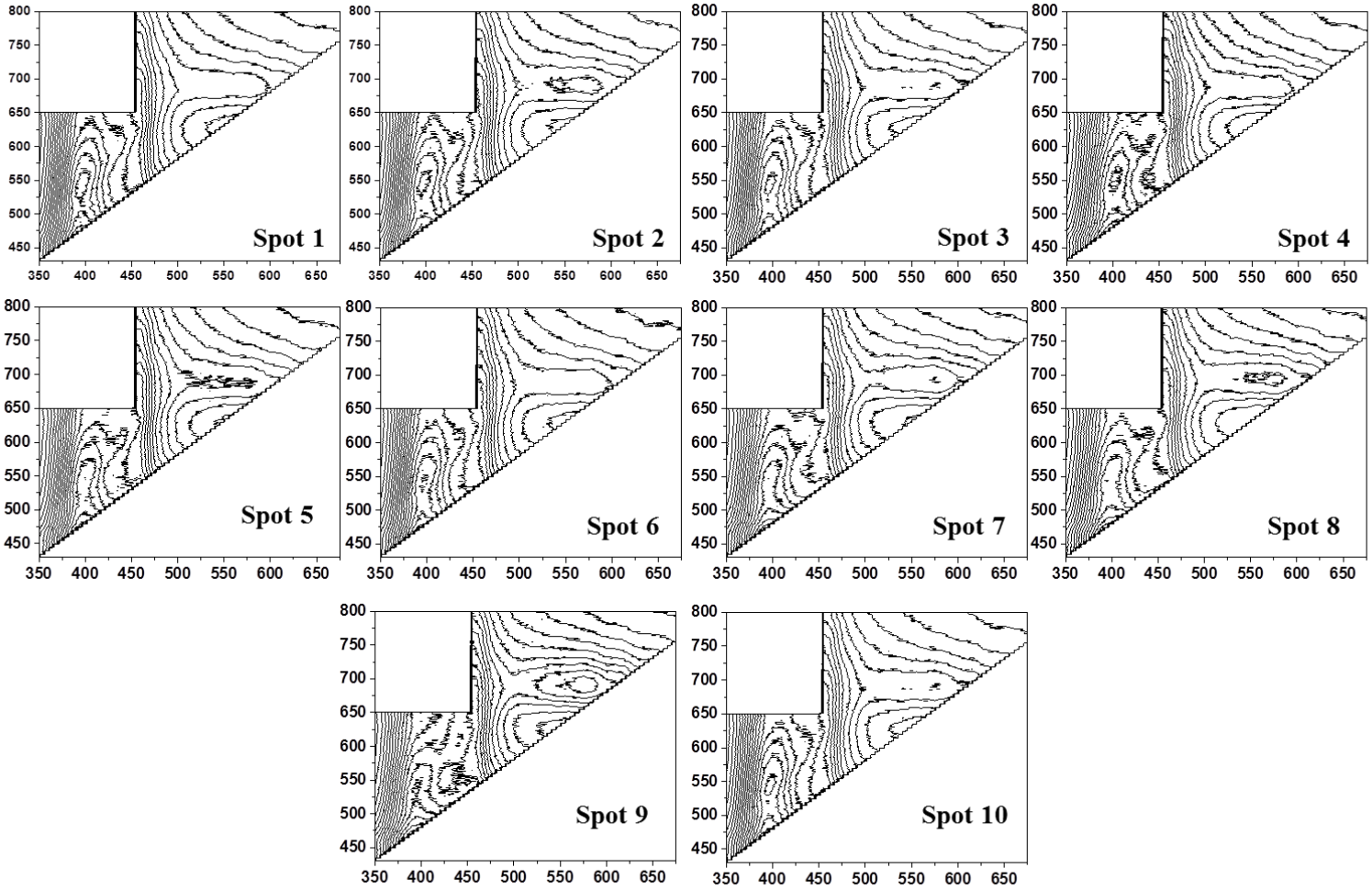

Figure B1: Reproducibility of EEMs recorded on ten spots on a single acid blue 25 fiber

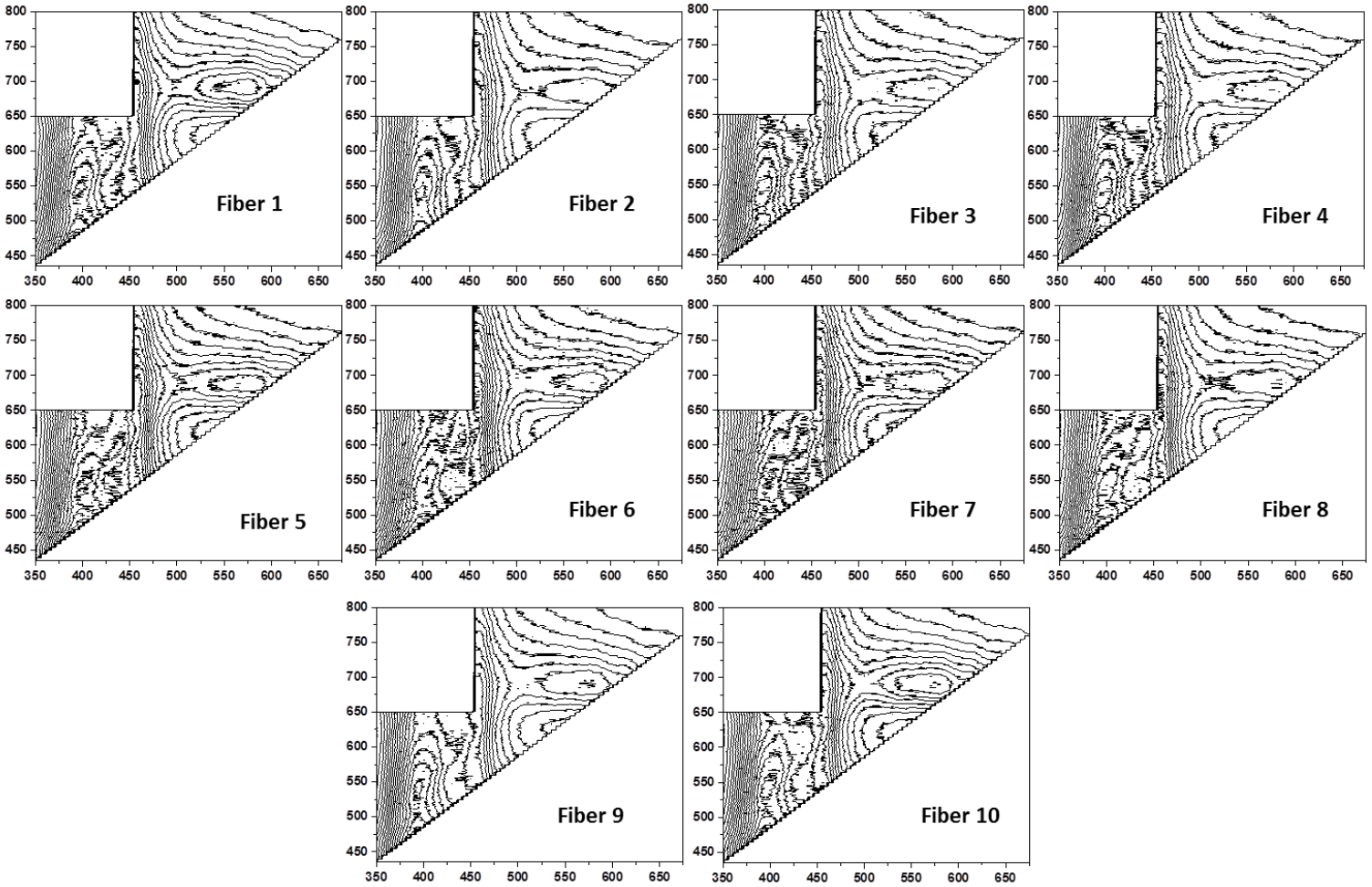

Figure B2: Reproducibility of EEMs recorded on ten fibers isolated from an acid blue 25 thread

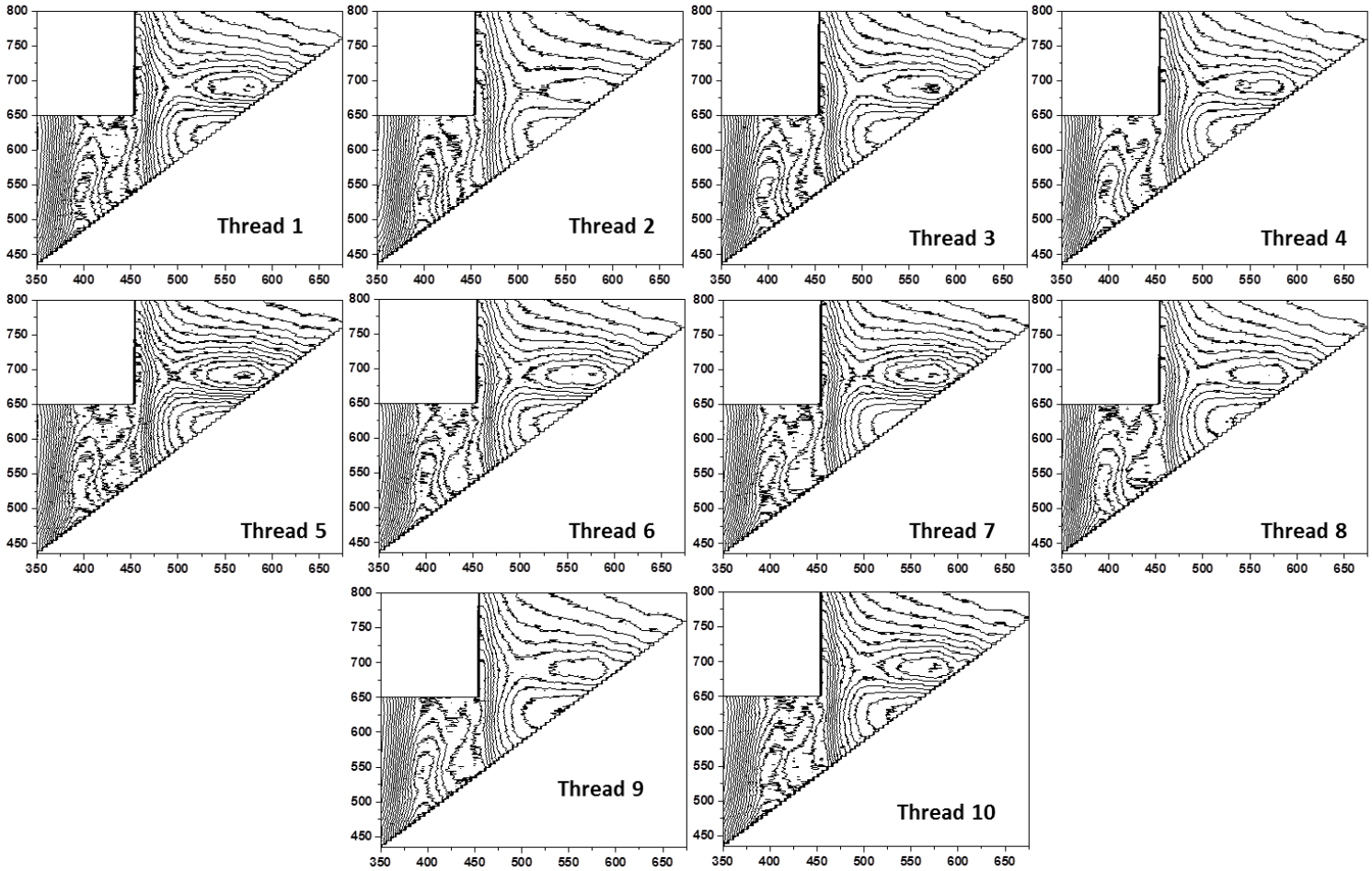

Figure B3: Reproducibility of EEMs recorded on ten threads isolated from a region of acid blue 25 cloth

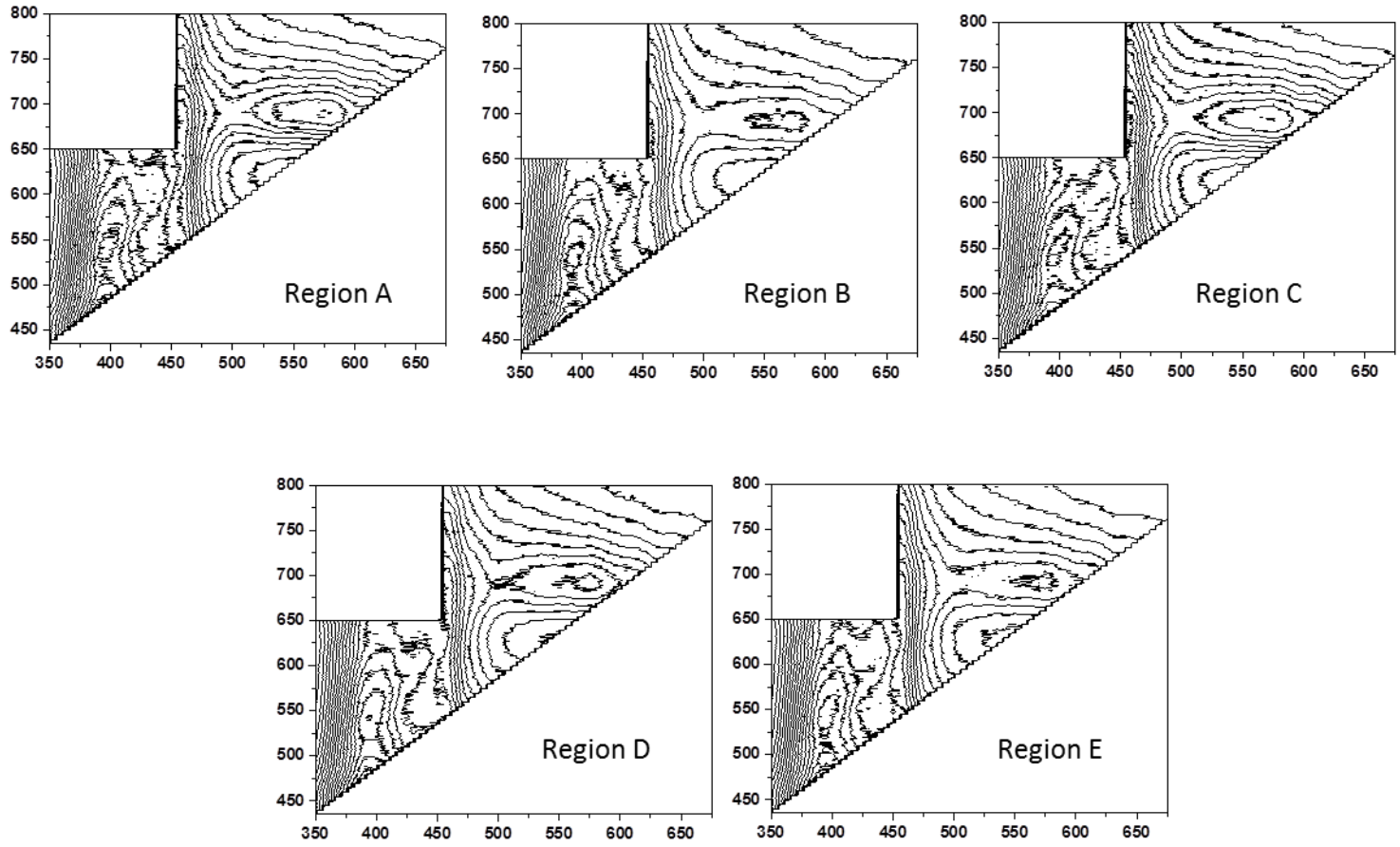

Figure B4: Reproducibility of EEMs recorded from five regions of acid blue 25 cloth

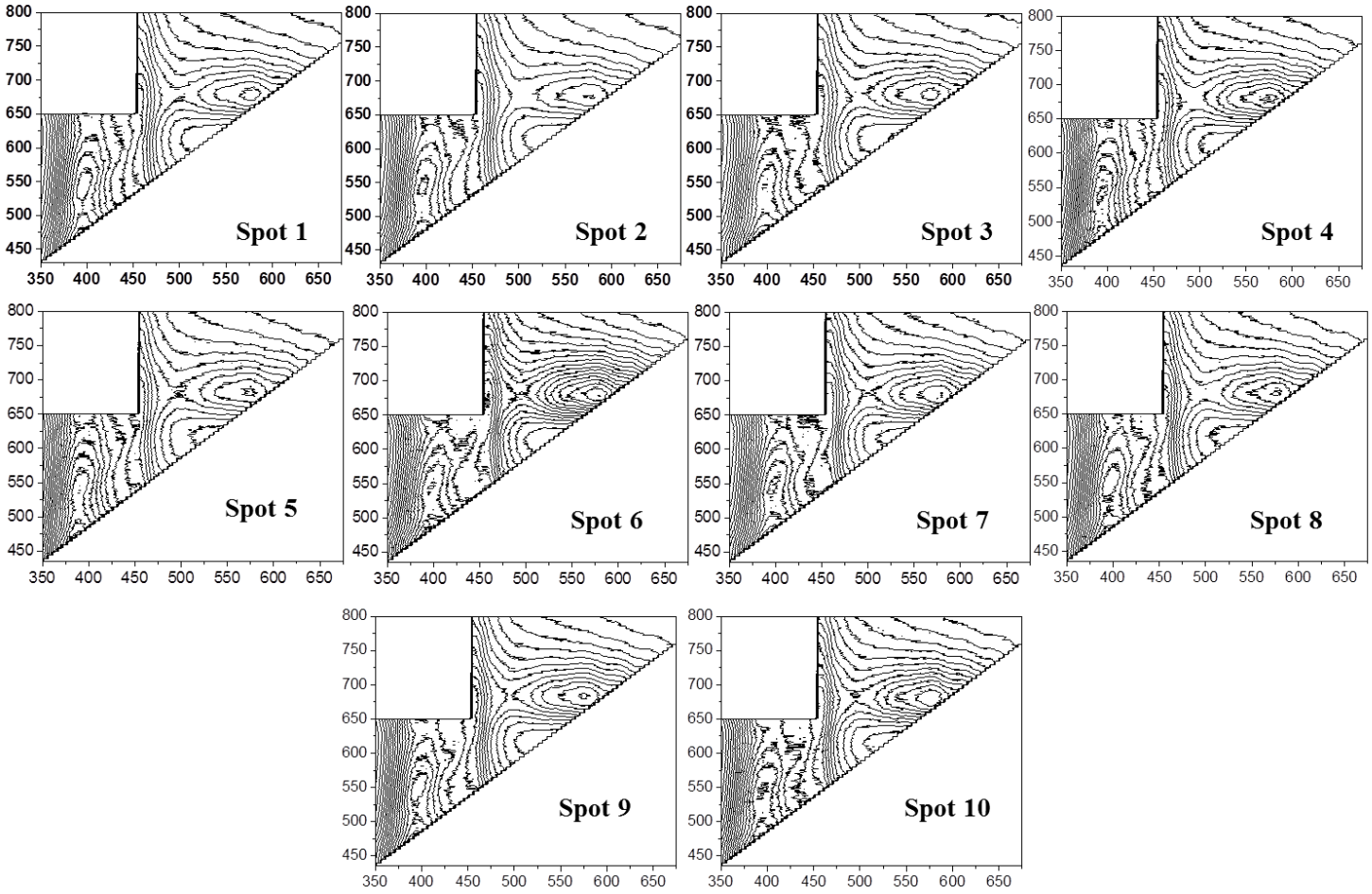

Figure B5: Reproducibility of EEMs recorded on ten spots on a single acid blue 41 fiber

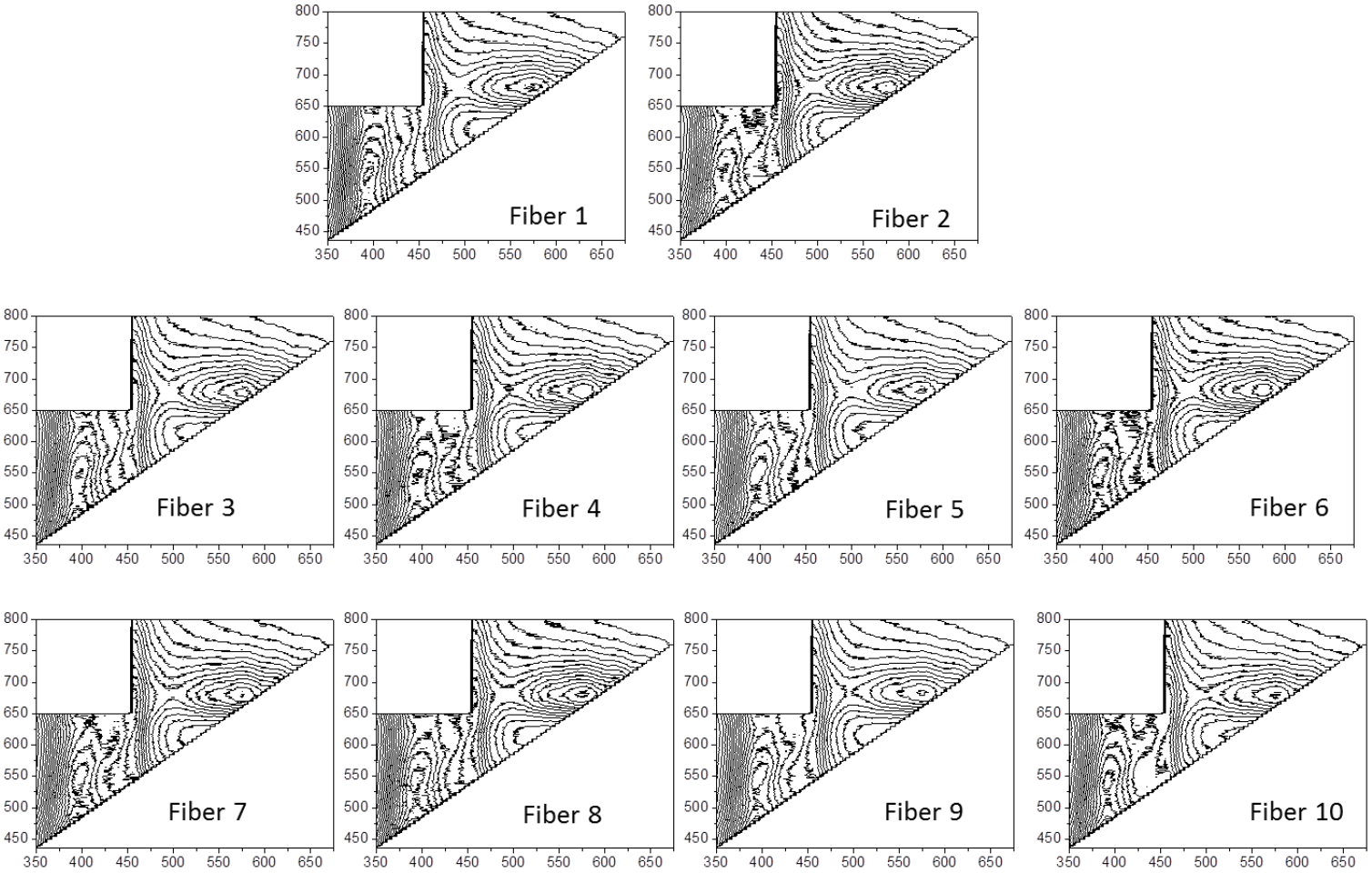

Figure B6: Reproducibility of EEMs recorded on ten fibers from an of acid blue 41 thread

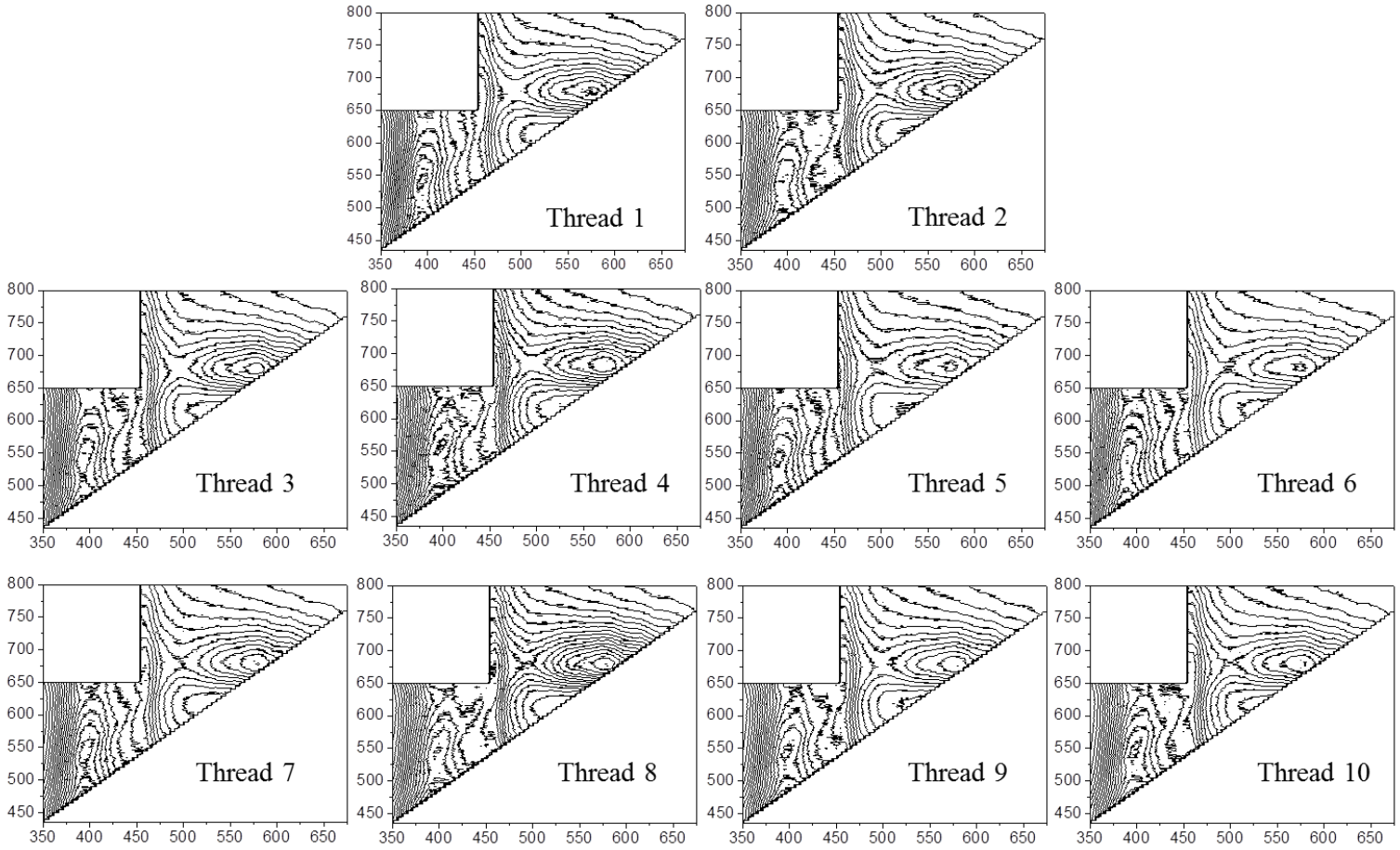

Figure B7: Reproducibility of EEMs recorded from ten threads of a region on acid blue 41 cloth

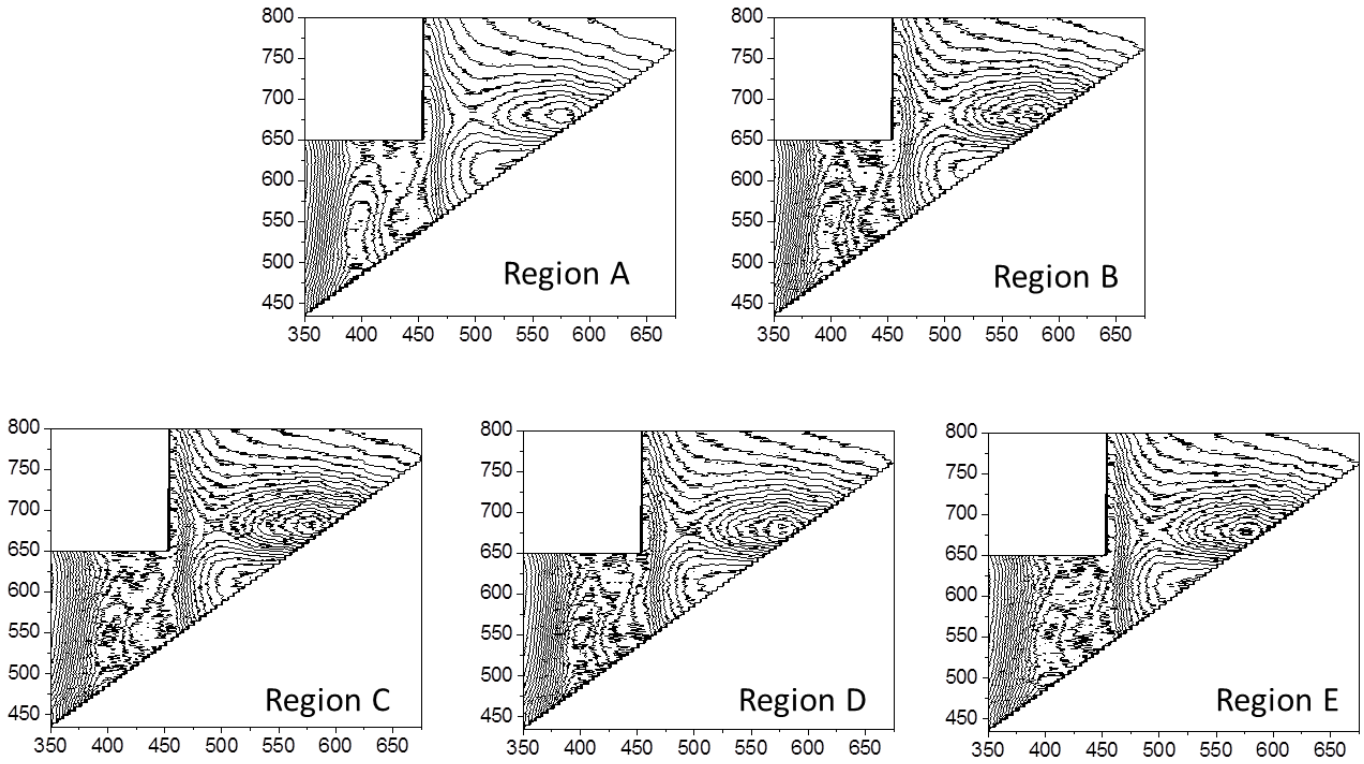

Figure B8: Reproducibility of EEMs recorded from 5 regions of acid blue 41 cloth

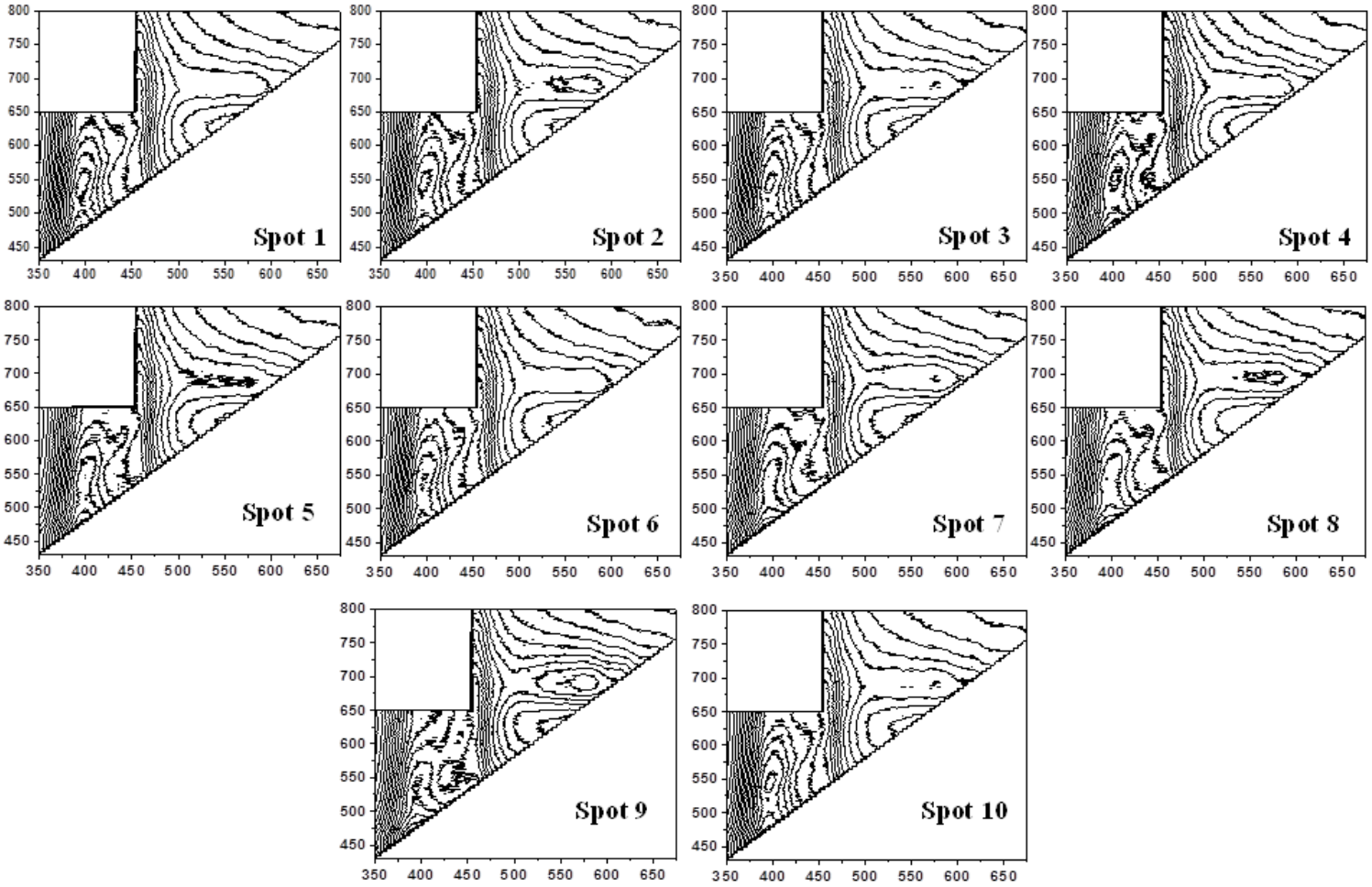

Figure B9: Reproducibility of EEMs recorded on ten spots on a direct blue 1 fiber

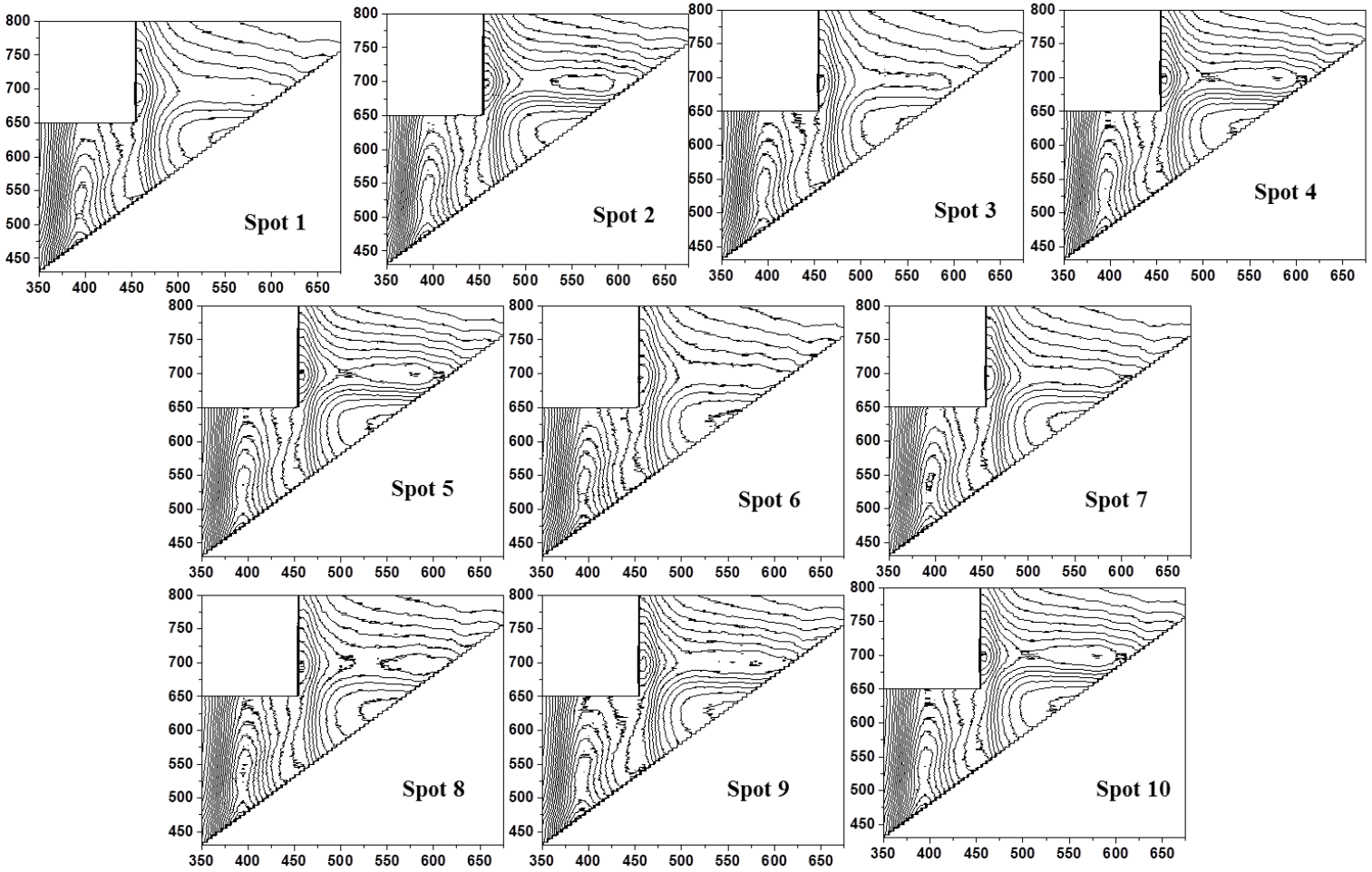

Figure B10. Reproducibility of EEMs recorded on ten spots on a direct blue 53 fiber

APPENDIX C: SPECTRAL REPRODUCIBILITY WITHIN THE LENGTH OF A THREAD

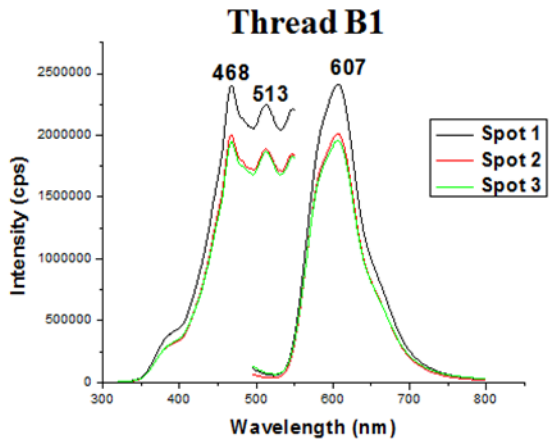

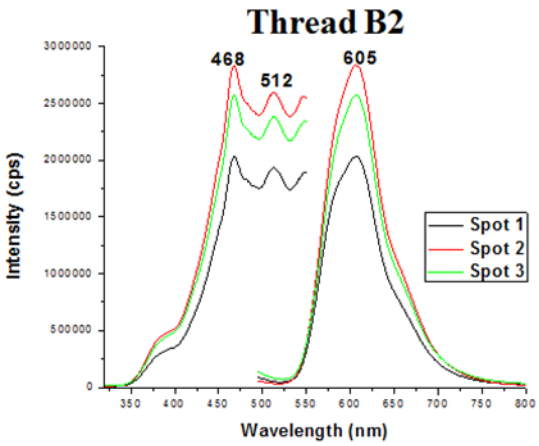

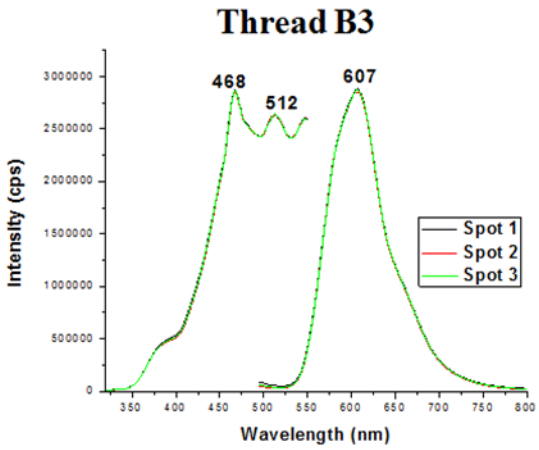

Thread	Average ± S.D*	R.S.D**
B1	2204256 ± 84346	3.83 %
B2	2475860 ± 232525	9.39 %
B3	2864373 ± 9023	0.32 %
B	**2390600 ± 101767**	**4.26 %**

*S.D = Standard deviation
**R.S.D = Relative standard deviation

Figure C1: Over lay of spectra collected from different spots on a threads from region B. Spectra were collected with excitation-emission monochromator bandpass of 12 nm under a 1000 µm pinhole diameter

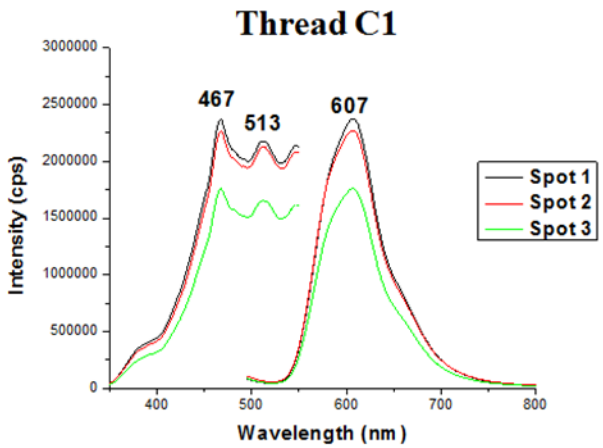

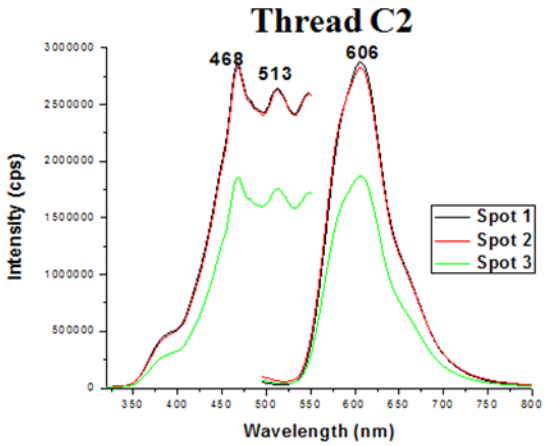

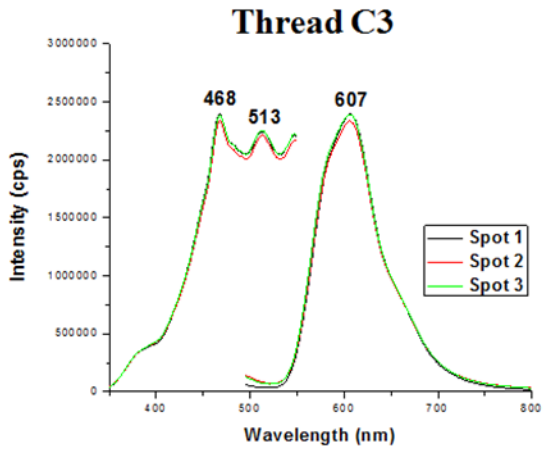

Thread	Average ± S.D	RSD
C1	2325770 ± 144769	6.23 %
C2	2522296 ± 321442	12.74 %
C3	2368773 ± 20537	0.87 %
C	**2373676± 108208**	**4.56 %**

Figure C2: Over lay of spectra collected from different spots on a threads from region C. Spectra were collected with excitation-emission monochromator bandpass of 12 nm under a 1000 µm pinhole diameter

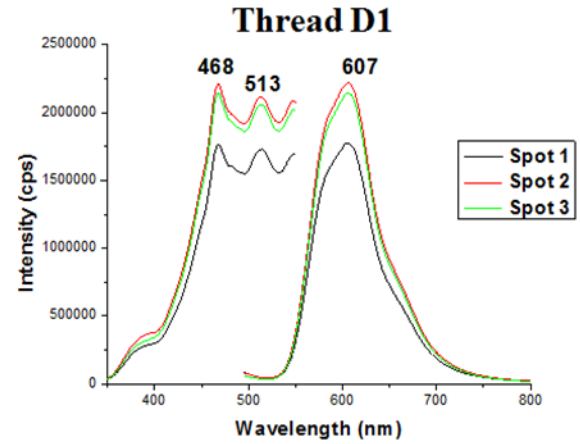

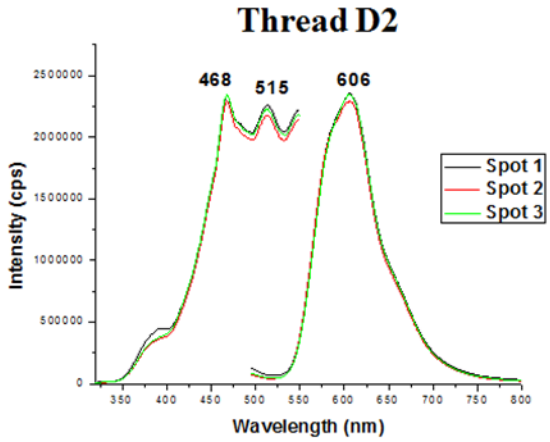

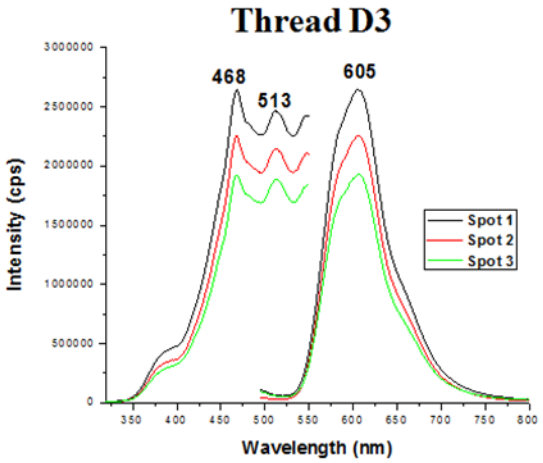

Thread	Average ± S.D	RSD
D1	1926283 ± 57802	3.00 %
D2	2328482 ± 21783	0.94 %
D3	2274670 ± 205173	9.02 %
D	**2076400 ± 75558**	**3.64 %**

Figure C3: Over lay of spectra collected from different spots on a threads from region D. Spectra were collected with excitation-emission monochromator bandpass of 12 nm under a 1000 µm pinhole diameter

APPENDIX D: EXCITATION AND FLUORESCENCE SPECTRA COLLECTED ON SINGLE TEXTILE FIBERS USING 40X-UV OBJECTIVE

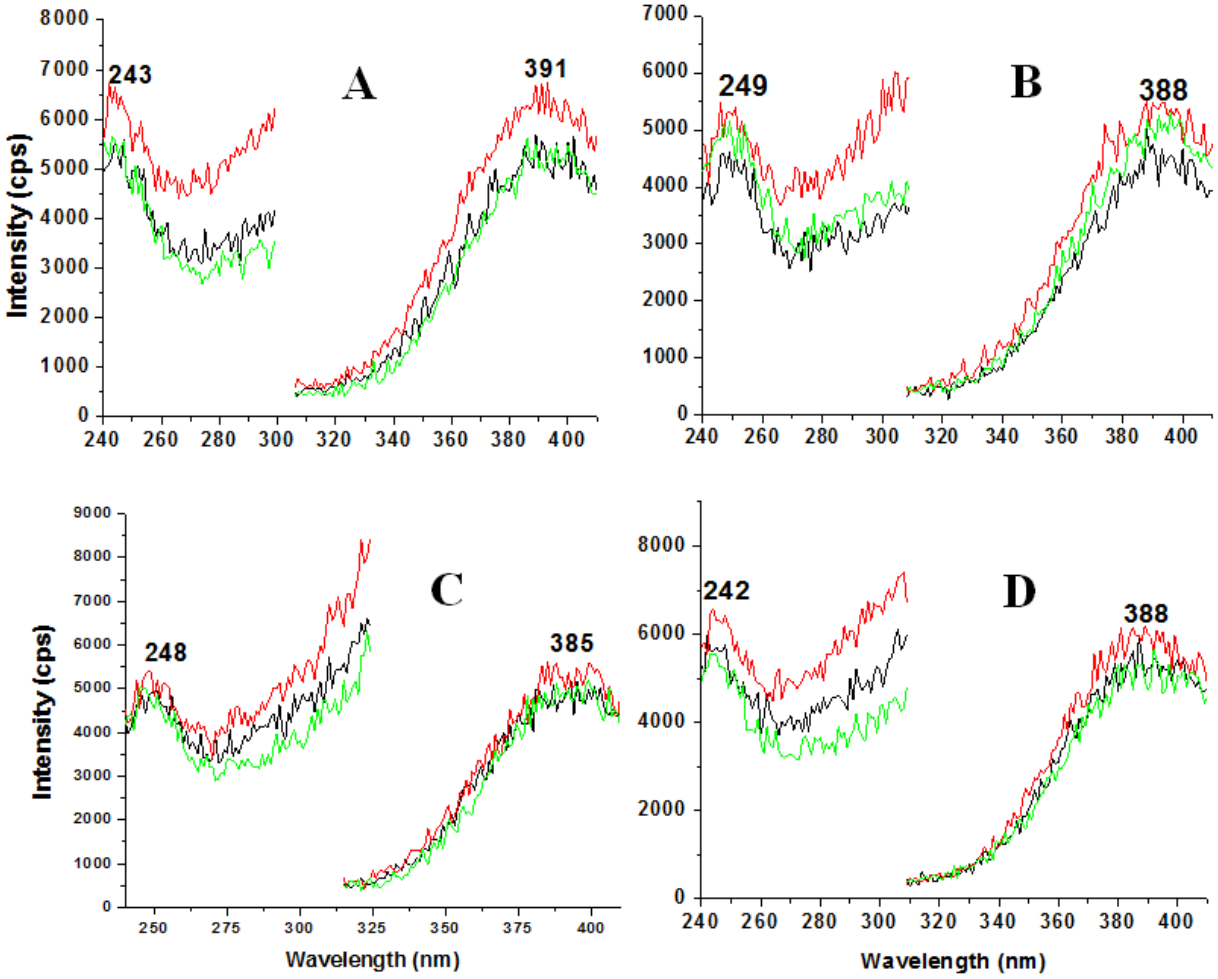

Figure D.1. Overlay of excitation-emission spectra of background (___), undyed nylon 361 fibers (___) and nylon 361 fibers pre-dyed (___) with A) Acid green 27 at $\lambda_{ex}/\lambda_{em}$=247/396 nm; B) Acid red 151 $\lambda_{ex}/\lambda_{em}$=249/392 nm; C) Acid yellow 17 $\lambda_{ex}/\lambda_{em}$=251/384 nm; D) Acid yellow 23 $\lambda_{ex}/\lambda_{em}$=240/387 nm. Spectra are collected under 40x-UV objective with excitation and emission bandpass at 28 nm.

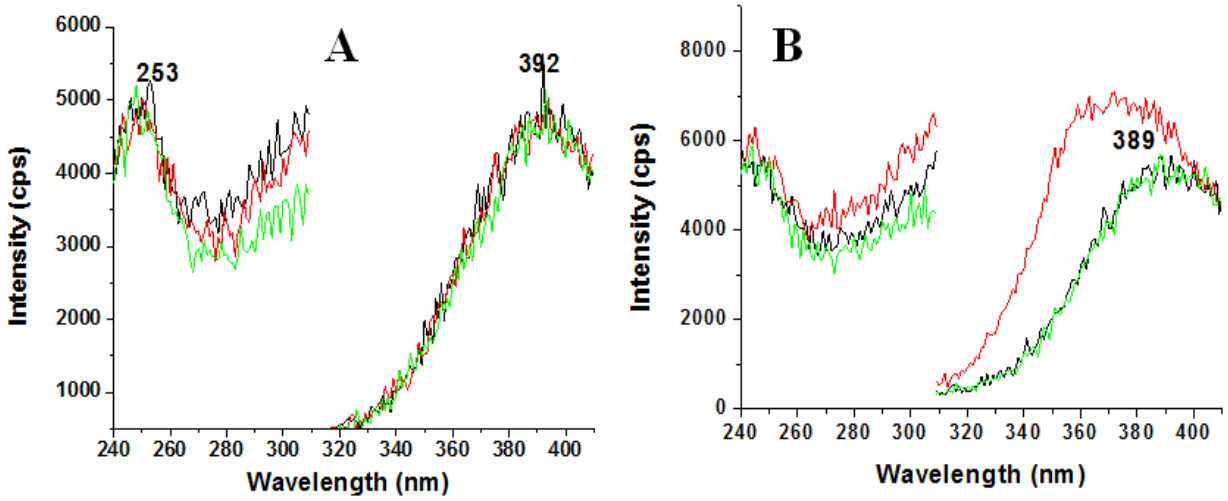

Figure D.2. Overlay of excitation-emission spectra of background (___), undyed cotton 400 fibers (___) and cotton 400 fibers pre-dyed (___) with A) Direct blue 1 at $\lambda_{ex}/\lambda_{em}$=253/392 nm; B) Direct blue 90 at $\lambda_{ex}/\lambda_{em}$=240/388 nm. Spectra are collected under 40x-UV objective with excitation and emission bandpass at 28 nm.

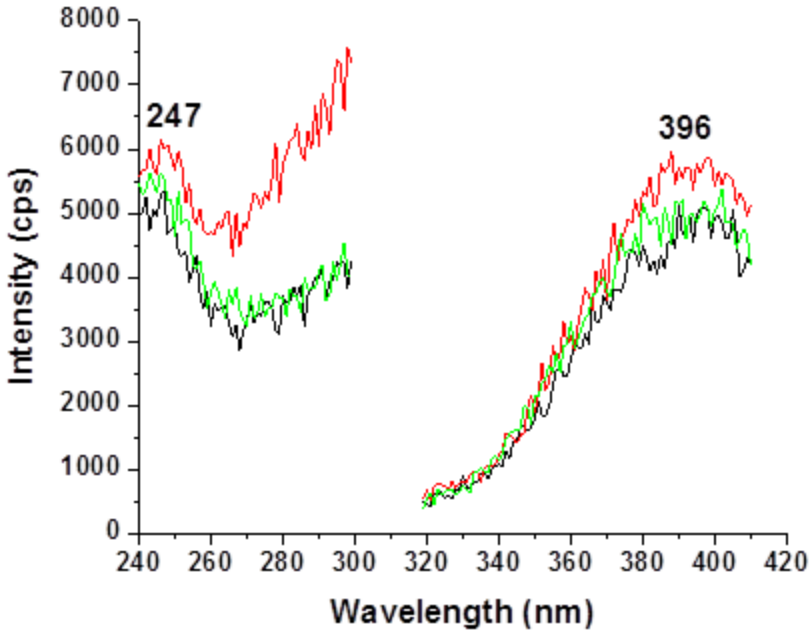

Figure D.3. Overlay of excitation-emission spectra of background (___), undyed poly-acrylic 864 fiber (___) and poly-acrylic 864 fiber pre-dyed (___) with Basic green 4 at $\lambda_{ex}/\lambda_{em}$=250/391 nm. Spectra are collected under 40x-UV objective with excitation and emission bandpass at 28 nm.

APPENDIX E: EXCITATION AND FLUORESCENCE SPECTRA OF REAGENT DYE SOLUTIONS IN THEIR CORRESPONDING BEST EXTRACTING SOLVENTS

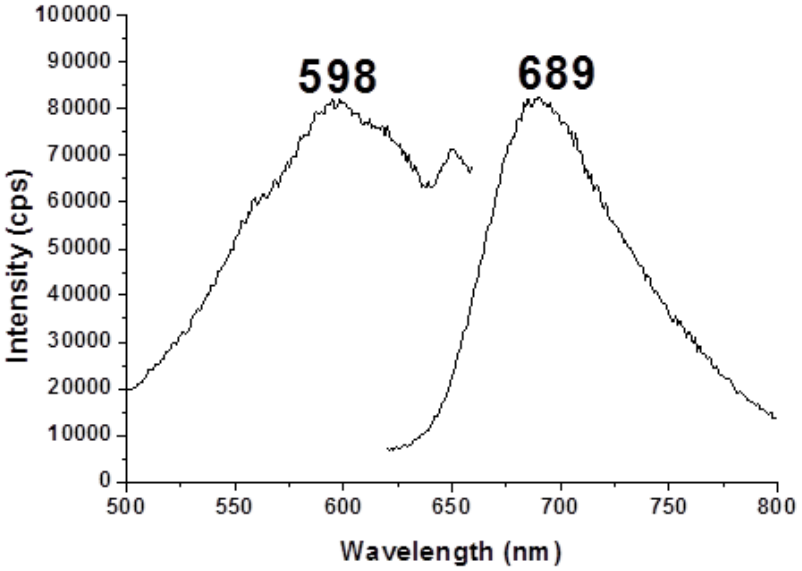

Figure E1. Excitation and fluorescence spectrum of a 10 ppm solution of acid green 27 reagent dye in 1:1 methanol/water (v:v). λ_{ex} = 598 nm and λ_{em} = 689 nm

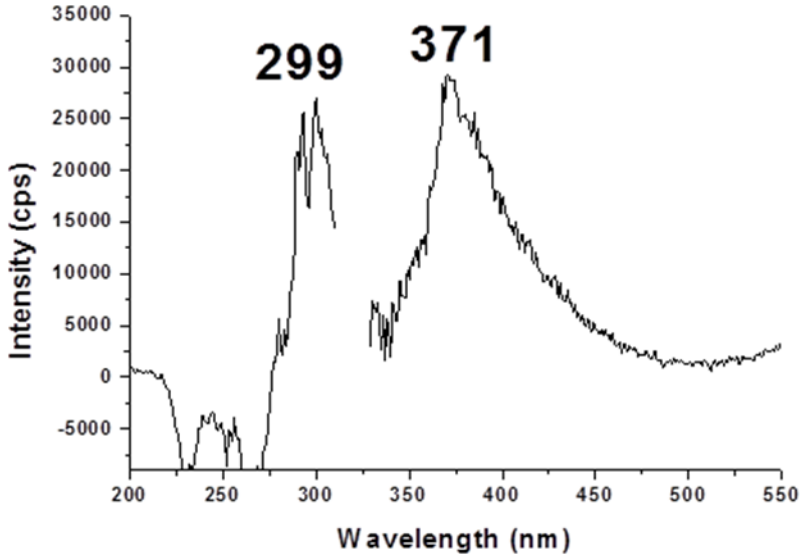

Figure E.2. Excitation and fluorescence spectrum of a 10 ppm solution of acid red 151 reagent dye in ethanol. λ_{ex} = 290 nm and λ_{em} = 371 nm

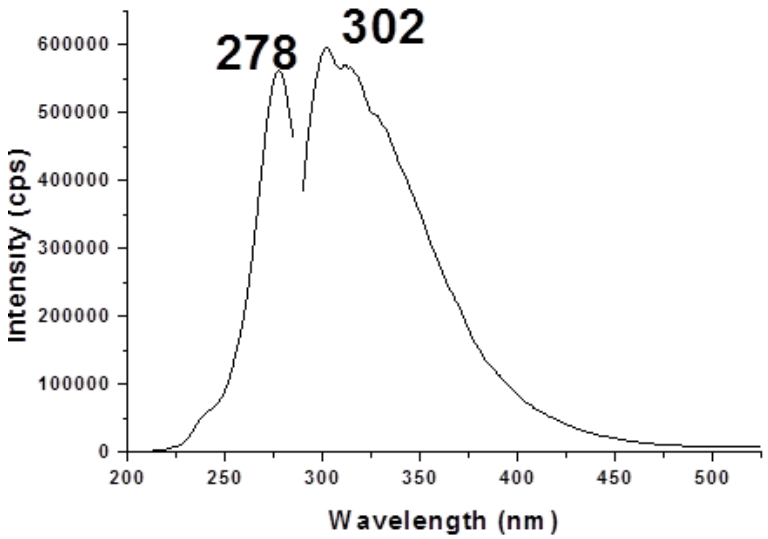

Figure E.3. Excitation and fluorescence spectrum of a 10 ppm solution of acid yellow 17 reagent dye in ethanol. λ_{ex} = 278 nm and λ_{em} = 302 nm

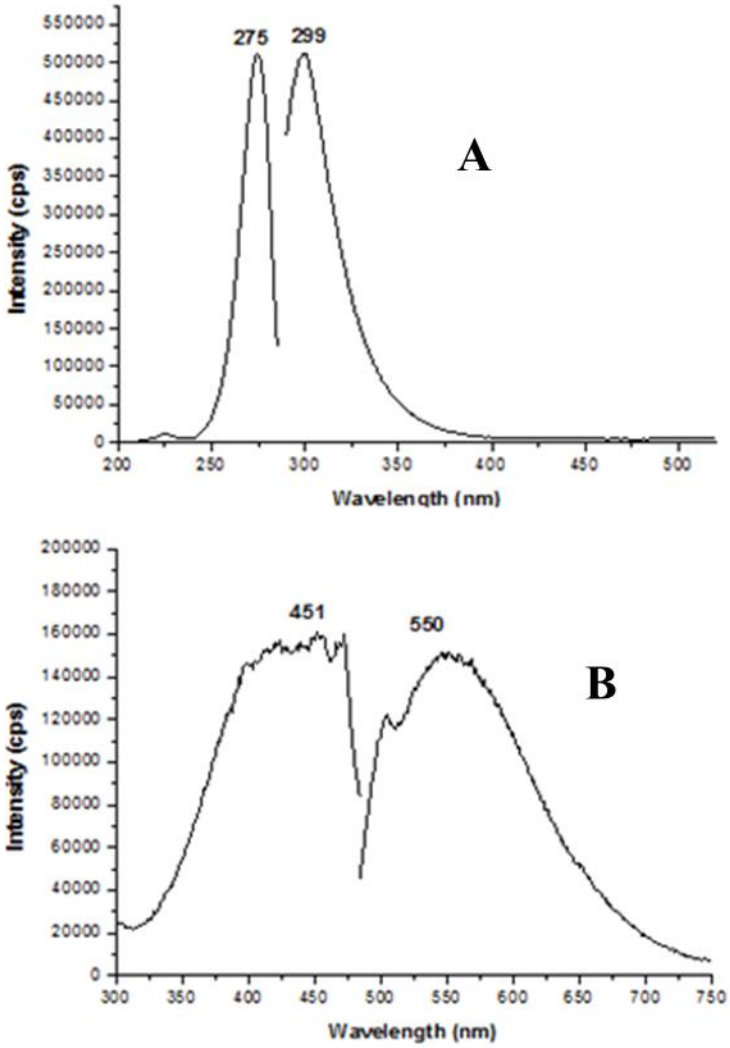

Figure E.4. Excitation and fluorescence spectrum of a 10 ppm solution of acid yellow 23 reagent dye in ethanol. A) λ_{ex} = 275 nm and λ_{em} = 299 nm; B) λ_{ex} = 451 nm and λ_{em} = 550 nm

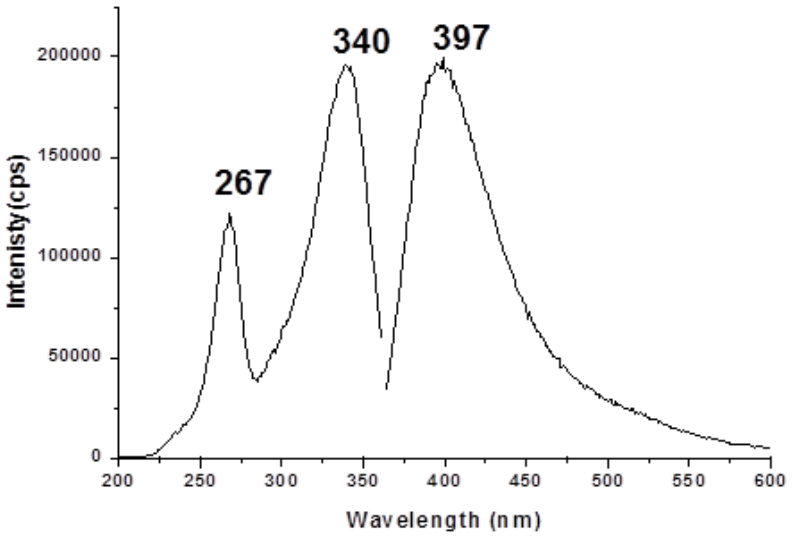

Figure E.5. Excitation and fluorescence spectrum of a 10 ppm solution of direct blue 1 reagent dye in ethanol; λ_{ex} = 340 nm and λ_{em} = 397 nm

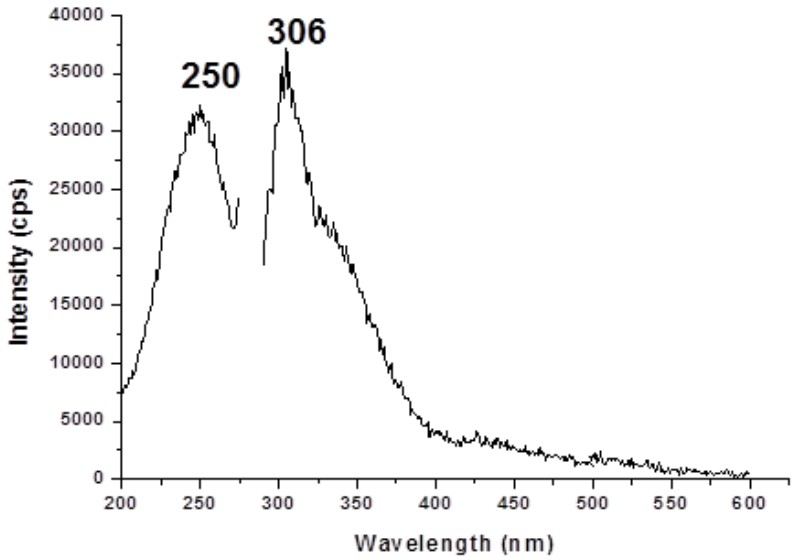

Figure E.6. Excitation and fluorescence spectrum of a 10 ppm solution of direct blue 90 reagent dye in 4:3 Pyridine/water (v:v); λ_{ex} = 250 nm and λ_{em} = 306 nm

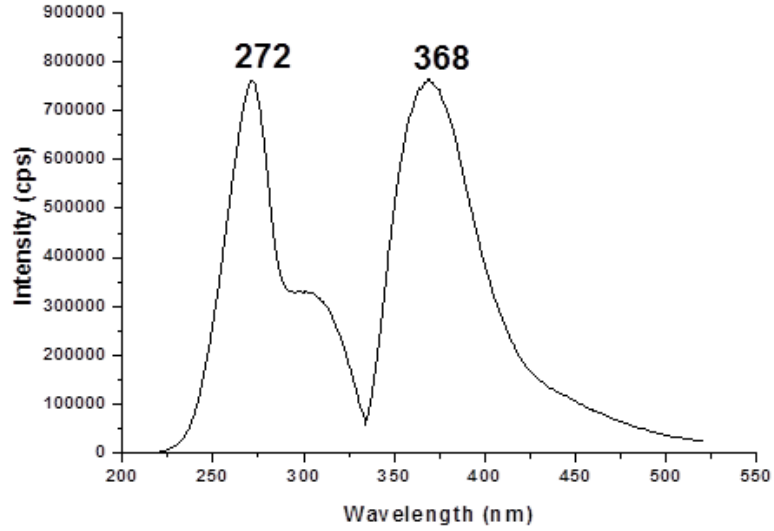

Figure E.7. Excitation and fluorescence spectrum of a 10 ppm solution of basic green 4 reagent dye in 1:1 acetonitrile/water (v:v); λ_{ex} = 272 nm and λ_{em} = 368 nm

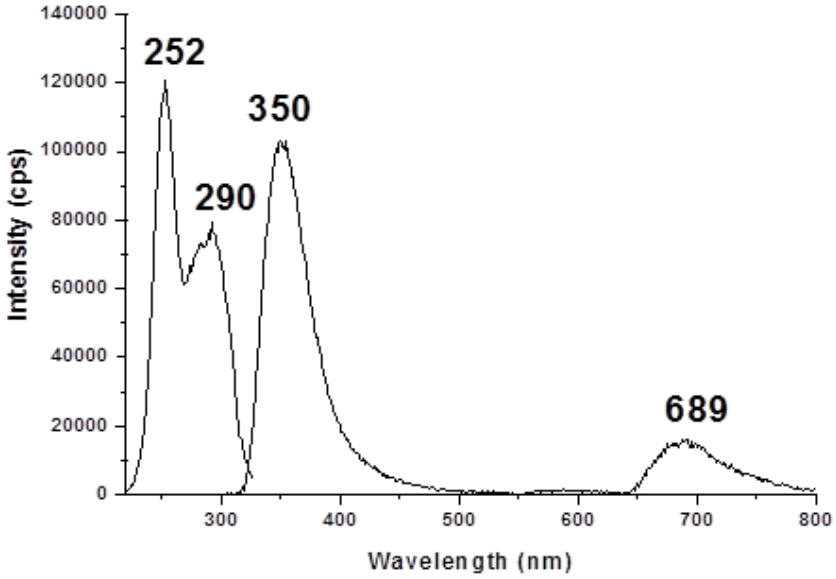

Figure E.8. Excitation and fluorescence spectrum of a 10 ppm solution of basic red 9 reagent dye in ethanol; λ_{ex} = 252 nm and λ_{em} = 350 nm

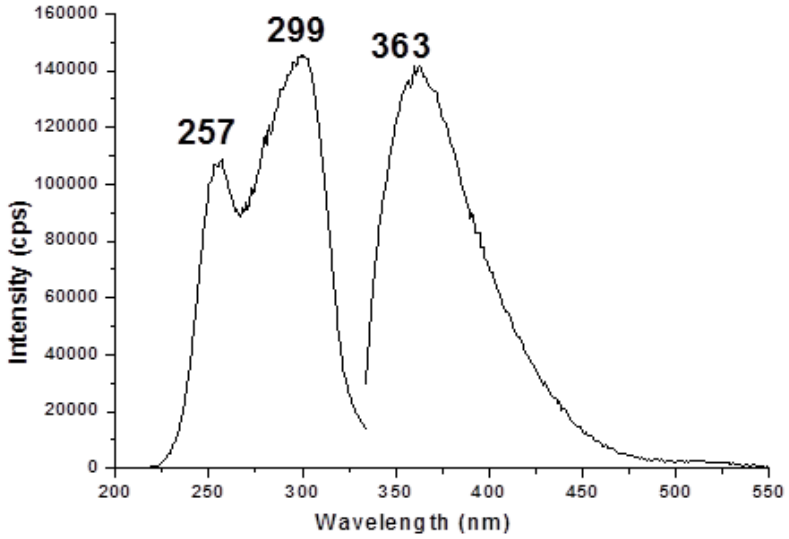

Figure E.9. Excitation and fluorescence spectrum of a 10 ppm solution of basic violet 14 reagent dye in ethanol; λ_{ex} = 299 nm and λ_{em} = 363 nm

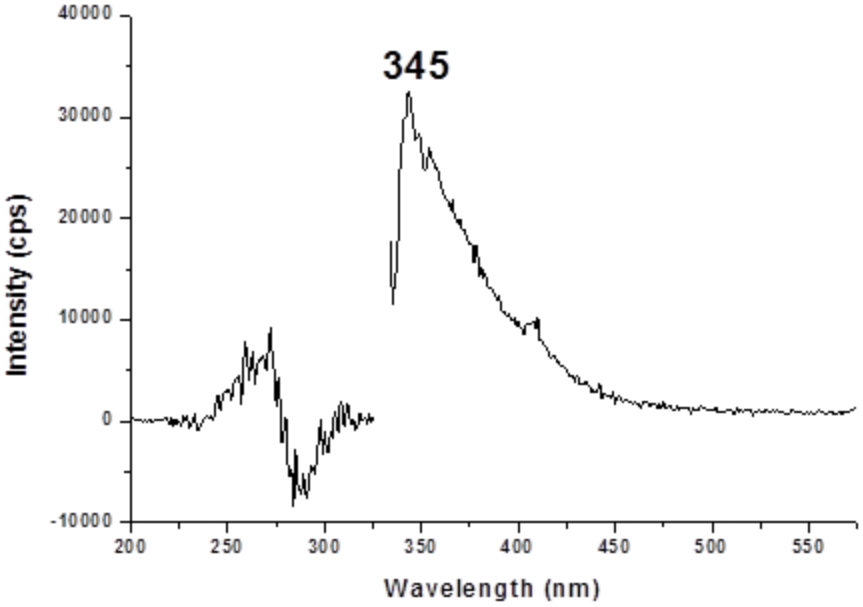

Figure E.10. Excitation and fluorescence spectrum of a 15 ppm solution of disperse red 13 reagent dye in ethanol; λ_{ex} = 300 nm and λ_{em} = 345 nm

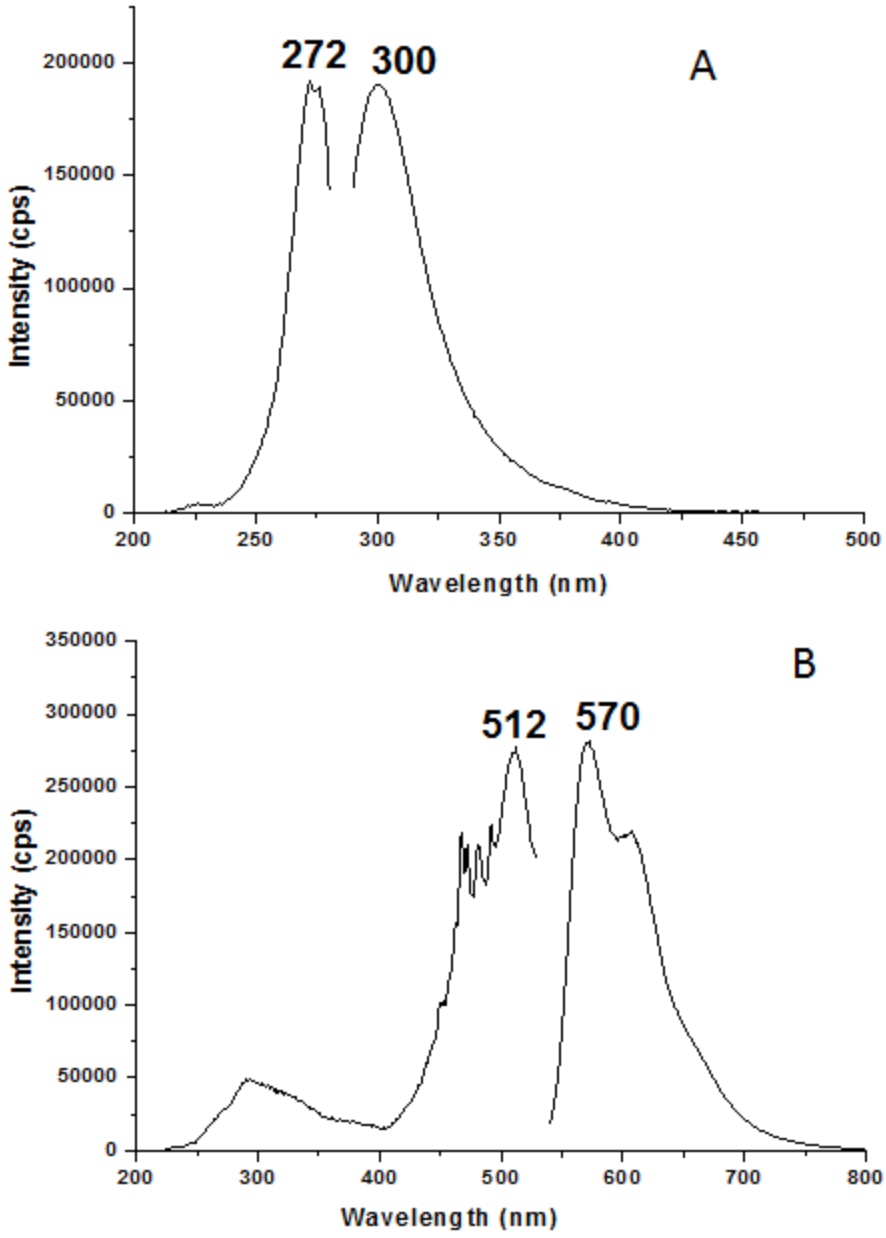

Figure E.11. Excitation and fluorescence spectrum of a disperse red 4 reagent dye in 50% v/v acetonitrile/water. A) λ_{ex} = 272 nm and λem = 300 nm; B) λex = 512 nm and λem = 570 nm

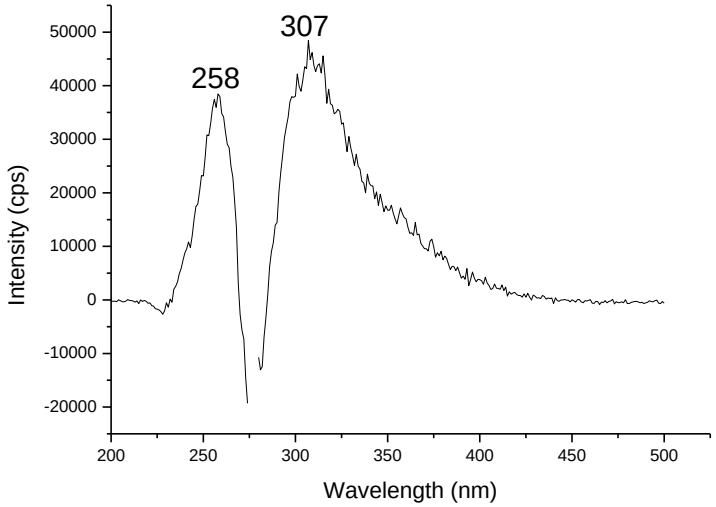

Figure E.12. Excitation and fluorescence spectrum of a disperse red 1 reagent dye in ethanol - λ_{ex} = 260 nm and λem = 307 nm

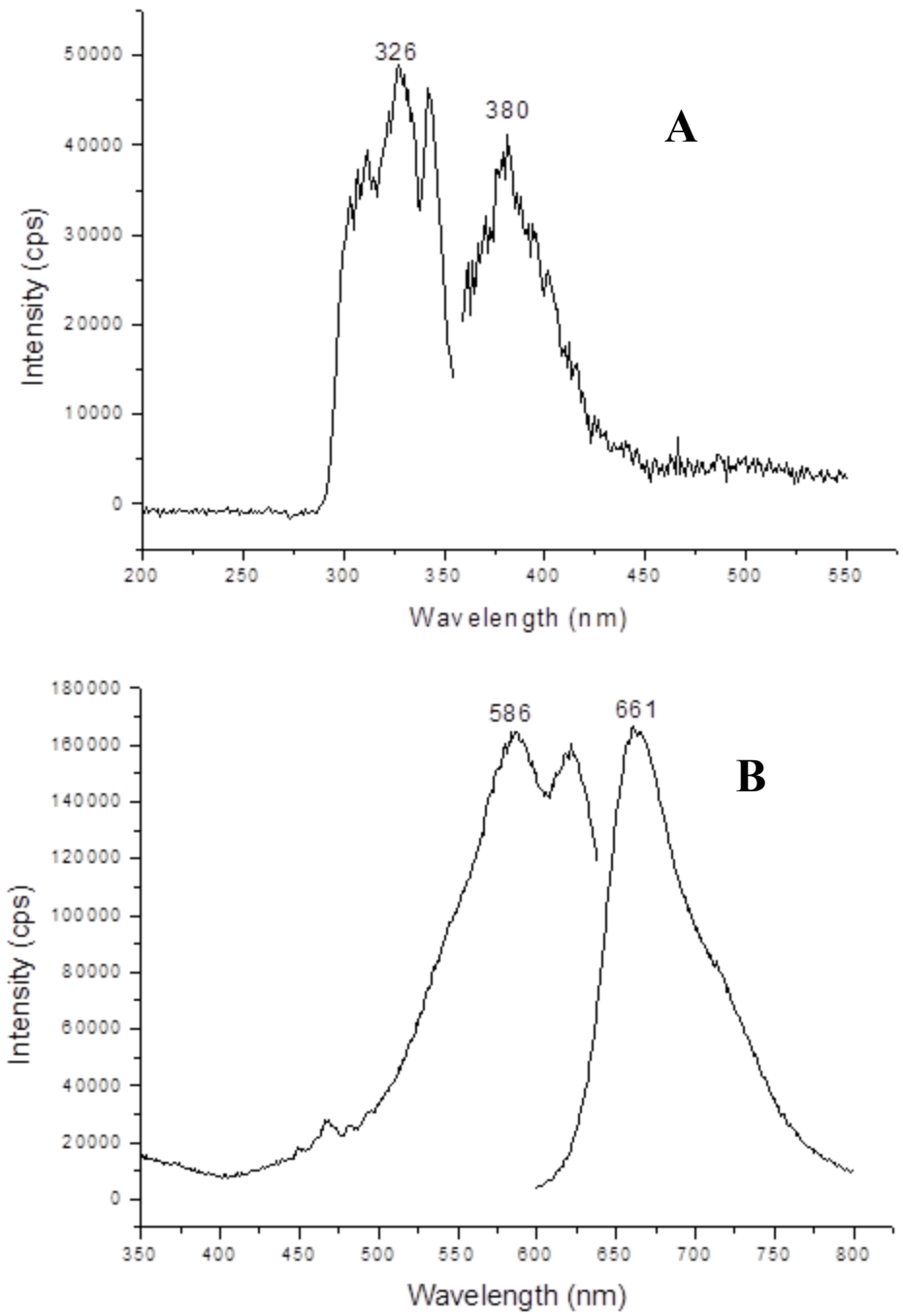

Figure E.13. Excitation and fluorescence spectrum of a disperse blue 56 reagent dye in 4:3 Pyridine/water. A) λ_{ex} = 310 nm and λem = 380 nm; B) λ_{ex} = 586 nm and λem = 661 nm

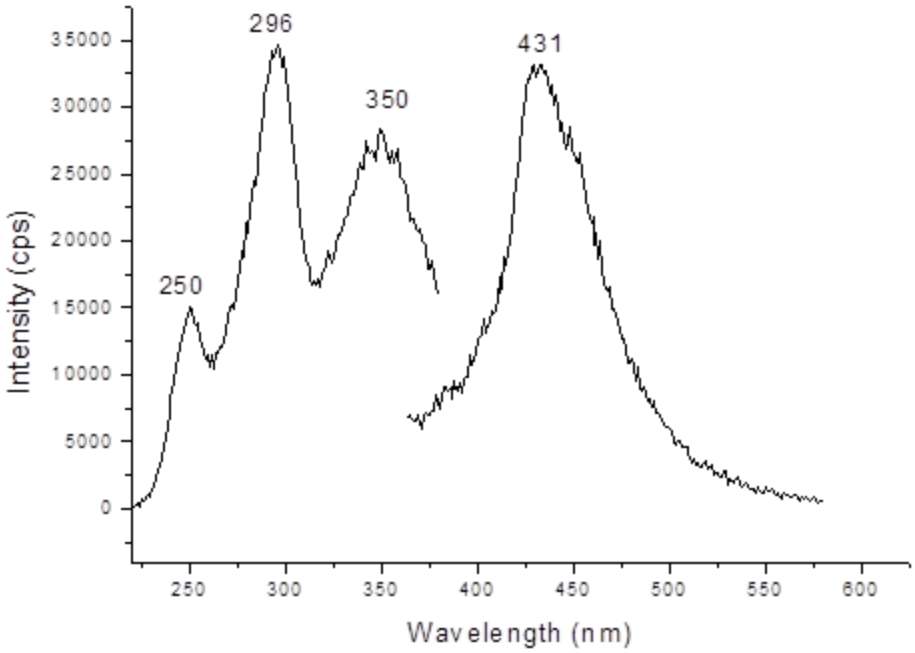

Figure E.14. Excitation and fluorescence spectrum of a direct blue 71 reagent dye in 50% acetonitrile/water - λ_{ex} = 300 nm and λem = 431 nm

APPENDIX F: TWO- DIMENSIONAL EXCITATION-EMISSION SPECTRA OF INSITINGUISBALE PAIR OF FIBERS

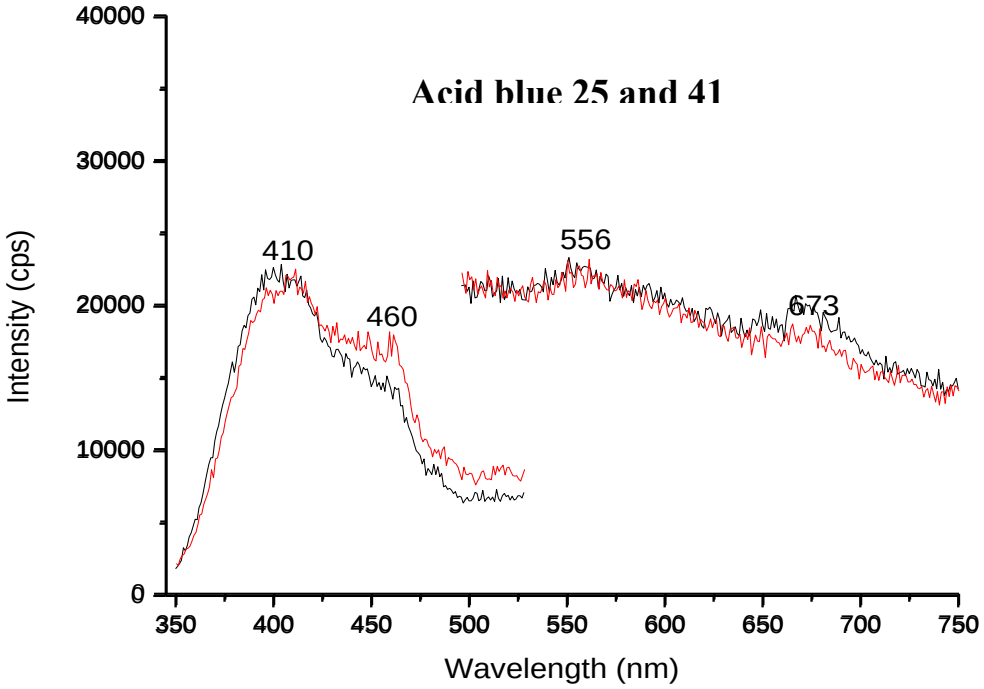

Figure F.1. Excitation and fluorescence spectrum of acid blue 25(___) and acid blue 41(___) fiber - λ_{ex} = 410 nm and λ_{em} = 556 nm

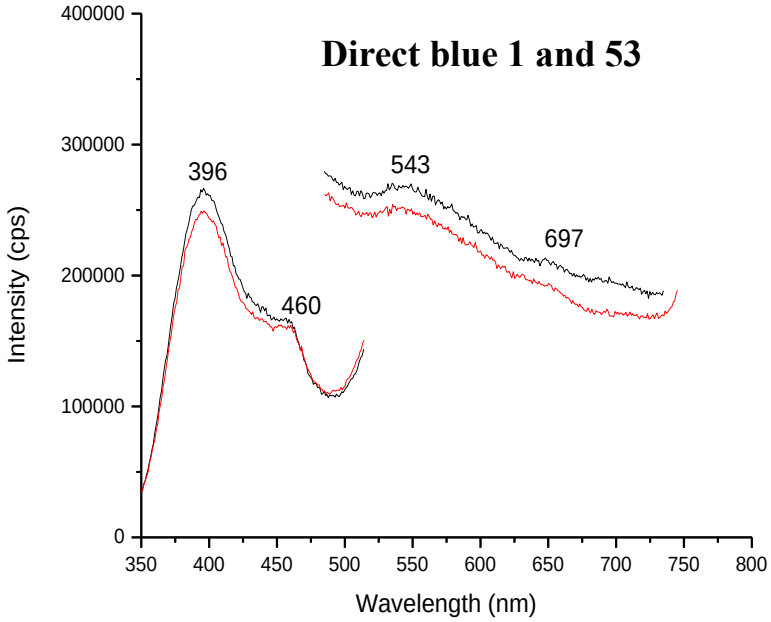

Figure F.2. Excitation and fluorescence spectrum of direct blue 1 (___) and direct blue 53 (___) fiber - λ_{ex} = 396 nm and λ_{em} = 554 nm

APPENDIX G: F-RATIOS FOR THE VALIDATION SETS OF ACID BLUE AND DIRECT BLUE FIBER PAIRS

Table G.1 Classification of acid blue 25 fibers based on the calculated F-ratio values

	F (AB25)	**F** (AB41)	**Identification**
AB 25 fiber 1	4.75	63.0	AB25
AB 25 fiber 2	0.51	51.4	AB25
AB 25 fiber 3	7.99	95.0	AB25
AB 25 fiber 4	3.47	61.4	AB25
AB 25 fiber 5	2.39	46.5	AB25
AB 25 fiber 6	1.78	24.0	AB25
AB 25 fiber 7	0.36	68.2	AB25
AB 25 fiber 8	1.95	46.1	AB25
AB 25 fiber 9	0.52	18.2	AB25
AB 25 fiber 10	0.52	55.4	AB25

Table G.2 Classification of acid blue 25 threads based on the calculated F-ratio values

	F (AB25)	**F** (AB41)	**Identification**
AB 25 thread 1	4.75	62.9	AB25
AB 25 thread 2	0.95	55.7	AB25
AB 25 thread 3	1.33	48.1	AB25
AB 25 thread 4	0.14	17.5	AB25
AB 25 thread 5	3.35	30.7	AB25
AB 25 thread 6	4.83	17.8	AB25
AB 25 thread 7	4.00	37.2	AB25
AB 25 thread 8	1.34	43.7	AB25
AB 25 thread 9	3.21	58.2	AB25
AB 25 thread 10	0.86	42.8	AB25

Table G.3 Classification of acid blue 25 regions based on the calculated F-ratio values

	F (AB25)	**F** (AB41)	**Identification**
AB 25 region 1	0.95	55.7	AB25
AB 25 region 2	1.04	42.0	AB25
AB 25 region 3	1.04	28.9	AB25
AB 25 region 4	1.76	50.2	AB25
AB 25 region 5	1.02	52.3	AB25

Table G.4 Classification of acid blue 41 fibers based on the calculated F-ratio values

	F (AB41)	**F (**AB25)	**Identification**
AB 41 fiber 1	0.24	132	AB41
AB 41 fiber 2	0.20	112	AB41
AB 41 fiber 3	2.30	28.8	AB41
AB 41 fiber 4	0.62	53.6	AB41
AB 41 fiber 5	0.38	66.5	AB41
AB 41 fiber 6	4.29	135	AB41
AB 41 fiber 7	0.19	149	AB41
AB 41 fiber 8	0.99	92.3	AB41
AB 41 fiber 9	8.34	167	AB41
AB 41 fiber 10	0.97	138	AB41

Table G.5 Classification of acid blue 41 threads based on the calculated F-ratio values

	F (AB41)	**F (**AB25)	**Identification**
AB 41 thread 1	0.24	132	AB41
AB 41 thread 2	0.43	141	AB41
AB 41 thread 3	0.35	105	AB41
AB 41 thread 4	9.69	148	AB41
AB 41 thread 5	23.2	146	Unclassified
AB 41 thread 6	10.1	109	AB41
AB 41 thread 7	1.11	181	AB41
AB 41 thread 8	0.59	169	AB41
AB 41 thread 9	0.88	143	AB41
AB 41 thread 10	0.70	131	AB41

Table G.6 Classification of acid blue 41 regions based on the calculated F-ratio values

	F (AB41)	**F (**AB25)	**Identification**
AB 41 region 1	0.43	141	AB41
AB 41 region 2	0.77	188	AB41
AB 41 region 3	4.40	179	AB41
AB 41 region 4	0.26	192	AB41
AB 41 region 5	0.52	168	AB41

Table G.7. Classification of direct blue 1 fibers based on the calculated F-ratio values

	F (DB1)	**F** (DB53)	**Identification**
DB1 fiber 1	3.21	43.6	DB1
DB1 fiber 2	1.55	29.2	DB1
DB1 fiber 3	2.28	39.4	DB1
DB1 fiber 4	7.42	21.7	DB1
DB1 fiber 5	0.82	70.6	DB1
DB1 fiber 6	9.64	91.8	DB1
DB1 fiber 7	1.24	36.7	DB1
DB1 fiber 8	2.36	50.0	DB1
DB1 fiber 9	16.0	64.7	Unclassified
DB1 fiber 10	16.6	47.3	Unclassified

Table G.8. Classification of direct blue 1 threads based on the calculated F-ratio values

	F (DB1)	**F** (DB53)	**Identification**
DB1 thread 1	8.83	53.3	DB1
DB1 thread 2	2.55	37.3	DB1
DB1 thread 3	1.96	31.5	DB1
DB1 thread 4	0.02	28.1	DB1
DB1 thread 5	0.07	54.7	DB1
DB1 thread 6	4.70	40.6	DB1
DB1 thread 7	0.77	48.3	DB1
DB1 thread 8	0.88	43.9	DB1
DB1 thread 9	0.61	36.1	DB1
DB1 thread 10	3.05	29.0	DB1

Table G.9. Classification of direct blue 1 regions based on the calculated F-ratio values

	F (DB1)	**F** (DB53)	**Identification**
DB1 region 1	8.84	53.3	DB1
DB1 region 2	3.40	61.8	DB1
DB1 region 3	1.53	47.8	DB1
DB1 region 4	5.73	84.8	DB1
DB1 region 5	3.88	48.3	DB1

Table G.10 Classification of direct blue 53 fibers based on the calculated F-ratio values

	F (DB53)	**F** (DB1)	**Identification**
DB53 fiber 1	2.56	96.0	DB53
DB53 fiber 2	7.97	118	DB53
DB53 fiber 3	1.67	154	DB53
DB53 fiber 4	17.1	60.8	Unclassified
DB53 fiber 5	6.11	142	DB53
DB53 fiber 6	23.2	61.5	Unclassified
DB53 fiber 7	2.60	123	DB53
DB53 fiber 8	0.30	113	DB53
DB53 fiber 9	4.71	45.3	DB53
DB53 fiber 10	0.08	40.4	DB53

Table G.11 Classification of direct blue 53 threads based on the calculated F-ratio values

	F (DB53)	**F** (DB1)	**Identification**
DB53 thread 1	1.42	328	DB53
DB53 thread 2	4.12	221	DB53
DB53 thread 3	7.07	123	DB53
DB53 thread 4	8.75	168	DB53
DB53 thread 5	0.48	189	DB53
DB53 thread 6	4.80	90.6	DB53
DB53 thread 7	0.22	221	DB53
DB53 thread 8	2.03	229	DB53
DB53 thread 9	2.92	140	DB53
DB53 thread 10	9.73	111	DB53

Table G.12 Classification of direct blue 53 regions based on the calculated F-ratio values

	F (DB53)	**F** (DB1)	**Identification**
DB53 region 1	1.42	328	DB53
DB53 region 2	2.61	110	DB53
DB53 region 3	2.21	117	DB53
DB53 region 4	14.34	73.4	Unclassified
DB53 region 5	0.21	96.7	DB53

REFERENCES

1. Rendle, D. F., Advances in chemistry applied to forensic science. *Chemical Society Reviews* **2005,** *34* (12), 1021-1030.
2. Goodpaster, J. V.; Liszewski, E. A., Forensic analysis of dyed textile fibers. *Anal. Bioanal. Chem.* **2009,** *394* (8), 2009-2018.
3. Bergfjord, C.; Holst, B., A procedure for identifying textile bast fibres using microscopy: Flax, nettle/ramie, hemp and jute. *Ultramicroscopy* **2010,** *110* (9), 1192-1197.
4. Kirkbride K., T. M., Infrared microspectroscopy of fibers. In *Forensic Examination of fibers*, 2nd ed.; Robertson J., G. M., Ed. CRC: New York, 1999; pp 179-222.
5. Causin, V.; Marega, C.; Guzzini, G.; Marigo, A., The effect of exposure to the elements on the forensic characterization by infrared spectroscopy of poly(ethylene terephthalate) fibers. *J. Forensic Sci.* **2005,** *50* (4), 887-893.
6. Causin, V.; Marega, C.; Guzzini, G.; Marigo, A., Forensic analysis of poly(ethylene terephthalate) fibers by infrared spectroscopy. *Applied Spectroscopy* **2004,** *58* (11), 1272-1276.
7. Macrae, R.; Dudley, R. J.; Smalldon, K. W., Characterization of dyestuffs on wool fibers with special reference to microspectrophotometry. *Journal of Forensic Sciences* **1979,** *24* (1), 117-129.
8. Adolf F., D. J., Microspectrophotometry/color measurement. In *Forensic Examination of fibers*, 2nd ed.; Robertson J., G. M., Ed. CRC: New York, 1999; pp 251-289.
9. Roux C., Scanning electron microscopy and elemental analysis. In *Forensic examination of fibers*, Robertson J., G. M., Ed. CRC: Newyork, 1999.
10. Grieve, M. C.; Dunlop, J.; Haddock, P., An investigation of known blue, red, and black dyes used in the coloration of cotton fibers. *Journal of Forensic Sciences* **1990,** *35* (2), 301-315.
11. Grieve, M. C.; Biermann, T. W.; Davignon, M., The evidential value of black cotton fibres. *Science & Justice* **2001,** *41* (4), 245-260.
12. Grieve, M. C.; Biermann, T.; Davignon, M., The occurrence and individuality of orange and green cotton fibres. *Science & Justice* **2003,** *43* (1), 5-22.
13. Biermann, T. W., Blocks of colour IV: The evidential value of blue and red cotton fibres. *Science & Justice* **2007,** *47* (2), 68-87.
14. Grieve, M. C.; Dunlop, J.; Haddock, P., An assessment of the value of blue, red, and black cotton fibers as target fibers in forensic-science investigations. *Journal of Forensic Sciences* **1988,** *33* (6), 1332-1344.
15. Challinor J.M., Fiber identification by pyrolysis techniques. In *Forensic examination of fibers*, 2nd ed.; Robertson J., G. M., Ed. CRC: Newyork, 1999; pp 223-237.
16. Huang, M.; Yinon, J.; Sigman, M. E., Forensic identification of dyes extracted from textile fibers by liquid chromatography mass spectrometry (LC-MS). *Journal of Forensic Sciences* **2004,** *49* (2), 238-249.
17. Rendle, D. F.; Crabtree, S. R.; Wiggins, K. G.; Salter, M. T., Cellulase digestion of cotton dyed with reactive dyes and analysis of the products by thin-layer chromatography. *Journal of the Society of Dyers and Colourists* **1994,** *110* (11), 338-341.

18. Wiggins, K. G.; Holness, J. A.; March, B. M., The importance of thin layer chromatography and UV microspectrophotometry in the analysis of reactive dyes released from wool and cotton fibers. *Journal of Forensic Sciences* **2005,** *50* (2), 364-368.
19. Wiggins, K. G.; Crabtree, S. R.; March, B. M., The importance of thin layer chromatography in the analysis of reactive dyes released from wool fibers. *Journal of Forensic Sciences* **1996,** *41* (6), 1042-1045.
20. Griffin R., S. J., Other methods of colour analysis: high performance liquid chromatography. In *Forensic examination of fibers,* 2nd ed.; Robertson J., G. M., Ed. CRC: Boca Raton, Florida, 1999.
21. Robertson J., Other methods of color analysis: capillary electrophoresis. In *Forensic examination of fibers,* 2nd ed.; Robertson J., G. M., Ed. CRC: Boca Raton, 1999.
22. Trojanowicz, M.; Wojcik, L.; Urbaniak-Walczak, K., Identification of natural dyes in historical Coptic textiles by capillary electrophoresis with diode array detection. *Chemia Analityczna* **2003,** *48* (3), 607-620.
23. Xu, X.; Leijenhorst, H.; Van den Hoven, P.; De Koeijer, J. A.; Logtenberg, H., Analysis of single textile fibres by sample-induced isotachophoresis - micellar electrokinetic capillary chromatography. *Science & Justice* **2001,** *41* (2), 93-105.
24. Golding, G. M.; Kokot, S., The selection of noncorrelated thin-layer chromatographic (tlc) solvent systems for the comparison of dyes extracted from transferred fibers. *Journal of Forensic Sciences* **1989,** *34* (5), 1156-1165.
25. Macrae, R.; Smalldon, K. W., Extraction of dyestuffs from single wool fibers. *J. Forensic Sci.* **1979,** *24* (1), 109-116.
26. Resua, R., Semi-micro technique for the extraction and comparison of dyes in textile fibers. *J. Forensic Sci.* **1980,** *25* (1), 168-173.
27. Wiggins, K. G.; Cook, R.; Turner, Y. J., Dye batch variation in textile fibers. *J. Forensic Sci.* **1988,** *33* (4), 998-1007.
28. Beattie, I. B.; Dudley, R. J.; Smalldon, K. W., Extraction and classification of dyes on single nylon, polyacrylonitrile and polyester fibers. *Journal of the Society of Dyers and Colourists* **1979,** *95* (8), 295-302.
29. Resua, R.; Deforest, P. R.; Harris, H., The evaluation and selection of uncorrelated paired solvent systems for use in the comparison of textile dyes by thin-layer chromatography. *J. Forensic Sci.* **1981,** *26* (3), 515-534.
30. Massonnet, G.; Buzzini, P.; Jochem, G.; Stauber, M.; Coyle, T.; Roux, C.; Thomas, J.; Leijenhorst, H.; Van Zanten, Z.; Wiggins, K.; Russell, C.; Chabli, S.; Rosengarten, A., Evaluation of Raman Spectroscopy for the analysis of colored fibers: A collaborative study. *J. Forensic Sci.* **2005,** *50* (5), 1028-1038.
31. Yinon, J.; Saar, J., Analysis of dyes extracted from textile fibers by thermospray high-performance liquid chromatography-mass spectrometry. *Journal of Chromatography* **1991,** *586* (1), 73-84.
32. Tuinman, A. A.; Lewis, L. A.; Lewis, S. A., Trace-fiber color discrimination by electrospray ionization mass spectrometry: A tool for the analysis of dyes extracted from submillimeter nylon fibers. *Analytical Chemistry* **2003,** *75* (11), 2753-2760.
33. Stefan, A. R.; Dockery, C. R.; Baguley, B. M.; Vann, B. C.; Nieuwland, A. A.; Hendrix, J. E.; Morgan, S. L., Microextraction, capillary electrophoresis, and mass spectrometry for

forensic analysis of azo and methine basic dyes from acrylic fibers. *Anal. Bioanal. Chem.* **2009,** *394* (8), 2087-2094.
34. Petrick, L. M.; Wilson, T. A.; Fawcett, W. R., High-performance liquid chromatography-ultraviolet-visible spectroscopy-electrospray ionization mass spectrometry method for acrylic and polyester forensic fiber dye analysis. *Journal of Forensic Sciences* **2006,** *51* (4), 771-779.
35. Morgan S.L., V. B. C., Baguley B.M., Stefan A.R.,, Advances in discrimination of dyed textile fibers using capillary electrophoresis/mass spectrometry. In *2007 trace evidence symposium*, Clearwater beach, Florida, 2007.
36. Soltzberg, L. J.; Hagar, A.; Kridaratikorn, S.; Mattson, A.; Newman, R., MALDI-TOF mass spectrometric identification of dyes and pigments. *Journal of the American Society for Mass Spectrometry* **2007,** *18* (11), 2001-2006.
37. Cochran, K. H.; Barry, J. A.; Muddiman, D. C.; Hinks, D., Direct Analysis of Textile Fabrics and Dyes Using Infrared Matrix-Assisted Laser Desorption Electrospray Ionization Mass Spectrometry. *Analytical Chemistry* **2013,** *85* (2), 831-836.
38. Zhou, C. Z.; Li, M.; Garcia, R.; Crawford, A.; Beck, K.; Hinks, D.; Griffis, D. P., Time-of-Flight-Secondary Ion Mass Spectrometry Method Development for High-Sensitivity Analysis of Acid Dyes in Nylon Fibers. *Analytical Chemistry* **2012,** *84* (22), 10085-10090.
39. Suszuki E., Forensic applications of infrared spectroscopy. In *Forensic science handbook*, Saferstein R., Ed. Regents/Prentice Hall: Upper Saddle River, New Jersey, 1993; pp 71-195.
40. Gilbert, C.; Kokot, S., Discrimination of cellulosic fabrics by diffuse-reflectance infrared fourier-transform spectroscopy and chemometrics. *Vib. Spectrosc.* **1995,** *9* (2), 161-167.
41. Kokot, S.; Crawford, K.; Rintoul, L.; Meyer, U., A DRIFTS study of reactive dye states on cotton fabric. *Vib. Spectrosc.* **1997,** *15* (1), 103-111.
42. Kokot, S.; Tuan, N. A.; Rintoul, L., Discrimination of reactive dyes on cotton fabric by Raman spectroscopy and chemometrics. *Applied Spectroscopy* **1997,** *51* (3), 387-395.
43. Keen, I. P.; White, G. W.; Fredericks, P. M., Characterization of fibers by Raman microprobe spectroscopy. *Journal of Forensic Sciences* **1998,** *43* (1), 82-89.
44. Jochem, G.; Lehnert, R. J., On the potential of Raman microscopy for the forensic analysis of coloured textile fibres. *Science & Justice* **2002,** *42* (4), 215-221.
45. Thomas, J.; Buzzini, P.; Massonnet, G.; Reedy, B.; Roux, C., Raman spectroscopy and the forensic analysis of black/grey and blue cotton fibres - Part 1. Investigation of the effects of varying laser wavelength. *Forensic Science International* **2005,** *152* (2-3), 189-197.
46. Massonnet, G.; Buzzini, P.; Monard, F.; Jochem, G.; Fido, L.; Bell, S.; Stauber, M.; Coyle, T.; Roux, C.; Hemmings, J.; Leijenhorst, H.; Van Zanten, Z.; Wiggins, K.; Smith, C.; Chabli, S.; Sauneuf, T.; Rosengarten, A.; Meile, C.; Ketterer, S.; Blumer, A., Raman spectroscopy and microspectrophotometry of reactive dyes on cotton fibres: Analysis and detection limits. *Forensic Science International* **2012,** *222* (1-3), 200-207.
47. Jurdana, L. E.; Ghiggino, K. P.; Nugent, K. W.; Leaver, I. H., CONFOCAL LASER RAMAN MICROPROBE STUDIES OF KERATIN FIBERS. *Textile Research Journal* **1995,** *65* (10), 593-600.
48. White, P. C.; Munro, C. H.; Smith, W. E., In situ surface enhanced resonance Raman scattering analysis of a reactive dye covalently bound to cotton. *Analyst* **1996,** *121* (6), 835-838.

49. Cho, L. L.; Reffner, J. A.; Gatewood, B. M.; Wetzel, D. L., Single fiber analysis by internal reflection infrared microspectroscopy. *J. Forensic Sci.* **2001,** *46* (6), 1309-1314.
50. Hartshorne, A. W.; Laing, D. K., Microspectrofluorimetry of fluorescent dyes and brighteners on single textile fibers .2. Color measurements. *Forensic Science International* **1991,** *51* (2), 221-237.
51. Hartshorne, A. W.; Laing, D. K., Microspectrofluorimetry of fluorescent dyes and brighteners on single textile fibers .3. Fluorescence decay phenomena. *Forensic Science International* **1991,** *51* (2), 239-250.
52. Palmer, R.; Chinherende, V., A target fiber study using cinema and car seats as recipient items. *J. Forensic Sci.* **1996,** *41* (5), 802-803.
53. Cantrell, S.; Roux, C.; Maynard, P.; Robertson, J., A textile fibre survey as an aid to the interpretation of fibre evidence in the Sydney region. *Forensic Science International* **2001,** *123* (1), 48-53.
54. Turro, N. J., *Modern molecular photochemistry*. Benjamin/Cummings Pub. Co: Menlo Park, Calif, 1978.
55. Ingle, J. D.; Crouch, S. R., *Spectrochemical analysis*. Prentice Hall: Englewood Cliffs, N.J, 1988.
56. da Silva, J.; Tavares, M.; Tauler, R., Multivariate curve resolution of multidimensional excitation-emission quenching matrices of a Laurentian soil fulvic acid. *Chemosphere* **2006,** *64* (11), 1939-1948.
57. DaCosta, R. S.; Andersson, H.; Wilson, B. C., Molecular fluorescence excitation-emission matrices relevant to tissue spectroscopy. *Photochemistry and Photobiology* **2003,** *78* (4), 384-392.
58. Warner, I. M.; Christian, G. D.; Davidson, E. R.; Callis, J. B., ANALYSIS OF MULTICOMPONENT FLUORESCENCE DATA. *Analytical Chemistry* **1977,** *49* (4), 564-573.
59. Warner, I. M.; Davidson, E. R.; Christian, G. D., QUANTITATIVE-ANALYSES OF MULTICOMPONENT FLUORESCENCE DATA BY METHODS OF LEAST-SQUARES AND NONNEGATIVE LEAST SUM OF ERRORS. *Analytical Chemistry* **1977,** *49* (14), 2155-2159.
60. Kasha M., Characterization of electronic transitions in complex molecules. *Discussions of the Faraday Society* **1950,** *9*, 14-19.
61. Vatsavai, K., *Analytical evaluation of the fluorescence characteristics of metabolites of polycyclic aromatic hydrocarbons at room, liquid nitrogen and liquid helium temperatures*. University of Central Florida: Orlando, Fla, 2007.
62. Blackledge, R. D., *Forensic analysis on the cutting edge : new methods for trace evidence analysis*. Wiley ;
John Wiley distributor: Hoboken, N.J.
Chichester, 2007; p xxvi, 446 p.
63. Robertson, J.; Grieve, M., *Forensic examination of fibres*. 2nd ed.; Taylor & Francis: London ; Philadelphia, 1999; p xix, 447 p.
64. Huang, M.; Russo, R.; Fookes, B. G.; Sigman, M. E., Analysis of fiber dyes by liquid chromatography mass spectrometry (LC-MS) with electrospray ionization: Discriminating between dyes with indistinguishable UV-Visible absorption spectra. *Journal of Forensic Sciences* **2005,** *50* (3), 526-534.

65. Muller, M.; Murphy, B.; Burghammer, M.; Snigireva, I.; Riekel, C.; Gunneweg, J.; Pantos, E., Identification of single archaeological textile fibres from the cave of letters using synchrotron radiation microbeam diffraction and microfluorescence. *Applied Physics a-Materials Science & Processing* **2006,** *83* (2), 183-188.
66. In *Forensic Science Communications*, 1999; Vol. Vol. 1.
67. Beattie, I. B.; Roberts, H. L.; Dudley, R. J., THIN-LAYER CHROMATOGRAPHY OF DYES EXTRACTED FROM POLYESTER, NYLON AND POLYACRYLONITRILE FIBERS. *Forensic Science International* **1981,** *17* (1), 57-69.
68. Home, J. M.; Dudley, R. J., THIN-LAYER CHROMATOGRAPHY OF DYES EXTRACTED FROM CELLULOSIC FIBERS. *Forensic Science International* **1981,** *17* (1), 71-78.
69. Hartshorne, A. W.; Laing, D. K., THE DYE CLASSIFICATION AND DISCRIMINATION OF COLORED POLYPROPYLENE FIBERS. *Forensic Science International* **1984,** *25* (2), 133-141.
70. Wiersema S., CAC Newsletter. March 1984.
71. Laing, D. K.; Dudley, R. J.; Hartshorne, A. W.; Home, J. M.; Rickard, R. A.; Bennett, D. C., THE EXTRACTION AND CLASSIFICATION OF DYES FROM COTTON AND VISCOSE FIBERS. *Forensic Science International* **1991,** *50* (1), 23-35.
72. Green F.J., Sigma Aldrich Handbook of Stains, Dyes and Indicators. 1990.
73. Pounds, C. A.; Smalldon, K. W., TRANSFER OF FIBERS BETWEEN CLOTHING MATERIALS DURING SIMULATED CONTACTS AND THEIR PERSISTENCE DURING WEAR .1. FIBER TRANSFERENCE. *Journal of the Forensic Science Society* **1975,** *15* (1), 17-27.
74. Goicoechea, H. C.; Calimag-Williams, K.; Campiglia, A. D., Multi-way partial least-squares and residual bi-linearization for the direct determination of monohydroxy-polycyclic aromatic hydrocarbons on octadecyl membranes via room-temperature fluorescence excitation emission matrices. *Analytica Chimica Acta* **2012,** *717*, 100-109.
75. Vatsavai, K.; Goicoechea, H. C.; Campiglia, A. D., Direct quantification of monohydroxy-polycyclic aromatic hydrocarbons in synthetic urine samples via solid-phase extraction-room-temperature fluorescence excitation-emission matrix spectroscopy. *Analytical Biochemistry* **2008,** *376* (2), 213-220.
76. Parker, C. A., SPECTROPHOSPHORIMETER MICROSCOPY - AN EXTENSION OF FLUORESCENCE MICROSCOPY. *Analyst* **1969,** *94* (1116), 161-&.
77. Hartshorne, A. W.; Laing, D. K., Microspectrofluorimetry of fluorescent dyes and brighteners on single textile fibers .1. Fluorescence emission-spectra. *Forensic Science International* **1991,** *51* (2), 203-220.
78. Nakamura, R.; Tanaka, Y.; Ogata, A.; Naruse, M., Dye Analysis of Shosoin Textiles Using Excitation-Emission Matrix Fluorescence and Ultraviolet-Visible Reflectance Spectroscopic Techniques. *Analytical Chemistry* **2009,** *81* (14), 5691-5698.
79. Fundamentals of light microscopy and electronic imaging, second edition. *Journal Of Biomedical Optics* **2013,** *18* (2), 29901-29901.
80. Shaloe W.U., D. N. J., High-sensitivity fluorescence detector for fluorescein isothiocyanate derivatives of amino-acids separated by capillary zone electrophoresis. *Journal of Chromatography* **1989,** *480*, 141-155.

81. Nakamura, R.; Tanaka, Y.; Ogata, A.; Naruse, M., Dye Analysis of Shosoin Textiles Using Excitation-Emission Matrix Fluorescence and Ultraviolet-Visible Reflectance Spectroscopic Techniques. *Analytical Chemistry* **2009,** *81*, 5691-5698.
82. Proefke, M. L.; Rinhart, K. L.; Raheel, M.; Ambrose, S. H.; Wisseman, S. U., Chemical Analysis of a Roman Period Egyptian Mummy. *Analytical Chemistry* **1992,** *64*, 105A-111A.
83. Wouters, J.; Rosariu-Chirinos, N., Dye Analysis of Pre-Columbian Peruvian Textiles with High-Performance Liquid Chromatography and Diode-Array Detection. *Journal of the American Institute for Conservation* **1992,** *31*, 237-255.
84. Goodpaster, J. V.; Liszewski, E. A., Forensic analysis of dyed textile fibers. *Anal Bioanal Chem* **2009,** *394*, 2009-2018.
85. Tuinman, A. A.; Lewis, L. A.; Lewis, S. S. A., Trace-Fiber Color Discrimination by Electrospray Ionization Mass Spectrometry: A Tool for the Analysis of Dyes Extracted from Submillimeter Nylon Fibers. *Analytical Chemistry* **2003,** *75*, 2753-2760.
86. Huang, M.; Russo, R.; Fookes, B. G.; Sigman, M. E., Analysis of Fiber Dyes by Liquid Chromatography Mass Spectrometry (LC-MS) with Electrospray Ionization: Discriminating Between Dyes with Indistinguishable UV-Visible Absorption Spectra. *J Forensic Sci* **2005,** *50*, 1-9.
87. Leona, M.; Stenger, J.; Ferloni, E., Application of surface-enhanced Raman scattering techniques to the ultrasensitive identification of natural dyes in works of art. *J Raman Spectrosc* **2006,** *37*, 981-992.
88. Wustholtz, K. L.; Brosseau, C. L.; Casadio, F.; Van Duyne, R. P., Surface-enhanced Raman spectroscopy of dyes: from single molecules to the artists' canvas. *Phys Chem Chem Phys* **2009,** *11*, 7350-7359.
89. Casadio, F.; Leona, M.; Lombardi, J. R.; Van Duyne, R. P., Identification of Organic Colorants in Fibers, paints, and Glazes by Surfaces Enhanced Raman Spectroscopy. *Acc Chem Res* **2010,** *43*, 782-791.
90. Xu, X.; Leijenhorst, H.; Van Den Jove, P.; de Koeijer, J.; Logetnberg, H., Analysis of single textile fibres by sample-induced isotachophoresis - micellar electrokinetic capillary chromatogrphy. *Sci Justice* **2000,** *41*, 93-105.
91. Markstrom, L. J.; Mabbott, G. A., Obtaining absorption spectra from single textile fibers using a liquid crystal tunable filter microspectrophotometer. *Forensic Sci International* **2011,** *209*, 108-112.
92. Palmer, R.; Hutchinson, W.; Fryer, V., The discrimination of (non-denim) blue cotton. *Sci Justice* **2009,** *49*, 12-18.
93. Barrett, J. A.; Siegel, J. A.; Goodpaster, J. V., Forensic Discrimination of Dyed Hair Color. *J Forensic Sci* **2011,** *56*, 95-101.
94. Yu, M. M. L.; Sandercock, P. M. L., Principal Component Analysis of Analysis of Variance on the Effects of Entellan New on the Raman Spectra of Fibers. *J Forensic Sci* **2012,** *57* (70), 70-74.
95. Sikirzhytski, V.; Sikirzhytskaya, A.; Lednev, I. K., Advanced statistical analysis of Raman spectroscopic data for the identification of body fluid traces: Semen and blood mixtures. *Forensic Sci International* **2012,** *222*, 259-265.

96. Bueno, J.; Sikirzhytski, V.; Lednev, I. K., Raman Spectroscopic Analysis of Gunshot Residue Offering Great Potential for Caliber Differentiation. *Analytical Chemistry* **2012,** *84*, 4334-4339.
97. Malinowski, E. R., Statistical F-Tests for Abstract Factor Analysis and Target Testing. *Journal of Chemometrics* **1988,** *3*, 49-60.
98. Green, F. J., *The Sigma-Aldrich handbook of stains, dyes, and indicators*. Aldrich Chemical Co: Milwaukee, Wis, 1990.